

METABOLIC ENGINEERING OF *Escherichia coli* FOR ETHANOL PRODUCTION
WITHOUT FOREIGN GENES

By

YOUNGNYUN KIM

A DISSERTATION PRESENTED TO THE GRADUATE SCHOOL
OF THE UNIVERSITY OF FLORIDA IN PARTIAL FULFILLMENT
OF THE REQUIREMENTS FOR THE DEGREE OF
DOCTOR OF PHILOSOPHY

UNIVERSITY OF FLORIDA

2007

© 2007 Youngnyun Kim

To my parents for their devoted support and encouragement in the pursuit of my education

ACKNOWLEDGMENTS

I deeply thank Dr. Keelnatham Shanmugam for scientific advice, support, and for guiding me to how to approach to science and think rationally in science. Without his expertise, direction and patience, I would not have accomplished my work. I also thank all my committee members, Dr. Lonnie Ingram, Dr. James Preston, Dr. Julie Maupin-Furlow and Dr. Shouguang Jin for helping me in achieving my work during my research period.

I also thank Mi-Jin Kim for encouraging me during the last moment of my work. I thank all my colleagues: Dr. Adnan Hasona, Dr. Tao Han, Phi Mihn Do, Mark Ou, Dr. Jinwoo Kim, Dr. Munsoo Rhee, Yue Su and Dr. Eunmin Cho for their experimental advice and friendship. Also I would like to express my thanks to all the laboratories in the department for helping me during my Ph.D course.

Finally, I thank my parents for their countless support and trust over the years.

TABLE OF CONTENTS

	<u>page</u>
ACKNOWLEDGMENTS	4
LIST OF TABLES	7
LIST OF FIGURES	8
LIST OF ABBREVIATIONS.....	10
ABSTRACT.....	13
CHAPTER	
1 LITERATURE REVIEW	15
Production of Bioethanol.....	15
Microbial Biocatalysts for Ethanol Production	17
Native Fermentation Profile, Mixed Acid Fermentation, of <i>E. coli</i>	20
The Importance of Redox Balance	21
Metabolism of Pyruvate.....	22
Pyruvate Dehydrogenase (PDH) Complex.....	25
Ethanologenic <i>Escherichia coli</i>	26
2 MATERIALS AND METHODS	33
Materials	33
Media and Growth Conditions.....	33
Gene Deletions.....	33
Transformation	34
Co-transduction Frequency.....	34
Sequencing DNA.....	35
Determination of the level of transcription of <i>pdh</i> operon	35
Construction of λ <i>Ppdh-lac</i>	35
Transduction.....	35
β -Galactosidase activity measurements.....	36
Quantitative RT-PCR	37
<i>in vitro</i> DNA Mutagenesis.....	37
Hydroxylamine Mutagenesis.....	37
PCR Mutagenesis	38
Construction of pTrc99A- <i>lpd</i> for Regulated Expression of <i>lpd</i>	38
Construction of pET-15b- <i>lpd</i> Plasmid for Purification of LPD	39
Expression of Dihydrolipoamide Dehydrogenase (LPD).....	39
Dihydrolipoamide Dehydrogenase (LPD) Assay	40
Purification of Pyruvate Dehydrogenase Complex	40
Pyruvate Dehydrogenase Assay	41

Protein Determination.....	42
SDS-Polyacrylamide Gel Electrophoresis.....	42
Fermentation.....	43
Analysis of Fermentation Products.....	43
3 RESULTS AND DISCUSSION.....	51
Isolation of Homo-Ethanol Producing <i>E. coli</i>	51
Mapping the Mutation(s) in Strain SE2378.....	52
Location(s) of the Mutation(s) in strain SE2378.....	54
Confirmation that the Mutation in <i>lpd</i> is Responsible for the Anaerobic Growth	
Phenotype of Strain SE2378.....	55
Additional Mutations.....	56
Metabolic Routes of Pyruvate with the Mutated LPD in Various Backgrounds.....	56
Aerobic and Anaerobic Expression Level of <i>pdh</i> Operon.....	57
LPD Purification and Characterization.....	58
NADH Sensitivity on Forward Reaction.....	59
NADH Sensitivity of the Reverse Reaction of LPD.....	60
PDH Purification and Characterization.....	61
Determination of Kinetic Constants of PDH Complex.....	62
Inhibition of PDH activity by NADH.....	62
Fermentation of Sugars to Ethanol.....	63
Glucose Fermentation.....	63
Xylose Fermentation.....	64
Removal of Trace Amount of Lactic Acid.....	65
Proposed Ethanologenic Fermentation Pathway.....	66
LIST OF REFERENCES.....	114
BIOGRAPHICAL SKETCH.....	127

LIST OF TABLES

<u>Table</u>	<u>page</u>
2-1 Bacterial strains and plasmids used in this study.....	44
2-2 List of primers used in this study.....	47
3-1 Growth and fermentation profile of the anaerobic (+) derivatives of <i>E. coli</i> strain AH242 grown in LB+glucose (0.3 %, w/v) in a batch culture without pH control.....	68
3-2 Growth characteristics of ethanologenic <i>E. coli</i> strain SE2378.....	74
3-3 Anaerobic growth and fermentation profile of <i>E. coli</i> with different <i>lpd</i> alleles.....	80
3-4 Fermentation profile of mutant strains with different pyruvate metabolic pathway composition.....	82
3-5 Pyruvate dehydrogenase mRNA, transcription and protein levels in aerobic and anaerobic <i>E. coli</i> wild type, strain W3110 and ethanologenic mutant, strain SE2378.....	83
3-6 Kinetic constants of the native (W3110) and the mutated (SE2378) LPD	88
3-7 Purification of native PDH complex from <i>E. coli</i> strain W3110.....	93
3-8 Purification of the mutated PDH complex from strain YK176.	94
3-9 Kinetics constants of the native (W3110) and the mutated (SE2378) PDH.....	100
3-10 Glucose fermentation characteristics of <i>E. coli</i> strain SE2378 and wild type strain W3110.....	106
3-11 Growth and ethanol production by <i>E. coli</i> strain SE2378 grown on glucose or xylose ^a	107
3-12 Xylose fermentation characteristics of <i>E. coli</i> strain SE2378 and wild type strain W3110.....	110
3-13 Fermentation characteristics of kanamycin-sensitive derivative of ethanologenic strain SE2378, YK1, and its $\Delta mgsA$ derivative strain YK96 in LB+glucose (50 g L ⁻¹) at pH 7.0 and 37 °C.....	112

LIST OF FIGURES

<u>Figure</u>	<u>page</u>
1-1 Mixed acid fermentation pathways of <i>E. coli</i>	29
1-2 Overall reaction catalyzed by the pyruvate dehydrogenase complex	29
1-3 Genetic organization of the <i>pdh</i> operon	30
1-4 Enzyme reaction diagram of the pyruvate dehydrogenase(PDH) complex	31
1-5 Elimination of lactate and formate production in the mixed acid fermentation pathway of <i>E. coli</i>	32
2-1 Construction of <i>lpd</i> in pTRC99a for complementation analysis	49
2-2 Construction of LPD expression construct in pET15b with PCR amplified <i>lpd</i> gene.....	50
3-1 HPLC analysis of fermentation products. (A) strain W3110, (B) strain SE2378 in LB+glucose (1 %, w/v) in batch fermentations	70
3-2 Metabolic fates of pyruvate in <i>E. coli</i>	71
3-3 Effect of deleting <i>pdh</i> genes in strain SE2378 on anaerobic growth	72
3-5 Promoter region and the transcription start site of <i>pdhR-aceEF-lpd</i> operon of <i>E. coli</i> K-12.	75
3-6 Comparison of amino acid sequence of PdhR from wild-type (W3110), and three ethanologenic mutants (SE2378, SE2377 and SE2382)	76
3-7 Nucleic acid sequence of intergenic region between <i>pdhR</i> and <i>aceE</i> genes of the ethanologenic mutants and the wild type	77
3-8 Comparison of the amino acid sequence of LPD among wild-type strain (W3110) and 6 isolates	78
3-9 Pyruvate metabolic enzymes in strain SE2378 and their affinity for pyruvate.	81
3-10 SDS-Polyacrylamide gel electrophoresis of purified dihydrolipoamide dehydrogenase (LPD) from wild-type, A) W3110 and B) the ethanologenic strain SE2378	84
3-11 Linearity of LPD protein concentration vs. activity of the enzyme in the forward reaction	85
3-12 Native LPD (W3110) activity with various NAD ⁺ concentrations	86

3-13	Mutated LPD (SE2378) activity with various NAD ⁺ concentrations.....	87
3-14	Inhibition of native LPD (W3110) forward activity by NADH	89
3-15	Inhibition of LPD activity by NADH (2.0 mM NAD ⁺) on forward reaction	90
3-16	Inhibition of mutated LPD (SE2378) by NADH	91
3-17	Activation of LPD reverse reaction by increasing NAD ⁺ /NADH ratio.....	92
3-18	SDS-PAGE of partially purified PDH complex	95
3-19	Native PDH (W3110) activity with various NAD ⁺ concentrations	96
3-20	Native PDH (W3110) activity with various pyruvate concentrations	97
3-21	Mutated PDH (SE2378) activity with various NAD ⁺ concentrations	98
3-22	Mutated PDH (SE2378) activity with various pyruvate concentrations.....	99
3-25	Inhibition of PDH complex by NADH at a fixed NAD ⁺ concentration of 1.0 mM	103
3-26	Growth and fermentation characteristics of wild type strain W3110 in LB + glucose (50 g L ⁻¹) at pH 7.0 and 37 °C.	104
3-27	Growth and fermentation characteristics of ethanologenic strain SE2378 in LB+ glucose (50 g L ⁻¹) at pH 7.0 and 37 °C.	105
3-28	Growth and fermentation characteristics of wild type strain W3110 in LB+ xylose (50 g L ⁻¹) at pH 7.0 and 37 °C.	108
3-29	Growth and fermentation characteristics of ethanologenic strain SE2378 in LB+ xylose (50 g L ⁻¹) at pH 7.0 and 37 °C.	109
3-30	Fermentation characteristics of kanamycin-sensitive derivative of ethanologenic strain SE2378, YK1, and its $\Delta mgsA$ derivative strain YK96 in LB+glucose (50 g L ⁻¹) at pH 7.0, 37 °C.....	111
3-31	Ethanologenic fermentation pathway	113

LIST OF ABBREVIATIONS

ACK	Acetate kinase
ACS	Acetyl-CoA synthetase
ADH	Alcohol dehydrogenase
ADP	Adenosine diphosphate
ATP	Adenosine-5'-triphosphate
BSA	Bovine serum albumin
bp	Base pair
cDNA	Complementary DNA
CoA	Coenzyme A
CTP	Cytosine-5'-triphosphate
da	Dalton
DOE	Department of energy
E1	Pyruvate decarboxylase/dehydrogenase
E2	Lipoamide acetyltransferase
E3	Dihydrolipoamide dehydrogenase
EDTA	Ethylenediamine tetraacetic acid
EIA	Energy information administration
EMS	Ethylmethane sulfonic acid
ETS	Electron transport system
FAD	Flavin adenine dinucleotide
FRT	Flipase recognition target site
GTP	Guanosine triphosphate
<i>K</i> _{cat}	Turnover number
kDa	Kilo dalton.

Km	Kanamycin resistance gene
<i>K_m</i>	Michaelis constant
LB	Luria broth
LDH	Lactate dehydrogenase
MOI	Multiplicity of infection
NAD ⁺	Nicotinamide adenine dinucleotide
NADH	Nicotinamide adenine dinucleotide reduced
NO	Nitric oxide
NOX	NADH oxidase
OAA	Oxaloacetic acid
ONPG	O-nitrophenyl-β-D-galactopyranoside
PAGE	Polyacrylamide agarose gel electrophoresis
PCR	Polymerase chain reaction
PFL	Pyruvate-formate lyase
POX	Pyruvate oxidase
PPC	Phosphoenolpyruvate carboxylase
PTA	Phosphotransacetylase
PTS	Phosphotransferase system
RFA	Renewable fuel association
rpm	Revolution per minute
RT-PCR	Real time PCR
SDS	Sodiumdodecyl sulfate
SSF	Simultaneoul saccharification and fermentation
TCA	Tricarboxylic acid cycle
Tn10	Transposable element containing tetracycline resistance gene

TPP	Thiamine pyrophosphate
UTP	Uridine-5'-triphosphate

Abstract of Dissertation Presented to the Graduate School
of the University of Florida in Partial Fulfillment of the
Requirements for the Degree of Doctor of Philosophy

METABOLIC ENGINEERING OF *Escherichia coli*
FOR ETHANOL PRODUCTION WITHOUT FOREIGN GENES

By

Youngnyun Kim

August 2007

Chair: K.T. Shanmugam

Major: Microbiology and Cell Science

Worldwide dependence on finite petroleum-based energy necessitates alternative energy sources that can be produced from renewable resources. A successful example of an alternative transportation fuel is bioethanol, produced by microorganisms, from corn starch that is blended with gasoline. However, corn, currently the main feedstock for bioethanol production, also occupies a significant role in human food and animal feed chains. As more corn is diverted to bioethanol, the cost of corn is expected to increase with an increase in the price of food, feed and ethanol. Using lignocellulosic biomass for ethanol production is considered to resolve this problem. However, this requires a microbial biocatalyst that can ferment hexoses and pentoses to ethanol. *Escherichia coli* is an efficient biocatalyst that can use all the monomeric sugars in lignocellulose, and recombinant derivatives of *E. coli* have been engineered to produce ethanol as the major fermentation product. In my study, ethanologenic *E. coli* strains were isolated from a *ldhA*-, *pflB*- derivative without introduction of foreign genes. These isolates grew anaerobically and produced ethanol as the main fermentation product. The mutation responsible for anaerobic growth and ethanol production was mapped in the *lpdA* gene and the mutation was identified as E354K in three of the isolates tested. Another three isolates carried an *lpdA* mutation, H352Y. Enzyme kinetic studies revealed that the mutated form of the dihydrolipoamide dehydrogenase

(LPD) encoded by the *lpdA* was significantly less sensitive to NADH inhibition than the native LPD. This reduced NADH sensitivity of the mutated LPD was translated into lower sensitivity to NADH of the pyruvate dehydrogenase complex in strain SE2378. The net yield of 4 moles of NADH and 2 moles of acetyl-CoA per mole of glucose produced by a combination of glycolysis and PDH provided a logical basis to explain the production of 2 moles of ethanol per glucose.

The development of *E. coli* provides a potential biocatalyst for conversion of pentoses derived from cellulosic biomass to biobased products without the introduction of new genes.

CHAPTER 1 LITERATURE REVIEW

Production of Bioethanol

Human society is sustained at present by petroleum-based energy, although this fossil-based energy is limited. The proven amount of oil reserves worldwide that can be extracted with existing technology is about 1.3 trillion barrels (EIA, DOE). Taking current annual oil production and consumption of about 30 billion barrels into consideration, this oil reserve will be exhausted in approximately 40 years. Other estimates of about 6 trillion barrels of oil reserves include estimates of potentially recoverable oil and require improvements in oil recovery. If all of these oil deposits, including unconventional oil reserves, can be economically tapped, the world-wide reserve can supply enough petroleum for about 240 years at current rate of use (47, 74, 141). The growth and increase in economy worldwide is expected to accelerate this rate of depletion of petroleum. United States (as of 2005) consumes each year approximately 30 % of total oil produced in the world (about 30 billion barrels per year) of which 60% is imported (13, 45). Of this total, more than 120 billion gallons of gasoline was consumed as automotive fuels. This equals the net import of petroleum (45, 74). Since the portion of automotive fuel in overall petroleum consumption is significant, alternative resources of fuels for automotive vehicles have received great attention (27, 40, 45, 54, 74, 100, 125, 132).

Ethanol has been recognized as one of the immediate and feasible alternative transportation energy source due to a number of advantages. Most of all, unlike petroleum-based fuels, ethanol can be produced in a renewable manner from biomass that can be produced continuously in large amounts (101). In the U.S., energy production from renewable biomass can potentially lead to as much as a 30 % reduction in gasoline use (45, 101). Ethanol that can be produced from biomass locally also reduces dependence on imported fuels (74). Since biomass is synthesized by

photosynthesis consuming CO₂ from the air, biomass-based fuel is a closed loop with no net CO₂ release into the atmosphere, mitigating the greenhouse effect of petroleum use. In addition, NO₂ emitted from combustion of petroleum-based fuels can be reduced by the use of ethanol due to its 35% oxygen content (5, 142) which also improves air quality. Eventually, as in the U.S., consideration on environment and fuel independence will encourage world-wide development of alternative clean energy sources (40, 54, 60-62, 100, 132). With these advantages of ethanol as a transportation fuel, ethanol production in the US is expanding and in 2006, fuel ethanol production has reached close to 5 billion gallons. With the corn to ethanol plants under construction, this capacity is expected to increase to over 12 billion gallons per year in the immediate future (45).

As mentioned above, one of the most favorable and critical points in ethanol production is the capability of using biomass. Solar energy is the fundamental energy source supporting almost all living organisms on earth and is mainly stored as biomass. This biomass is produced in a renewable manner and only a fraction of this biomass, corn starch, is currently used to produce ethanol. Fermentation of corn starch accounts for > 93 % of the total ethanol production in US while petroleum-based chemical synthesis accounts for < 7 % (13, 45, 74). Using corn, an important food and feed source, as a feedstock for ethanol production is expected to lead to relatively high cost of ethanol production due to the limitation in the availability of corn and expanding corn starch based ethanol industry (13, 54). An increase in ethanol production in the future will require more corn to be diverted away from food and feed requirements with further increase in the price of other commodities. This necessitates the need for alternate feedstock that does not compete with food and feed sources, such as lignocellulose, for ethanol fermentation (45, 74, 78, 125).

Lignocellulose is a complex substrate composed of cellulose (20 to 50 %), hemicellulose (20 to 40 %), lignin (10 to 20 %) and others (2 to 20 %) (45, 125). Among the components of lignocellulose, cellulose, a β -1,4-glucose linear polymer, is formed as a ribbon structure into fibers. The hydrogen bonding between cellulose ribbons results in insoluble and anhydrous crystalline structure. This structural complexity prevents ready access to cellulases toward hydrolysis of the polymer, resulting in the need for higher level of enzymes or chemical pretreatments to hydrolyze cellulose into glucose before fermentation to ethanol (5, 60). Unlike cellulose, hemicellulose is composed of heterogeneous polymers of pentoses, hexoses and sugar acids (60-62). The high concentration of pentoses in hemicellulose is another obstacle for ethanol production, because none of the traditional industrial microbial biocatalysts used for ethanol production ferments pentoses (12, 60-62, 74).

Thus, converting lignocellulosic biomass to fermentable sugars and to ethanol is the most challenging part in utilizing this feedstock. Isolating microorganisms capable of fermenting all the sugars present in lignocellulosic materials has been one of the main issues in achieving the goal of maximizing ethanol production (12, 45, 60, 62, 74).

Microbial Biocatalysts for Ethanol Production

Historically yeast has been utilized to produce various fermentation products for human use historically and technology for fermentation with yeast is well established (74, 131). In addition to these technical and historical advantages, genetic and metabolic engineering enabled yeast to become a major microbial biocatalyst for ethanol production as well as other useful fermentation products such as xylitol (12, 88, 131). Since most yeasts do not ferment xylose, the second most abundant saccharide in the hemicellulose component in biomass, one of the main issues of ethanol production research with using yeast has been the isolation and construction of

pentose fermenting yeast. Although *Pichia stipitis* and *Candida tropicalis* ferment xylose, these microbes have several critical problems such as low ethanol production yield with xylose (45, 62, 63), inability to ferment arabinose (45, 65), and an oxygen requirement for growth (39, 128). In spite of the successful introduction of genes for xylose metabolism such as the ones encoding xylose reductase and xylitol dehydrogenase from *Pichia stipitis* into *Saccharomyces*, the recombinant strain still produces low ethanol yield from xylose and low growth rate on xylose due to cofactor imbalance compared to glucose (3, 70, 115). Although introduction of heterologous xylose isomerase into *Saccharomyces* helped overcome cofactor imbalance, this did not improve ethanol yield from xylose (67). Despite improvement in expanding the range of fermentable carbohydrates in yeast (36, 39, 48, 126, 135), the problems caused by genetic engineering, such as differences in internal pH between bacteria and yeasts, unsuitable protein folding, incorrect post-translational modification, low ethanol yield, and low specific growth rate, have hampered the development of yeast as efficient biocatalysts for fuel ethanol production from lignocellulosic biomass, especially the hemicellulose component (38, 39, 65, 88, 94).

Zymomonas mobilis that metabolizes sugars by Entner-Doudoroff pathway is another extensively studied traditional microorganism in ethanol production, with its several advantages, such as homo-ethanol fermentation, high ethanol production yield (up to 120 g/l), high ethanol tolerance and high specific ethanol productivity (85, 104, 121). In spite of these attractive points, limited ability of sugar utilization by *Z. mobilis* has restricted use of this bacterium by the ethanol industry. Therefore, like yeast, genetic engineering of *Z. mobilis* to improve its ability to metabolize all the sugars in biomass is in progress (32, 35, 143). The recombinant *Z. mobilis* strains that can ferment xylose or arabinose require long fermentation times, despite high ethanol yield (12, 35, 74). As seen with yeast and *Z. mobilis*, expanding the substrate range of traditional

microbial biocatalysts for optimal ethanol production at industrial scale using lignocellulosic biomass as the feedstock is still one of the main challenges (64).

While none of the traditional yeast or ethanologenic bacteria metabolizes both pentoses and hexoses (57, 61, 74), enteric bacteria, such as *Escherichia coli*, can use all of these sugars as carbon sources (12, 60). *E. coli* is used as a work horse by the industry to produce various products because genetic systems as well as physiological aspects of *E. coli* are well established (8, 44, 118, 137). However, despite these advantages, mixed acid production by fermenting *E. coli* is a hurdle to overcome towards developing a recombinant strain for homo-ethanol fermentation (18, 22, 23, 61, 129).

Genetic engineering of *E. coli* resulted in development of *E. coli* strain KO11, a most promising ethanol producer that ferments all the sugars in lignocellulosic biomass to high yield of ethanol. The pyruvate decarboxylase gene (*pdh*) and alcohol dehydrogenase gene (*adhB*) from *Z. mobilis* were combined into a portable ethanol operon cassette (103) and integrated into the chromosomal DNA of *E. coli* in the construction of strain KO11 (61, 93). This genetic modification was able to draw all the advantages from *E. coli* and *Z. mobilis* and provided an efficient metabolic route for converting pyruvate into ethanol. However, lower ethanol tolerance and specific productivity by *E. coli* compared to *Z. mobilis* are being addressed. Enteric bacteria other than *E. coli* with additional beneficial characteristics have also been investigated for ethanol production. Integrating the PET operon into *Klebsiella oxytoca* enabled a genetically engineered biocatalyst (strain P2) that metabolizes cellobiose and cellotriose, hydrolysis products of cellulose, in addition to fermenting monomeric sugars (89). The best performance obtained using recombinant *K. oxytoca* strain P2 resulted in successful fermentation of glucose or cellobiose to a yield of 45 g/l ethanol within 48 hours (140). When partially hydrolyzed cellulose

was used as a feedstock to utilize the ability of *K. oxytoca* to ferment cellobiose, the recombinant *K. oxytoca* strain P2 produced 38.6 g/l ethanol, indicating a potential to reduce the cost of cellulase supplement in a simultaneous saccharification and fermentation (SSF) process (140). Another approach towards developing a microbial biocatalyst to reduce the cost of SSF was to integrate the genes encoding endoglucanase, a component of cellulase mixtures, into an appropriate host such as *K. oxytoca* strain P2. Two extracellular endoglucanase genes, *celZ* and *celY*, from *Erwinia chrysanthemi*, were integrated into *K. oxytoca* P2 chromosomal DNA (strain SZ21) and cellulase exporter (*out*) genes were also introduced into this construct with a plasmid (pCPP2006) (144, 145). In SSF of highly crystalline cellulose, Sigmacell 50, with a fixed amount of cellulase Spezyme CP or CE, the ethanol yield was higher with strain SZ21 (pCPP2006) as the microbial biocatalyst than that from the parent strain without the *cel* and *out* genes (144). Overall, comparison among biocatalysts developed for ethanol production mentioned above, *E. coli* KO11 and its derivative (LY01) obtained after long-term adaptation for higher ethanol tolerance produced more ethanol in shorter fermentation time than any other biocatalyst, especially on high xylose concentration (140 g L⁻¹) (60, 62, 144).

Native Fermentation Profile, Mixed Acid Fermentation, of *E. coli*

Escherichia coli, one of the most studied microorganisms, has mixed acid fermentation as the main fermentation pathway (22) (Figure 1-1). End products of fermentation are a mixture of lactic acid, acetic acid, formic acid, succinic acid and ethanol, with the possibility of gas formation from formate (CO₂ and H₂) (6, 7, 87). The pathways to these products diverge mostly from pyruvate produced by glycolysis from sugars (22, 92). Pyruvate is converted into either lactic acid by lactate dehydrogenase (LDH) (9, 22, 68) or acetyl-CoA and formate by pyruvate formate-lyase (PFL) (22, 69). Acetyl-CoA is subsequently converted to equimolar amounts of acetic acid and ethanol (22). Acetic acid production is carried out by phosphotransacetylase

(PTA) and acetate kinase (101) (22, 73) and ethanol is produced via acetaldehyde by alcohol dehydrogenase (ADH) (21, 22, 42). In addition, phosphoenolpyruvate carboxylase and malate dehydrogenase, fumarase and fumarate reductase lead to succinic acid from the oxaloacetate generated from phosphoenolpyruvate (22, 83). This divergence of pyruvate metabolism into these products functions to meet both the energy requirement (22) and redox balance depending upon growth condition. Thus, in order to maximize the flux from sugar to ethanol, the carbon flux to other fermentation products should be lowered or blocked while also maintaining redox balance and producing enough energy to support cell growth under a given condition.

The Importance of Redox Balance

As a facultative anaerobe, *Escherichia coli* grows under both aerobic and anaerobic conditions. One of the key issues in *E. coli* growth is to maintain redox balance (NADH/NAD⁺) in metabolism because some of the metabolic pathways proceed with oxidation-reduction coupled reactions (2, 22). During glycolysis, when glyceraldehyde-3-phosphate is oxidized into 1,3-bisphosphoglycerate, 1 mol of NAD⁺ is reduced to NADH with an introduction of 1 mol of inorganic phosphate (55). This is one of the important steps in the generation of ATP by substrate-level phosphorylation (10, 24, 90). Since this oxidation step requires NAD⁺ as a substrate, and the 1,3-bisphosphoglycerate leads to ATP production, maintaining the level of NAD⁺ pool is crucial for glycolysis of sugars to pyruvate. Under aerobic conditions, *E. coli* maintains its redox balance via respiratory electron transport systems (ETS) that oxidize NADH produced from glycolysis and TCA cycle, where O₂, as the terminal electron acceptor, is eventually reduced to H₂O (22, 59). Proton motive force generated when NADH is re-oxidized by the ETS is linked to ATP production by ATP synthase (33, 133, 134). However, under fermentative conditions in the absence of external electron acceptors, the cell maintains the redox

balance by producing fermentation products such as lactate and ethanol, due to the nature of the system (Figure 1-1) (22).

Metabolism of Pyruvate

Pyruvate is the key intermediate in the catabolic pathways of *E. coli* (58, 107), regardless of growth condition. Under aerobic conditions, the major catabolic pathway from pyruvate is the oxidative decarboxylation of pyruvate to acetyl-CoA and CO₂ with reduction of NAD⁺ to NADH catalyzed by pyruvate dehydrogenase (PDH) (22, 99, 136) (Figure 1-2). The PDH complex is active *in vivo* only under aerobic growth condition and is induced by pyruvate. However, despite the expression of PDH under anaerobic conditions, the activity of the PDH complex is inhibited during fermentative growth (17, 37, 46, 51, 122-124). The PDH complex consists of 3 subunits that are pyruvate dehydrogenase / decarboxylase (E1), dihydrolipoamide acetyltransferase (E2), and dihydrolipoamide dehydrogenase (E3; LPD), encoded by the *aceE*, *aceF* and *lpd* genes, respectively (99). The expression of *aceEF-lpd* genes is controlled at the transcriptional level by PdhR encoded by *pdhR* gene that is promoter proximal of the *pdhR-aceEF-lpd* operon (*pdh* operon) (98). In the absence of pyruvate, PdhR binds to the operator region of *pdhR* gene inhibiting transcription of the *pdhR-aceEF-lpd* genes (51) (Figure 1-3). The *lpd* is also expressed independently, since LPD is shared with 2-oxoglutarate dehydrogenase. The link between dihydrolipoamide dehydrogenase and 2-oxoglutarate dehydrogenase is co-regulation at the transcriptional level primarily by ArcA (26, 99, 120). Acetyl-CoA produced by PDH is oxidized by the enzymes of the TCA cycle and subsequently the NADH is oxidized by respiratory ETS (59, 83, 113).

During anaerobic growth, pyruvate formate-lyase (PFL) encoded by *pflB* takes over the role of PDH in pyruvate metabolism converting pyruvate to acetyl-CoA and formate (69, 109, 110). Subsequently, acetyl-CoA produced from pyruvate is converted to acetate by

phosphotransacetylase (PTA) encoded by *pta* and acetate kinase (101) encoded by *ackA* or reduced to ethanol by alcohol dehydrogenase (ADH) encoded by *adhE* (Figure 1-1) (22). The 2 moles of NADH produced during glycolysis per mole of glucose are used to reduce one mole of acetyl-CoA to one mole of ethanol to maintain the redox balance. The other acetyl-CoA from the pyruvate is converted to acetate generating one additional ATP at the acetate kinase step to increase the net ATP yield /glucose to 3.0 (50). Thus, the expected ratio between ethanol and acetate production is 1 (22). In addition to the *pflB* gene, *E. coli* genome also has a second putative pyruvate formate-lyase encoded by the *pflCD* genes. However, this is a silent operon and deleting the *pflCD* genes has no effect on the PFL activity of the cell (146).

The second pathway branching from pyruvate under fermentative condition that enables NAD^+ to be regenerated is that of lactate production (Figure 1-1). When 1 mol of pyruvate is converted into 1 mol of lactate by lactate dehydrogenase (LDH) encoded by *ldhA*, NADH is oxidized to NAD^+ . Thus, lactate production alone is sufficient to maintain the redox balance to support cell growth under fermentative conditions (9, 15, 22, 23).

Another metabolic pathway originating from pyruvate is direct oxidation to acetate by pyruvate oxidase (Pox) encoded by the *poxAB* genes (1, 19, 20). PoxB, a membrane-bound flavoprotein, catalyzes decarboxylation of pyruvate to acetate with the reduction of an enzyme-bound flavin adenine dinucleotide, FAD. The *poxA* gene product plays a regulatory role in the expression of *poxB* (130). The *pox* genes are primarily induced at the transient phase from the exponential to the stationary phase of growth since the transcription of *poxB* is dependent on stationary phase sigma factor (*rpoS*) (20). Since pyruvate oxidase is induced during the stationary phase of growth, the phenotype of a mutant lacking PDH activity is acetate-dependence for aerobic growth in glucose mineral salts medium. Although Pox is also expressed

and active during anaerobic growth, its level of expression is lower than that of aerobic conditions.

Phosphoenolpyruvate (PEP) is an intermediate immediately preceding pyruvate during glycolysis (22, 107). Therefore, a catabolic pathway branching from PEP should also be considered as a branch of pyruvate during glucose fermentation. PEP is converted to small amount of succinate in sequential reactions (22, 66, 119) catalyzed by phosphoenolpyruvate carboxylase, malate dehydrogenase, fumarase, and fumarate reductase (22). During this production of succinate, malate dehydrogenase oxidizes 1 NADH to 1 NAD⁺. Reduction of fumarate to succinate utilizes a second reductant. Hence, 2 NADHs produced during glycolysis of glucose to 2 PEP can be oxidized in this route. However, since 1 PEP is consumed to transport glucose into a cell through the phosphotransferase system (PTS), only one PEP is available for succinate production. Purified fumarate reductase failed to use NADH as an electron donor suggesting that in vivo the fumarate reductase utilizes some other form of reductant other than NADH (119). This shortage of PEP combined with the lack of NADH use by fumarate reductase prevents the cell from maintaining redox balance by the succinate production pathway alone. Succinyl-CoA required as a precursor for amino acid synthesis (81) is made from either succinate or α -ketoglutarate by α -ketoglutarate dehydrogenase (α -KGDH). Under fermentative conditions, expression of α -KGDH, encoded by *sucAB*, is negatively regulated by ArcAB and Fnr proteins (95) so that the complete TCA cycle is interrupted at the α -ketoglutarate dehydrogenase step although a basal amount of α -KGDH is maintained to produce succinyl-CoA for growth (22). Based on these results and the observation that a fumarate reductase minus mutant of *E. coli* does not require succinate implies that succinate production for growth of *E. coli* under anaerobic conditions can be accomplished by alternate pathways (25). Consumption

of one PEP for transport of glucose by PTS and the second for succinate production affects not only the redox balance, but also ATP production (86) because the net ATP production under these conditions is only 1 mole of ATP per mole of glucose (97). Unless another non-ATP (PEP)-dependent glucose transport system is used, such as transportation by galactose permease (GalP) (52, 53), the succinate production pathway is not the main pathway to re-oxidize NADH, due to the shortage of PEP and energetic constraints.

Based on the metabolic fates of pyruvate reviewed above, lactate production (LDH) and ethanol production (ADH) pathways play key roles in maintaining redox balance under fermentative conditions. When both *ldh* and *pfl* genes are deleted, although all the downstream enzymes (ADH and ACK) are present, *E. coli* can not grow anaerobically due to a decrease in the NAD⁺ pool.

Pyruvate Dehydrogenase (PDH) Complex

The structural ratio among each component of the pyruvate dehydrogenase complex, a multimeric protein of 4.6 MDa, is 24:24:12 (E1:E2:E3), respectively (116). Structural modeling and reconstitution of the pyruvate dehydrogenase complex revealed that dihydrolipoamide transacetylase (E2) plays a central role in forming a multi-subunit complex with enzymatic activity (103, 108). The dimer form of pyruvate dehydrogenase/decarboxylase (E1) with a molecular mass of 199 KDa is noncovalently bound to E2 (34). The E1 catalyses oxidative decarboxylation of pyruvate leading to acyl-TPP (thiamine pyrophosphate) (28). The acyl group is transferred to CoA by E2, yielding acetyl-CoA. Dihydrolipoamide dehydrogenase (LPD; E3) reducing NAD⁺ to NADH as a terminal enzymatic subunit in PDH is also homodimeric containing 2 moles of FAD per dimer (103). FAD insertion is critical in forming non-covalent assembly of PDH and activity (75) (Figure 1-4).

In addition to the regulation at the transcription level by PdhR depending on the presence of pyruvate, the activity of PDH is also regulated at the enzyme level (16, 17, 117). Glycolytic intermediates, such as fructose-6-phosphate, fructose-1,6-diphosphate, and 3-phosphoglycerate, positively regulate PDH activity (114). The enzyme level is inhibited by acetyl-CoA in a competitive manner (112, 114). In contrast to acetyl-CoA, GTP regulates PDH activity noncompetitively (112). ATP, CTP, and UTP have no effect on PDH activity. The inhibition by GTP is reversed by GMP and GDP (112). Since the acetyl-CoA produced by PDH is a key precursor entering the TCA cycle leading to production of NADH and energy through the electron transport system, maintaining a higher energy state may be the main reason to negatively regulate PDH activity (112, 114). The activity of PDH is also partially inhibited by glucose, acetate, and TCA cycle intermediates. A *lacZ* fusion study showed that the intracellular ratio between NADH and NAD⁺ (NADH/NAD⁺) has a significant effect on PDH level (17) and activity (114). In particular, the expression or activity of LPD seems to be highly sensitive to NADH levels (105, 138). Under anaerobic conditions, the NADH/NAD⁺ ratio (0.34) is several fold higher than found for growth under aerobic conditions (0.19) (aerobic:anaerobic::0.19:0.34) (49). Values demonstrating an even greater difference were also recently reported by Snoep *et al.* (aerobic:anaerobic::0.03:0.70)(121). This sensitivity of LPD to NADH inhibition makes PDH inactive during fermentative growth due to the higher NADH pool and is probably another regulatory mechanism of this critical enzyme. Finally, while mammalian PDH is also regulated by phosphorylation of the E1 component, there is no evidence of phosphorylation of PDH in *E. coli* and other bacteria (102).

Ethanologenic *Escherichia coli*

Ethanol is one of the most promising candidates as a transportation energy source in the near future. For ethanol to replace petroleum as the fuel of choice, ethanol production by

fermentation should be cost effective. As indicated above, fermentation of renewable biomass is the best way to produce ethanol in terms of substrate cost. Based on composition of biomass, the ability of microorganisms to ferment various carbohydrates present in biomass is one of the key factors. In addition to substrate range, appropriate metabolic pathways to maximize ethanol production yield is an important requirement for developing cost effective microbial biocatalysts for ethanol fermentation. In this connection, strain KO11 and other enteric recombinant biocatalysts fulfill the need for a robust biocatalyst that can metabolize all the sugars present in a variety of feedstocks. The presence of *Z. mobilis* genes in *E. coli* strain KO11 and other enteric microbial biocatalysts has led to reluctance in wider use of these ethanologens at an industrial scale. Despite the development of significant new microbial biocatalysts for fermentation of multiple sugars to ethanol, none of the reported microorganisms (yeast, *Z. mobilis*, enteric bacteria) was engineered without the introduction of foreign gene(s). Is it possible to construct a microbial biocatalyst that ferments all the sugars in biomass to ethanol that also lacks foreign gene input? As mentioned earlier, based on the ability to utilize carbohydrates from various sources, enteric bacteria provide the best platform for further engineering for production of a multitude of compounds. *E. coli* is the ideal organism of choice to address this challenge since this organism already has the metabolic versatility to ferment all the sugars of biomass and also produces ethanol during fermentation, although as a minor product.

Towards construction of a microbial biocatalyst lacking foreign genes, production of lactate, acetate and formate produced during fermentation by *E. coli*, must be eliminated. Lactate production and ethanol/acetate production steps are redundant for redox balance maintenance and the lactate pathway can be deleted without a detrimental effect on growth. In an *ldhA* mutant, ethanol production is the only way for the cell to maintain redox balance and removal of this

pathway by deleting the *pflB* gene, whose product generates acetyl-CoA used for ethanol production prevents growth of the organism (22). Although PDH has the ability to produce the required acetyl-CoA and the needed second NADH per acetyl-CoA generated, this enzyme is inactive in the anaerobic cell due to its inhibition by NADH. An altered form of PDH that is less sensitive to NADH can support fermentation of sugars to ethanol (Figure 1-5). However, a price for utilizing this pathway would be the loss of an ATP per glucose that could reduce the growth rate of the bacterium. A net ATP yield of two per glucose may not be that critical for the growth of *E. coli* with glucose (50).

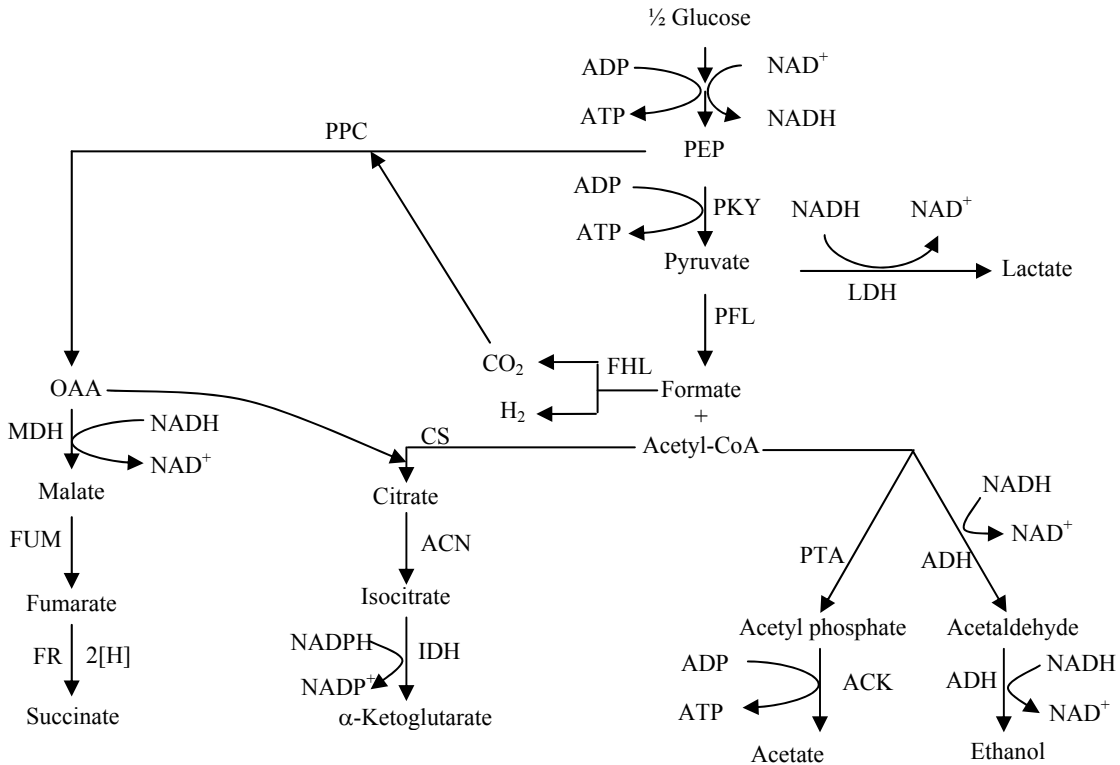


Figure 1-1. Mixed acid fermentation pathways of *E. coli*.

PPC: phosphoenolpyruvate carboxylase, PKY: pyruvate kinase, LDH: lactate dehydrogenase, PFL: pyruvate formate-lyase, FHL: formate hydrogen-lyase, PTA: phosphotransacetylase, ACK: acetate kinase, ADH: alcohol dehydrogenase, MDH: malate dehydrogenase, FUM: fumarase, FR: fumarate reductase, CS: citrate synthase, ACN: aconitase, IDH: isocitrate dehydrogenase.

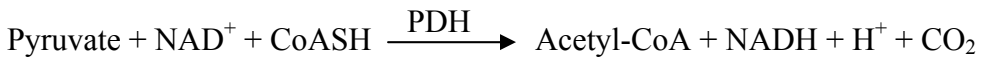


Figure 1-2. Overall reaction catalyzed by the pyruvate dehydrogenase complex.

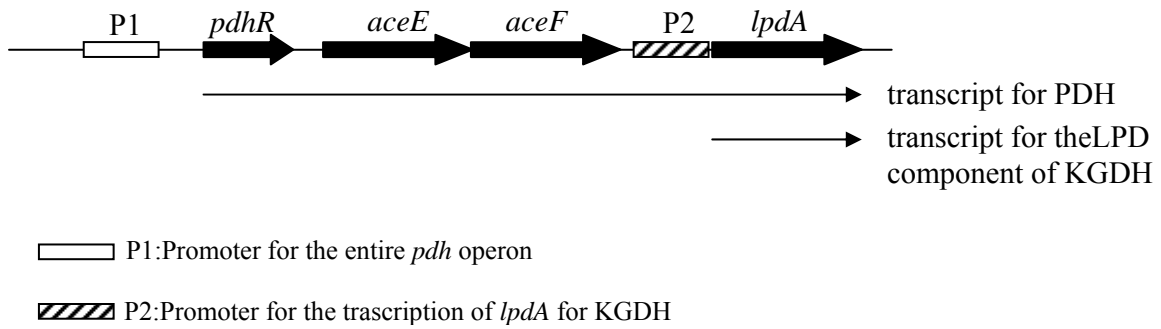


Figure 1-3. Genetic organization of the *pdh* operon.

pdhR : regulator gene, *aceE* : pyruvate decarboxylase, *aceF* : dihydrolipoamide acetyltransferase, *lpdA* : dihydrolipoamide dehydrogenase, KGDH : α -ketoglutarate dehydrogenase.

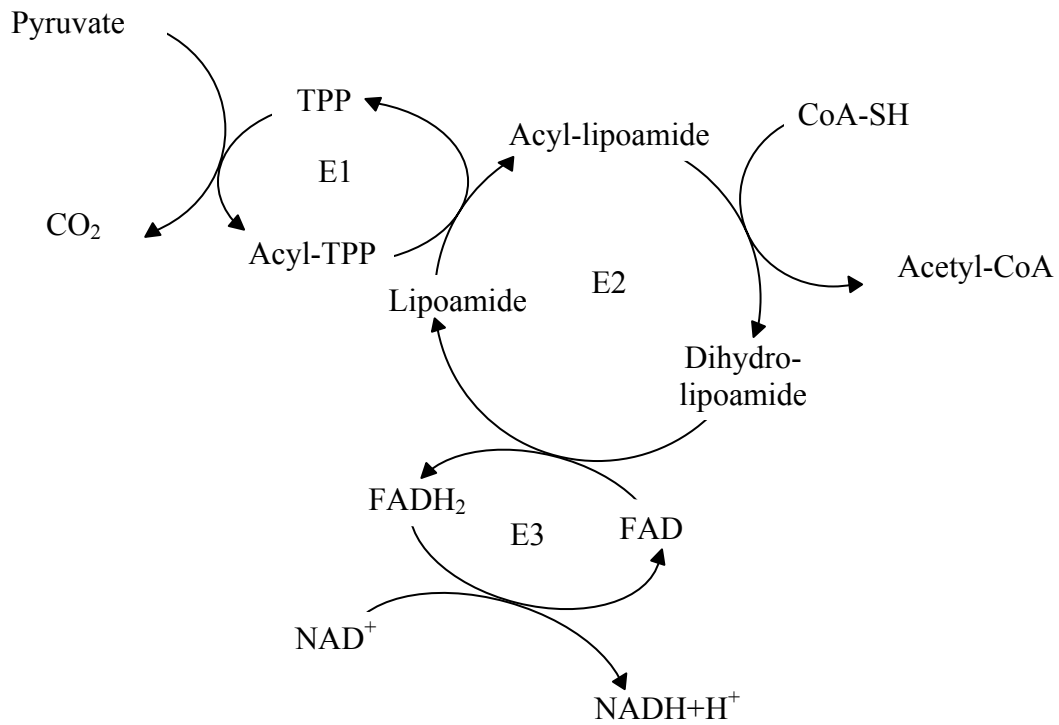


Figure 1-4. Enzyme reaction diagram of the pyruvate dehydrogenase(PDH) complex.
 TPP: thiamine pyrophosphate, E1: pyruvate decarboxylase/dehydrogenase, E2:
 dihydrolipoamide acetyltransferase, E3: dihydrolipoamide dehydrogenase.

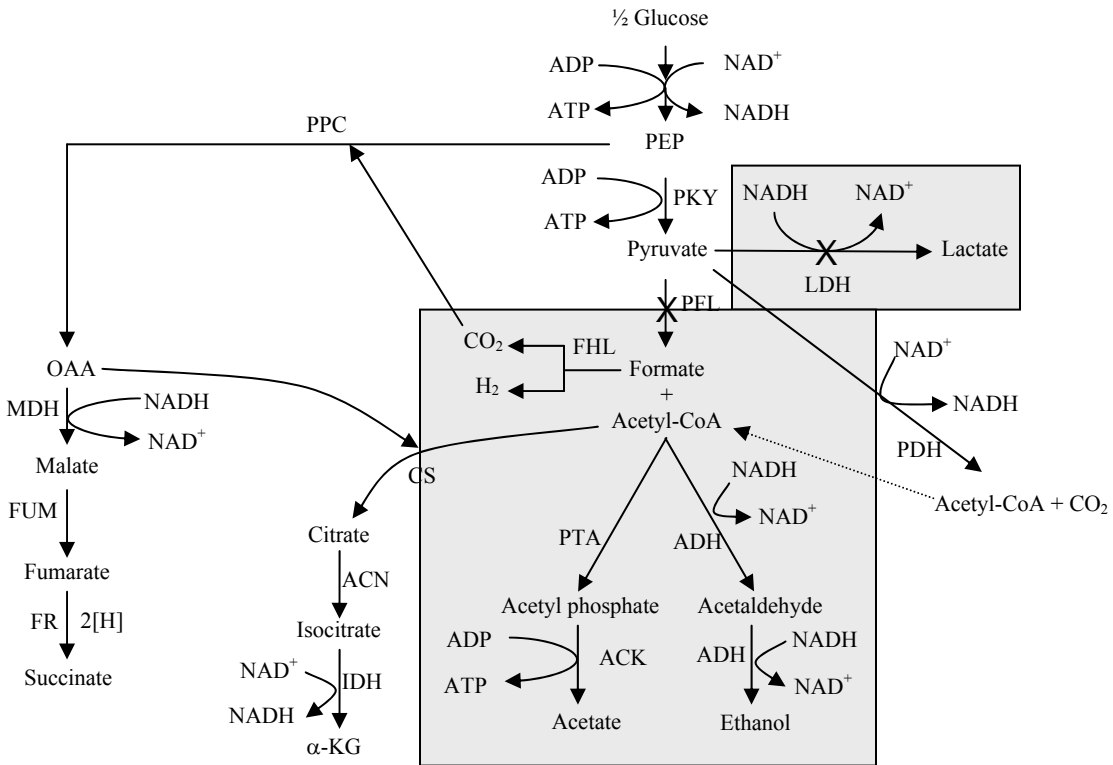


Figure 1-5. Elimination of lactate and formate production in the mixed acid fermentation pathway of *E. coli*. PKY: pyruvate kinase, PPC: phosphoenolpyruvate carboxylase, MDH: malate dehydrogenase, FUM: fumarase, FR: fumarate reductase, LDH: lactate dehydrogenase, PFL: pyruvate-formate lyase, FHL: formate-hydrogen lyase, PTA: phosphotransacetylase, ACK: acetate kinase, ADH: alcohol dehydrogenase, CS: citrate synthase, ACN: aconitase, IDH: isocitrate dehydrogenase, PDH: pyruvate dehydrogenase.

CHAPTER 2 MATERIALS AND METHODS

Materials

Biochemicals were purchased from Sigma-Aldrich Chemicals Co. Organic and inorganic chemicals were purchased from Fisher Scientific Co. and were analytical grade. DNA restriction endonucleases, T4 DNA ligase and DNA polymerases were obtained from New England Biolabs Inc., Invitrogen or Clontech Laboratories. Real-time PCR reagents were from Bio-Rad Laboratories, Inc. Plasmid extraction and DNA gel-extraction kits were from Qiagen Inc.

Media and Growth Conditions

Luria broth was prepared as described previously (96). Glucose-minimal medium contained Na_2HPO_4 (6.25 g), KH_2PO_4 (0.75 g), NaCl (2.0 g), $\text{FeSO}_4 \cdot 7\text{H}_2\text{O}$ (10 mg), $\text{Na}_2\text{MoO}_4 \cdot 2\text{H}_2\text{O}$ (10 mg), $\text{MgSO}_4 \cdot 7\text{H}_2\text{O}$ (0.2 g), and $(\text{NH}_4)_2\text{SO}_4$ (1 g) in 1 L of deionized water. Sugars were added after autoclaving the medium at a final concentration of glucose at $3 \text{ g} \cdot \text{L}^{-1}$ for aerobic growth and $10 \text{ g} \cdot \text{L}^{-1}$ for anaerobic growth. Aerobic liquid cultures were grown in a shaker at 200 RPM and routine anaerobic cultures were grown in screw-cap tubes filled to the top and incubated without mixing. Solid medium was prepared by the addition of agar ($15 \text{ g} \cdot \text{L}^{-1}$) into liquid medium. Top-agar for growing phage contained 0.7 % agar instead of 1.5 %. Media used for propagation of phage P1, λ and transduction were as per Miller (84).

Gene Deletions

Construction of gene disruption in *E. coli* was as described by Datsenko *et al.* (29). Genes disrupted were amplified by PCR and cloned into TOPO pCR2.1 plasmid vector (Invitrogen). After removal of the gene, a DNA cassette containing kanamycin-resistance gene, flanked by FRT sequences, was integrated into the deleted area. The antibiotic resistance gene with the flanking *E. coli* DNA was PCR-amplified and the PCR product was transformed into *E. coli*

strain BW25113 (pKD46) that was pre-grown in LB+arabinose (0.3% w/v) to O.D. 0.6 at 420 nm. Transformants with the deletion were selected on the corresponding antibiotic markers and the deletion was verified by PCR with the primers flanking the antibiotic marker gene inserted in the deleted gene. The deletion mutation was transduced by phage P1 to other genetic backgrounds before use (84).

Transformation

Chemical transformation was carried out as described previously with minor modification (79). Cells inoculated from an overnight culture (0.1 ml) were grown in a 125 ml flask containing 5 ml LB medium at 37 °C for about 1.5 hours. After harvest by centrifugation at room temperature (1,200 x g; 5 min), cells were resuspended in 0.5 ml of cold 0.1 M CaCl₂. Plasmid DNA was added to 0.2 ml of the cell suspension and the cell-DNA mixture was incubated on ice for 20 min. After heat-shock (1 min, 42 °C), the mixture was incubated on ice for an additional 5 min. One ml of LB was added to the reaction mixture and incubated for 2 hours at 37 °C, standing. Transformants were selected on appropriate antibiotic medium. Electroporation of cells for plasmid transformation was as recommended by Bio-Rad (MicroPulser electroporation apparatus operating instructions and applications guide).

Co-transduction Frequency

Co-transduction frequency of two genes was calculated by a formula described by Sanderson et al (106) (Eqn. 2-1).

$$C = 1 - [d / L]^3 \quad (\text{Eqn. 2-1})$$

C, cotransduction frequency; d, distance between the two genes; L, size of the DNA fragment transferred (usually the average DNA size packaged by phage P1; about 95 kbp).

Sequencing DNA

Nucleotide sequence of DNA was determined by the Interdisciplinary Center for Biotechnology Research, DNA Sequencing Core Facility at the University of Florida. Invitrogen and Sigma-Genosys synthesized oligonucleotide primers used for sequencing and the primers are listed in Table 2-2.

Determination of the level of transcription of *pdh* operon

Construction of λ *Ppdh-lac*

The promoter DNA with operator corresponding to the *pdh* operon (-326 to -15 of the *pdhR* with the “A” in the start codon ‘ATG’ as +1) was prepared by digestion of the DNA from plasmids pKY10 (SE2378 *Ppdh*) and pKY13 (W3110 *Ppdh*) with BlnI and AflII endonucleases. Ends of the digested DNA products were filled in by Klenow-fragment of DNA polymerase and cloned into SmaI restriction site of plasmid pTL61t (77), 208 base pairs upstream of promoterless *lacZ* gene. The plasmid constructs (pKY15 for SE2378 *Ppdh* and pKY17 for W3110 *Ppdh*) were selected after transformation of *E. coli* Top10 as blue colonies on LB-ampicillin medium with X-Gal (5-bromo-4-chloro-3-indolyl- β -D-galactopyranoside, 40 $\mu\text{g}\cdot\text{ml}^{-1}$). The cloned *pdh* promoter DNA was sequenced to confirm the sequence. The plasmid constructs were transformed into strain LE392, and the transformants were grown in LB+maltose (0.3 %). Strain LE392 with plasmid was infected with λ RZ5, mixed with 2.0 ml of top-agar and poured as an overlay over LB-agar. Phage was propagated, at 37 °C for about 6 hours, collected and stored for further studies.

Transduction

An overnight culture of strain SE2366 was inoculated (1% v/v) into 3 ml of LB+ maltose in a 125 ml flask and incubated in a shaker (200 RPM) for about 2 hrs. Cells from 1 ml of the culture were harvested by centrifugation at room temperature and resuspended in 0.4 ml of 10

mM MgSO₄. Five µl of phage stock (0.2 of MOI) was added to 0.2 ml of the cell suspension and the mixture was incubated at room temperature for 20 min. MOI is the average number of phage per bacterium. After adding 1.8 ml of LB, the transduction mixture was incubated at 37 °C for 2 hours. Transductants were selected for resistance to ampicillin and blue color on LB-agar containing ampicillin and X-Gal. Transductants with the lowest β-galactosidase activity, presumptive single lysogens, were used in *pdh* operon transcription studies.

β-Galactosidase activity measurements

Transductants carrying $\lambda Ppdh-lac$ fusion were grown in LB+glucose under aerobic or anaerobic conditions for 4 hours. Cells were harvested by centrifugation, washed with 2.0 ml of cold Z-buffer (60 mM Na₂HPO₄·7H₂O, 40 mM NaH₂PO₄, 10 mM KCl, 1 mM MgSO₄·7H₂O, 50 mM β-mercaptoethanol, pH 7.0) and resuspended in 1.0 ml of Z-buffer. Optical density of culture was adjusted to 2.4 (420 nm; Beckman DU 640) in 1.0 ml as a final volume. To 1.0 ml of this cell suspension, 54 µl of chloroform and 27 µl of 0.1 % SDS was added. After the suspension was mixed for 10 seconds in a vortex mixer to permeabilize the cells for the substrate ONPG, the cells were kept on ice. Permeabilized cells (0.1 ml) were added to 0.9 ml of Z-buffer. Z-buffer (1.0 ml) only was used as a control. The tubes were placed in a water bath at 28 °C. After 2 min, 0.2 ml of ONPG (4 mg ml⁻¹) was added to each tube and incubation was continued until the appearance of yellow color. Sodium carbonate (1 M) solution (0.5 ml) was added to stop the reaction. For calculation of β-galactosidase activity, 2.4 O.D. units at 420 nm represented 350 µg protein ml⁻¹ and one nmole of O-nitrophenol ml⁻¹ had an absorbance of 0.0045 at 420 nm (1 cm light path). The specific activity of β-galactosidase was expressed as nmoles min⁻¹ mg cell protein⁻¹.

Quantitative RT-PCR

For isolation of total RNA from aerobic cultures, cells were grown in 10 ml of LB in a 250 ml flask at 37 °C with shaking at 200 RPM. For anaerobic cultures, cells were grown in 9 ml of LB medium in a 13x100 mm screw-cap tube filled to the top. Cells were harvested at early to mid exponential phase of growth. Total RNA was extracted by a hot phenol method (4). Isolated RNA was further processed with Qiagen RNA cleaning kit as per the Manufacturer's protocol. Treating with ribonuclease-free DNase (Sigma) removed contaminating DNA from the RNA.

Reverse transcription to generate cDNA was carried out as described previously (4) using a primer based on the *aceE* sequence (72 to 240 from A of start codon, ATG, within coding sequence). The 20 µl reaction mixture contained 4 µl of iScript reaction mix (5x), 1 µl of iScript reverse transcriptase, dH₂O and 2 µg RNA sample. The reaction was conducted at 25 °C for 5 min, at 42 °C for 30 min and at 85 °C for 5 min. Quantitative RT-PCR was carried out with SYBR-Green-490 as per the Manufacturer's instructions (Bio-Rad) with the *aceE* cDNA as the template and a set of *aceE* specific primers (forward primer, CATCCGTGAAGAAGGTGTTG; reverse primer, GCGTTCCAGTTCCAGATTAC). The PCR conditions were 3.5 min at 95 °C followed by 65 cycles of 30 sec at 95 °C, 50 sec at 55 °C, 20 sec at 72 °C.

in vitro DNA Mutagenesis

Hydroxylamine Mutagenesis

The *lpd*⁺ gene in plasmid pKY32, was mutagenized *in vitro* as described by Davis et. al. (30) with minor modification. A 200 µl reaction mixture containing 7.5 µg plasmid DNA (30 µl), 40 µl phosphate-EDTA buffer (0.5 M K-phosphate, pH 6.5; 5 mM EDTA), 80 µl of freshly prepared hydroxylamine-hydrochloride, pH 6.0 (1.0 M NH₂OH-HCl, 0.45 M NaOH) and 50 µl deionized H₂O was incubated at 37°C for 18 hours. DNA was purified by 3 successive phenol

extractions and 3 successive chloroform extractions. DNA was precipitated with 100 % ethanol and dissolved in dH₂O.

PCR Mutagenesis

The *lpd* gene was also mutagenized by error-prone PCR as described by Ichiro *et al.* (82) with plasmid pKY32 as the template. PCR reaction was conducted with the same primer set as used for cloning the *lpd* gene into plasmid pET15b. Mutagenic buffer contained 8 mM dTTP, 8 mM dCTP, 48 mM MgCl₂ and 5 mM MnCl₂ in addition to Taq DNA polymerase and its supplied buffer. PCR reaction was performed using the following cycle: 1 min at 95°C followed by 5 cycles of 1 min at 95 °C, 30 sec at 45 °C, 2 min at 72 °C followed by 30 cycles of 1 min at 95 °C, 30 sec at 55°C, 2 min at 72 °C, followed by 15 min at 72 °C. The PCR product was purified and stored at 4 °C.

Construction of pTrc99A-*lpd* for Regulated Expression of *lpd*

The *lpd* gene was amplified by PCR from the genomic DNA of *E. coli* wild type, strain W3110 or SE2378. The forward primer (5'-GCGACCATGGAGAAGGAGATATACCATGAGTACT-3') contained an NcoI restriction site at the 5' end (underlined), and the reverse primer (5'-GCGAAAGCTTTTACTTCTTCTTCGCTTTCG-3') contained a HindIII restriction site at 5' end (underlined). A Shine-Dalgarno sequence (ribosomal binding site) was located 10 nucleotides upstream of the start codon (ATG). Both the PCR product and plasmid pTrc99A were digested with NcoI and HindIII restriction enzymes and ligated together to construct plasmids pKY32 and pKY33 containing wild-type *lpd* and *lpd* gene with mutation, respectively (Figure 2-1). The cloned DNA sequence was verified by sequencing the DNA.

Construction of pET-15b- *lpd* Plasmid for Purification of LPD

The *lpd* gene was amplified by PCR with the forward priming oligonucleotide (5'-GAGCCTCGAGATGAGTACTGAAATC-3') and reverse priming oligonucleotide (5'-GCGTGGATCCTTACTTCTTCTTCG-3'). The forward primer contains XhoI restriction site at the 5' end and the reverse primer has BamHI restriction site at the 5' end. PCR product digested with XhoI and BamHI was ligated with plasmid pET-15b also digested with XhoI and BamHI (Figure 2-2). *E. coli* TOP10 competent cells were transformed with the ligation product and the transformants were selected for resistance to ampicillin on LB medium. The plasmid constructs (pKY36 with *lpd* from W3110 or pKY37 with the *lpd* from SE2378) were used for protein purification.

Expression of Dihydrolipoamide Dehydrogenase (LPD)

Dihydrolipoamide dehydrogenase (LPD) was produced in strain JM109(λ DE3) transformed with pKY36 or pKY37 encoding LPD. A 500 ml LB+ampicillin (100 μ g ml⁻¹) culture was grown at 37°C with shaking at 250 rpm in a 2.8 liter Fernbach flask to an O.D. of 0.6 at 420 nm (Beckman DU 640 spectrophotometer). The T7-RNA polymerase was induced by addition of arabinose (1.5 %) (91). After 4 hours of incubation at room temperature with shaking, cells were harvested by centrifugation (12,000 xg; 15 min; 4 °C), washed with 50 mM potassium phosphate buffer (pH 8.0) (Buffer A) and resuspended in 5 ml of the same buffer. Cells were passed through a French pressure cell at 20,000 psi. The crude extract was clarified by centrifugation (30,000 x g; 45 min), and the supernatant was filtered through a 0.22 μ m filter. The filtered protein solution was loaded onto a Hi Trap chelating column (5 ml; General Electric) that was pre-washed with 0.1 M NiCl₂ in the Buffer A. Unadsorbed and loosely-bound proteins were washed with 5 volumes of Buffer A followed by 5 volumes of Buffer A with 50

mM imidazole. (His)₆-tagged LPD protein was eluted with an imidazole gradient of 0.05 M to 0.5 M in K-phosphate buffer (pH 8.0). All the fractions containing LPD activity were combined. The His-tag was cleaved off the protein by incubation with Thrombin (25 unit mg protein⁻¹; General Electric) at 4 °C, overnight. Thrombin and the small peptide were removed by gel filtration through a Sephacryl S-200 HR column (2.6/60 cm; General Electric). The protein was eluted with Buffer A containing 0.1 M NaCl at 0.5 ml.min⁻¹ flow rate. All the fractions with LPD activity were combined and dialyzed against 50 mM potassium phosphate buffer, pH 8.0. Purity of the protein was confirmed by 12 % SDS-PAGE.

Dihydrolipoamide Dehydrogenase (LPD) Assay

Dihydrolipoamide dehydrogenase was assayed as described by Wei *et al.* (136). The standard reaction mixture for forward reaction contained 0.1 M KH₂PO₄ (pH 8.0), 3 mM NAD⁺, 3 mM DL-dihydrolipoic acid, and 1.5 mM EDTA in 1 ml, at room temperature. The enzyme uses both dihydrolipoamide and dihydrolipoic acid as substrates and replacement of dihydrolipoamide with dihydrolipoic acid only reduces the LPD activity by 20 % (136). One unit of enzyme activity is defined as the amount of NADH produced (μmol NADH·min⁻¹mg protein⁻¹). The reverse reaction mixture included 0.1 M KH₂PO₄ (pH 8.0), 0.1 mM NAD⁺, 0.1 mM NADH, 3 mM DL-lipoamide, and 1.5 mM EDTA in 1 ml at room temperature. Both the forward and reverse reactions were carried out at room temperature. One unit of activity is defined as the amount of NADH oxidized (μmol NADH min⁻¹ mg protein⁻¹).

Purification of Pyruvate Dehydrogenase Complex

Pyruvate dehydrogenase (PDH) complex was purified from strains YK175 (native form) and YK176 (mutated form) as described by Bisswanger (11) with minor modification. Cells were cultured in six liters of glucose-minimal medium (1 L per 2.8 L Fernbach flask). When cell

density reached a density of approximately 2.0 (O.D. 420 nm; Beckman DU640), cells were harvested by centrifugation ($10,000 \times g$, 15 min, 4°C) and washed with 100 ml 50 mM K-phosphate buffer (pH 8.0; referred to as Buffer A). Cells were lysed by passage through a French pressure cell (20,000 psi) in the presence of protease inhibitor cocktail (5 ml / 20 g cell wet weight) (Sigma). DNase I and RNase I were added to the extract at $100 \mu\text{g}\cdot\text{ml}^{-1}$ each and incubated at 37°C for 1 hour with gentle mixing in a centrifuge tube to reduce the viscosity. After nuclease treatment, cell extract was centrifuged at $12,000 \times g$ for 30 min to remove cell debris and all operations from this point on were at 4°C . The supernatant was further centrifuged at $150,000 \times g$ for 4 h to sediment the PDH complex. The supernatant was immediately decanted and the pellet was dissolved in 6 ml of phosphate buffer for 2 h with gentle mixing with a rocker. The protein solution was centrifuged at $12,000 \times g$ for 15 min to remove particulate that did not dissolve. The supernatant was passed through a hydroxyapatite column (15 x120 mm; Bio-Rad) that was equilibrated with Buffer A. The PDH complex was eluted from the column with a linear gradient of 50 mM to 500 mM K-phosphate (pH 8.0) at 0.15 ml min^{-1} flow rate. All the fractions containing PDH activity were combined, dialyzed in Buffer A and concentrated. The concentrated protein solution was further purified with a gel filtration column (Sephacryl S-200HR, 2.6 X 60 cm) with Buffer A as the eluant at a flow rate of 0.5 ml min^{-1} . All the active fractions were pooled and used immediately for the enzyme assay.

Pyruvate Dehydrogenase Assay

Activity of pyruvate dehydrogenase was determined in both crude extracts as well as in partially purified protein. Two different assay conditions were used to determine the pyruvate dehydrogenase activity in crude extracts. A standard assay for determination of the activity of the pyruvate dehydrogenase complex in crude extract or purified protein was based on pyruvate-

dependent reduction of NADH at 340 nm ($\epsilon = 6,220 \text{ M}^{-1}\text{cm}^{-1}$) at room temperature as described by Hinman (56). One ml reaction mixture contained 0.2 mM thiamine pyrophosphate, 0.1 mM CoA, 1.0 mM MgCl_2 , 0.3 mM dithiothreitol, 2.5 mM NAD^+ , $100 \mu\text{g}\cdot\text{ml}^{-1}$ of BSA and crude extract or purified protein in Buffer A. The reaction was started with the addition of 5 mM pyruvate. The K_m for NAD^+ was estimated from a double reciprocal (Lineweaver-Burk) plot of substrate concentration and velocity (76). Effect of NADH on enzyme activity was determined in the same reaction mixture with the addition of various concentrations of NADH.

A reaction that only determined the activity of the E1 component of the PDH complex contained 12.5 mM MgCl_2 , 0.18 mM thiamine pyrophosphate, 0.175 mM CoA, 2.0 mM NAD^+ , 5.0 mM pyruvate and 1.0 mM potassium ferricyanide in one ml of 50 mM sodium phosphate buffer (pH 7.0). The reaction was based on the pyruvate-dependent reduction of ferricyanide at 430 nm ($\epsilon=1,030 \text{ M}^{-1}\text{cm}^{-1}$). The reaction was started with the addition of pyruvate.

Protein Determination

Protein concentration was determined using Coomassie Blue G-250 as described by Bradford (14) with bovine serum albumin as the standard.

SDS-Polyacrylamide Gel Electrophoresis

SDS-PAGE was performed with 12.5 % gels as described by Laemmli (72). Broad molecular weight standards used in SDS-PAGE were myosin (200,000 da), β -galactosidase (116,250 da), phosphorylase b (97,400 da), bovine serum albumin (66,200 da), ovalbumin (45,000 da), carbonic anhydrase (31,000 da), soybean trypsin inhibitor (21,500 da), lysozyme (14,400 da) and aprotinin (6,500 da) (Bio-Rad). Proteins were visualized with Coomassie blue R250.

Fermentation

Batch fermentation without pH control was carried out in 13 x 100 mm screw-cap tubes filled to the top with appropriate medium. Inoculum (1% v/v) for these fermentations was grown aerobically for about 16 h. pH-controlled fermentation was conducted at 37 °C in a 500 ml vessel containing 250 ml of corresponding medium in a custom-made pH-stat as described before (96). Culture pH was maintained by the addition of 1 N or 2 N KOH (80) unless specified otherwise.

Analysis of Fermentation Products

Sugars and fermentation products were analyzed by HPLC (Hewlett Packard 1090 series II equipped with a filter photometric detector (210 nm) and a refractive index detector in series) fitted with a Bio-Rad Aminex HPX-87H ion exclusion column as described previously (129).

Table 2-1 Bacterial strains and plasmids used in this study

Strains	Relevant Genotype	Reference or Source
W3110	Wild type	ATCC 27325
BW25113	<i>lacIq rrnB</i> _{T14} Δ <i>lacZ</i> _{W116} <i>hsdR514 araBAD</i> _{AH33} Δ <i>rhaBAD</i> _{LD78}	B. Wanner
AH218	BW25113 Δ (<i>focA-pflB</i>)-FRT-Km-FRT	This study
AH241	W3110 Δ <i>ldhA</i>	Lab collection
AH242	AH241 Δ (<i>focA-pflB</i>)-FRT-Km-FRT Δ <i>ldhA</i>	AH241 X P1(AH218)
SE2377	AH242 Anaerobic-(+)	Isolate
SE2378	AH242 Anaerobic-(+)	Isolate
SE2382	AH242 Anaerobic-(+)	Isolate
SE2383	AH242 Anaerobic-(+)	Isolate
SE2384	AH242 Anaerobic-(+)	Isolate
SE2385	AH242 Anaerobic-(+)	Isolate
YK1	SE2378-FRT Km ^S	This study
YYC186	Δ (<i>aroP-aceF</i>)73 <i>yac-284::Tn10 lacZ608</i> (Am) <i>A-</i>	Chang et al
YK2	YK1 Δ (<i>aroP-aceF</i>), <i>yac-284::Tn10</i>	YK1 X P1(YYC186)
CAG12025	<i>zad-220::Tn10 l- rph-1</i>	CGSC
YK29	AH242-FRT Km ^S	This study
YK55	SE2378 Tc ^R Anaerobic (+)	SE2378 X P1(CAG12025)
YK93	YK1 Δ <i>aceF</i> -FRT-Km-FRT	This study
YK95	BW25113, Δ <i>mgsA</i> -FRT-Km-FRT	This study
YK96	YK1, Δ <i>mgsA</i> -FRT-Km-FRT	This study
YK98	BW25113 Δ <i>lpd</i> -FRT-Km-FRT	This study
YK99	YK1 Δ <i>lpd</i> -FRT-Km-FRT	YK1 X P1(YK98)
YK100	YK29 Δ <i>lpd</i> -FRT-Km-FRT	YK29 X P1(YK98)
YK111	YK100, Km ^S , aerobic+	YK100 X P1(YK1)
YK112	YK101-P1(YK55), Tc ^R	YK101-P1(YK55)
YK121	W3110-P1YK(112)	W3110-P1(YK112)
YK122	SE2377 Tc ^R Anaerobic (+)	SE2377 X P1(CAG12025)

Table 2-1 Continued.

Strains	Relevant Genotype	Reference or Source
YK123	SE2382 Tc ^R Anaerobic (+)	SE2382 X P1(CAG12025)
YK126	YK100 Tc ^R Anaerobic (+)	YK100 X P1(YK123)
YK127	YK100 Tc ^R Anaerobic (+)	YK100 X P1(YK122)
YK128	YK100 (+pKY32)	This study
YK129	YK100 (+pKY33)	This study
YK130	YK99 (+pKY32)	This study
YK131	YK99 (+pKY33)	This study
YK132	W3110 (+pKY32)	This study
YK133	W3110 (+pKY33)	This study
YK134	W3110 Δ lpd-FRT-Km-FRT	W3110 X P1(YK98)
YK135	YK134 (+pKY32)	This study
YK136	YK134 (+pKY33)	This study
YK137	YK101 (+pKY32)	This study
YK138	YK101 (+pKY33)	This study
YK139	YK100, Km ^S , anaerobic (+)	YK100 X P1(SE2377)
YK140	YK134 Km ^S , aerobic+	YK134 X P1(SE2377)
YK141	YK100, Km ^S , anaerobic+	YK100 X P1(SE2382)
YK142	YK134 Km ^S , aerobic+	YK134 X P1(SE2382)
YK143	AH241, Δ lpd-FRT-Km-FRT	AH241 X P1 (YK98)
YK146	YK143, Km ^S , aerobic+	YK143 X P1 (SE2382)
YK149	YK96, Km ^S , Amp ^S	This study
YK150	JM109(λ DE3)(+pKY36)	This study
YK151	JM109(λ DE3)(+pKY37)	This study
YK152	YK29, Km ^R , aerobic-	YK29 X P1(YK93)
YK153	W3110, Km ^R , aerobic-	W3110 x P1(YK93)
YK154	YK93, Km ^S , aerobic+	YK93 X P1(W3110)
YK156	YK93, Km ^S , aerobic+	YK93 X P1(SE2378)

Table 2-1 Continued.

Strains	Relevant Genotype	Reference or Source
YK157	YK152, Km ^S , aerobic+	YK152 X P1(W3110)
YK158	YK152, Km ^S , aerobic+	YK152 X P1(SE2378)
YK161	JM109(λ DE3)(+pKY38)	This study
YK167	YK142, Δ (<i>focA-pflB</i>)-FRT-Km-FRT	YK142 X P1(AH240)
YK168	YK134, Km ^S , Amp ^S	This study
YK169	YK168, Δ (<i>focA-pflB</i>)-FRT-Km-FRT	YK168 X P1(AH240)
YK170	YK169 (+pKY33)	This study
YK175	AH241, Δ <i>ldhA</i> , Δ <i>adhE</i> -FRT-Km-FRT	AH241 X P1(YK87)
YK176	YK141, Δ <i>adhE</i> -FRT-Km-FRT	YK141 X P1(YK87)
Top 10	F- <i>mcrA</i> Δ (<i>mrr-hsdRMS-mcrBC</i>) ϕ 80 <i>lacZ</i> Δ M15 Δ <i>lacX74</i> <i>deoR</i> <i>nupG</i> <i>recA1</i> <i>araD139</i> Δ (<i>ara-leu</i>)7697 <i>galU</i> <i>galK</i> <i>rpsL</i> (Str ^R) <i>endA1</i> λ^-	Invitrogen
Plasmids		Reference or Source
pTrc99A	pTrc expression vector, Amp ^R	Lab collection
pET15b	T7 expression vector, Amp ^R	Novagen
pTL61t	transcriptional fusion vector	Linn et al
pKY32	W3110 <i>lpd</i> in pTRC99a	This study
pKY33	SE2378 <i>lpd</i> in pTRC99a	This study
pKY36	W3110 <i>lpd</i> in pET15b	This study
pKY37	SE2378 <i>lpd</i> in pET15b	This study
pKY38	SE2377 <i>lpd</i> in pET15b	This study
Phage		
P1	Tn9 Cm ^R <i>clr-100</i>	Lab collection
λ 5ZP	λ' <i>bla lacZ lacY</i> ⁺	Lab collection

Table 2-2 List of primers used in this study.

Primer list	Oligonucleotide sequence	Use
<i>pdhR</i> -P1	AATGGTATGCGGCAGCGAAT	<i>pdhR</i> sequencing
<i>pdhR</i> -P2	GGCGTTCAGTTCAGATTA	
<i>pdhR</i> -P3	TGATCCTCGAAGGCACTCTC	
<i>pdhR</i> -P4	CAGATGGCGATGCGATGCTT	
<i>pdhR</i> -P5	TCGCTTCGAGACGTTGAATC	
<i>pdhR</i> -P6	CGCCAGAACTTCGAATTGCT	
P1	GAAGCATCGCATCGCCATCT	P1 to R17 <i>aceEF-lpd</i> sequencing primers
F2	AGGTGTTGAGCGTGCTCAGT	
F3	AGTTCACGGCAATGGCCTCT	
F4	GGTCACCGGTAACGGCAAGA	
P2	GCACACCGTCCATGTTCATT	
F6	CGTGCTCTGAACGTGATGCT	
F7	CGAAGGTCTGCAGCACGAAG	
P3	GGTGGTCACGATCCGAAGAA	
F9	CCGGCGCACTGATTATGATT	
F10	TACCGGCTCGCTGATTATGG	
P5	TTCGCTGAGCAGGTCCGTA	
F12	CTGCAGCTCTTGAGCAGATG	
F14	ACTCAGGTCGTGGTACTTGG	
F15	CCGCATGAAGATCCGCGTAT	
F16	GTACCAACGTACCGCACATC	
P2	GCACACCGTCCATGTTCATT	
R2	GCGATAGCACGACCAGAAGC	
R3	TACCAGCACGGCGTCGTAAC	
R4	TGCCGTTCTCACCTTCAACT	
R5	CAACGGAAGGCAGCGGAGTA	P1 to R17 <i>aceEF-lpd</i> sequencing primers
P4	TTGTCGCCTTCTACGGTGAT	

Table 2-2 Continued.

Primer list	Oligonucleotide sequence	Reference
R7	TTCCGGCGCGTTCACAATCG	
P6	TCAGGTTTCGCACCAGAGATT	
R9	GCTTATGTTACGCGACTCC	
R10	CATAATCAGCGAGCCGGTAG	
P8	CGCTTGCTACCTTGCTGC	
R12	ACGGACCTGCTCAGCGAACA	
R13	CACCGTACATACGCTCCAGA	
P9	CGCCGTCTGGTGATGTAAGTA	
P10	CGAGCAACGGTCAGCAGTAT	
R14	CGGCAGATTGTTGGTGCTGT	
R16	TGCCTTCCAGTTCGTTGATG	
R17	CCAGCTGCTCCTGAGTCAGA	
48 <i>mgsA</i> -F	ACAAATGCTGATGAGCTGGGTGGAACGGCATCAA CCGTTACTGGAGTGCTGCAAGGCGATTAAGT	<i>mgsA</i> deletion
<i>mgsA</i> -R	AGAATATCGACCGCGTCGTTGAAATGCGGCGACT GGATTATGAAGGATTACGAATTCCGGTCTCC	
<i>lpd</i> -pTrc99a-NcoI	GCGACCATGGAGAAGGAGATATACCATGAGTACT GAAATCAA AACTC	<i>lpd</i> for pTrc99a construct
<i>lpd</i> -pTrc99a-HindIII	GAGCAAGCTTTTACTTCTTCTTCGCTTTCG	
<i>lpd</i> -pET15b F-XhoI	GAGCCTCGAGATGAGTACTGAAATC	<i>lpd</i> for pET15b construct
<i>lpd</i> -pET15b F-BamHI	GCGTGGATCCTTACTTCTTCTTCG	
<i>adhE</i> -F	ATCACCGCACTGACTATACTCTCG	
<i>adhE</i> -R	CCTGTTGTGGAAGCCGTTAT	

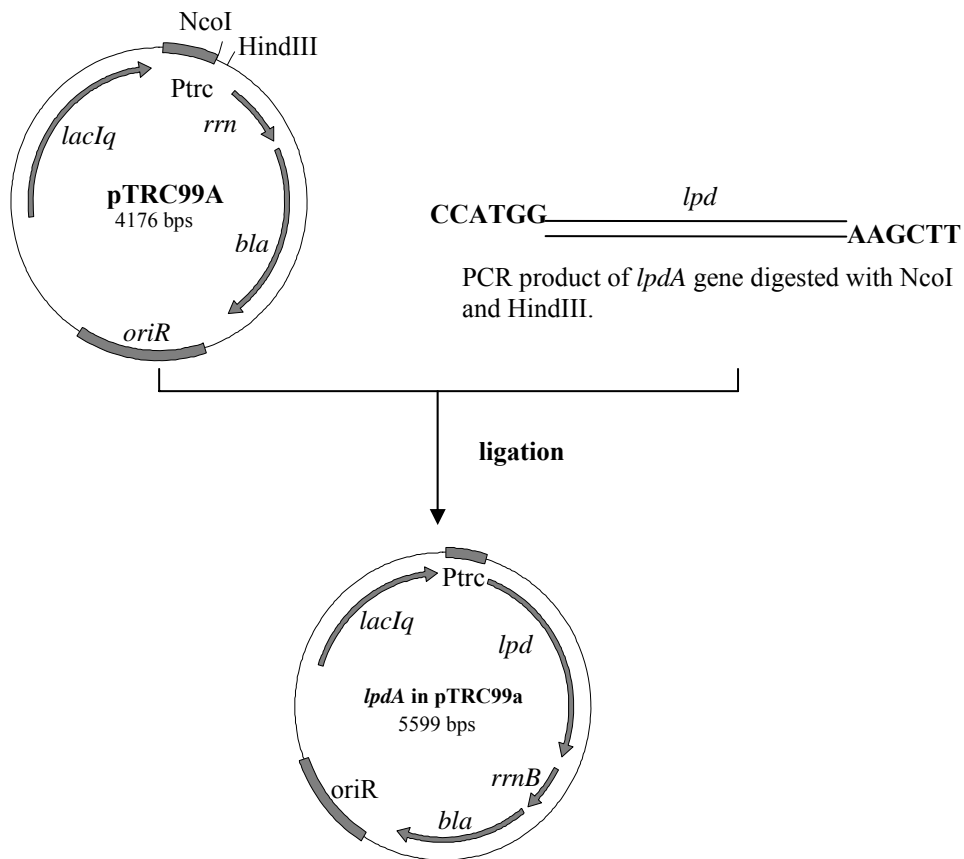


Figure 2-1 Construction of *lpd* in pTRC99a for complementation analysis. *lpd*, lipoamide dehydrogenase gene; *bla*, β -lactamase; *lacI*, lac repressor; *oriR*, origin of replication; *rrnB*, transcription termination sequence.

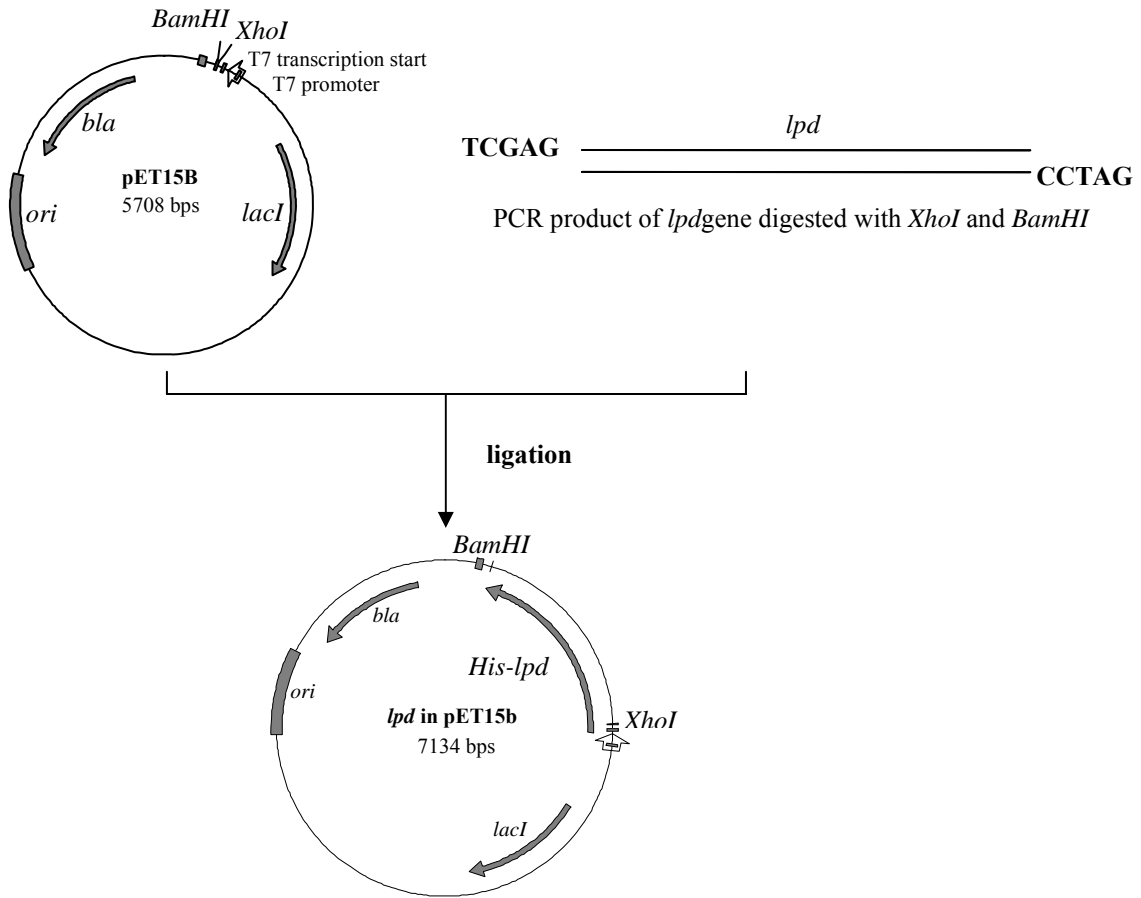


Figure 2-2 Construction of LPD expression construct in pET15b with PCR amplified *lpd* gene.

CHAPTER 3 RESULTS AND DISCUSSION

Isolation of Homo-Ethanol Producing *E. coli*

Production of either lactate or ethanol catalyzed by lactate dehydrogenase or alcohol dehydrogenase (encoded by *ldhA* or *adhE*, respectively), is a key fermentation pathway that allows *E. coli* maintain redox balance under fermentative growth conditions. In a *pflB* mutant, although *adhE* gene is intact, pyruvate is not converted to ethanol due to the absence of acetyl-CoA, the substrate for alcohol dehydrogenase. An *ldhA*, *pflB* double mutant is defective for anaerobic growth due to a shortage of NAD⁺ for the activity of glyceraldehyde-3-phosphate dehydrogenase, a key enzyme of glycolysis. Isolating a mutant starting from a *pflB*, *ldhA* deletion strain that can grow under anaerobic conditions would help identify new pathways by which NADH is reoxidized by *E. coli* to maintain the overall redox balance.

Towards this objective, strain AH242 ($\Delta pflB$, $\Delta ldhA$) was mutagenized by EMS (ethylmethane sulfonate) and 31 mutant strains that grew anaerobically on LB+glucose solid medium were isolated. All the isolates produced ethanol as the primary fermentation product (Table 3-1). The level of succinate produced by these isolates was similar to that of the wild type strain, W3110, indicating that the succinate production pathway is not responsible for the observed anaerobic growth of the isolates. Although the genes encoding PTA and ACK for acetate production from acetyl-CoA were not deleted in the isolates, these isolates produced very low levels of acetate. These results suggest that ethanol production is not due to activation of the second PFL enzyme encoded by the silent *pflCD* operon or another PFL-like protein. In addition, the absence of formate among the fermentation products also suggests that the ethanol produced by these isolates did not originate from PFL activity. Interestingly, a trace amount of lactate was observed in the fermentation broth, despite the deletion of *ldhA* gene in this mutant, (Table 3-1;

Figure 3-1). One isolate that grew faster than others, strain SE2378, was used in further studies (Table 3-1).

Mapping the Mutation(s) in Strain SE2378

Based on the fermentation profile and growth pattern, ethanol production is the new pathway that helps maintain redox balance in the mutants derived from the *ldhA*, *pflB* double mutant. Since lactate yield was minimal and formate was not detected, lactate dehydrogenase and pyruvate-formate lyase activity were not restored in strain SE2378. This suggests an induction of a new anaerobic pathway in strain SE2378 and other similar isolates for ethanol production that is responsible for oxidation of NADH to NAD⁺ under fermentative conditions. The known pathway for production of ethanol as the major fermentation product from glucose utilizes pyruvate decarboxylase and alcohol dehydrogenase, found in *Z. mobilis* and a few other bacteria (Figure 3-2). This enzyme activity was not detected in *E. coli* and a gene corresponding to *pdh* was not found in the annotated genome of *E. coli*. An alternate pathway is to generate acetyl-CoA from pyruvate and reduce this to ethanol in two steps by alcohol dehydrogenase. Pyruvate oxidase and acetyl-CoA synthetase could serve this function (Figure 3-2). However, pyruvate oxidase is reported to be only produced during the stationary phase of growth, and ACS is an ATP-dependent reaction. A fermenting cell is not likely to have the ATP needed to support ethanol production by this latter pathway. In addition, the ADH-E dependent reduction of acetyl-CoA requires two NADH per acetyl-CoA and glycolysis followed by the POX pathway does not generate the needed two NADH per acetyl-CoA. An alteration of pyruvate dehydrogenase (PDH) complex that is not normally active in an anaerobic cell is of high probability in strain SE2378 (Figure 3-2) (17).

To evaluate the role of PDH complex in supporting anaerobic growth of strain SE2378, $\Delta(\textit{aroP-aceF})$, $\textit{zac}::\textit{Tn10}$ was transduced into strain SE2378. The cotransduction frequency of

$\Delta(\text{aroP-aceF})$ with *Tn10* was close to 100%. Transductants were first selected for resistance to tetracycline on rich medium with tetracycline. Since a *pdh* mutant required acetate for optimal aerobic growth in glucose-minimal medium, all the tetracycline-resistant transductants were tested for growth on glucose-minimal medium. All the tested transductants required acetate for growth on glucose-minimal medium (Figure 3-3). These transductants lost the anaerobic growth positive phenotype of the parent, strain SE2378. When the same deletion mutation was transduced into wild type strain, W3110, the $\Delta(\text{aroP-aceF}), \text{zac}::\text{Tn10}$ transductants grew normally under anaerobic conditions (Figure 3-4). These results show that the PDH is not required for anaerobic growth of *E. coli* but is only required for the anaerobic growth of strain SE2378 that lacks both *ldhA* and *pflB*. However, the possibility that a mutation in another gene that is near the *pdh* operon is responsible for the anaerobic growth of strain SE2378 can not be ruled out from these experiments. To distinguish between the two alternatives, a part of the *aceF* gene of the *pdh* locus (*pdhR-aceEF-lpd*) was deleted in strain SE2378 and the phenotype of the new derivative (strain YK93) was determined. Strain YK93 was acetate-dependent for aerobic growth in minimal medium and anaerobic growth defective in all media tested (Figure 3-4). Similar results were also obtained when a Δlpd mutation was introduced into strain SE2378. Restoration of aerobic growth phenotype of strain YK93 by transducing the *aceF*⁺ gene from strain SE2378 (strain YK158) also restored anaerobic growth. Although the anaerobic growth rate of strain YK158 was about 50% of that of strain W3110, this growth rate was comparable to that of strain SE2378 (Table 3-2). Strain YK158 also produced ethanol as the major fermentation product. In contrast, when aerobic growth was restored by transducing the *aceF*⁺ gene from the wild type strain, W3110, about 93 % of the transductants still retained the anaerobic growth defect of the recipient (Table 3-2). However, the anaerobic growth of the 7% of the transductants

carrying the *aceF*⁺ from the wild type suggests that the mutation that supported anaerobic growth of strain SE2378 is not located in the *aceF* gene but in a gene within 0.05 minute (about 2.25 kbp) (based on co-transduction frequency) of *aceF* in the *E. coli* genome. While the aerobic growth of strain YK152 was restored with the *aceF*⁺ from wild type strain, W3110, none of the transductants grew anaerobically.

Location(s) of the Mutation(s) in strain SE2378

The genetic analysis revealed that a mutation in the *pdh-aceEF-lpd* operon or in a closely linked gene in strain SE2378 is responsible for the anaerobic growth of SE2378. In order to explore the nature of the mutation(s), the DNA sequence of the entire *pdh* operon of strain SE2378 and 2 other isolates (SE2377, SE2382) was determined. This included the upstream promoter region also (Figure 3-5) (99). None of the three mutant strains carried a mutation in the promoter region or further upstream of the *pdh* operon (up to -243). The DNA sequence revealed 2 mutations within the coding region of *pdhR* gene of strain SE2378 (T to C of 34th nucleotide & insertion of TGC between 352th and 353th nucleotide from the start codon 'ATG' of *pdhR*), which lead to an amino acid substitution (S12P) and an amino acid insertion (leucine as 118th amino acid) (Figure 3-6).

A single nucleotide substitution (G to A) was also found in the intergenic region between *pdhR* and *aceE* in SE2378 at position -59 from the 'A' of start codon 'ATG' of *aceE* gene. However, no mutation was found in *pdhR* gene or the intergenic region of the other two isolates (Figures 3-6 and 3-7). Since strains SE2377 and SE2382 also grew anaerobically, a mutation in another gene in the *pdh* operon other than the *pdhR* appears to be responsible for the anaerobic growth phenotype (Table 3-1).

The genes *aceE* and *aceF* encode E1 component (pyruvate decarboxylase / dehydrogenase) and E2 component (dihydrolipoamide transacetylase), respectively, of pyruvate dehydrogenase

complex. The DNA sequence of these two genes was unaltered in all the strains tested. These three strains carried a single nucleotide substitution (G to A at position +1,060 or C to T at position +964 from 'A') in the *lpd*. This nucleic acid change led to an amino acid substitution from glutamate to lysine (E354K) or histidine to tyrosine (H322Y) (Figure 3-8). Since the *lpd* mutation in the three mutants was in one of two amino acid positions, the *lpd* genes in three other mutants (SE2383, SE2384 and SE2385) were also sequenced. Mutation in these three mutants was also in the amino acid position 322 or 354 as with the other three ethanologenic mutants (Figure 3-8). In concert with mapping experiments, the sequencing results provide high probability that pyruvate dehydrogenase plays an essential role in restoring anaerobic growth of SE2378 and other similar derivatives.

Confirmation that the Mutation in *lpd* is Responsible for the Anaerobic Growth Phenotype of Strain SE2378

DNA sequence analysis identified a single amino acid substitution in the *lpd* in the six mutants that grew anaerobically in a mutant lacking LDH and PFL (Figure 3-8). The role of this mutation in *lpd* gene in supporting the anaerobic growth phenotype of these mutants was examined directly by complementation analysis. For these experiments, an *lpd* deletion mutation was introduced into a kanamycin-sensitive derivative of strain AH242, the parent of strain SE2378 and other anaerobic-plus isolates. The resulting strain, YK100, was transformed with plasmids that express the *lpd* gene either from the wild type or strain SE2378 from a *lac* promoter. Since strain AH242 is the parent strain of SE2378, this strain should be free of any of the mutation(s) responsible for the anaerobic-plus phenotype of strain SE2378 (Table 3-3). Complementation of the *lpd* mutation with the native *lpd*⁺ gene (strain YK128) supported aerobic growth in minimal medium but not anaerobic growth. Complementation of the same *lpd* mutation in strain YK100 with the *lpd* gene alone from SE2378 supported both aerobic and

anaerobic growth with ethanol as the main fermentation product (Table 3-3). These results indicate that the mutation found in the *lpd* gene is sufficient to support anaerobic growth of strain SE2378 and other isolates.

Additional Mutations

In order to further confirm that the mutation in the *lpd* is sufficient for the observed ethanologenic phenotype of the *ldhA*, *pflB* mutant, the *lpd*⁺ gene from wild type strain, W3110, was mutagenized by either hydroxylamine or by error-prone PCR amplification. When plasmid pKY32 with the wild type *lpd*⁺ gene was mutagenized with hydroxylamine hydrochloride and transformed into strain YK100 ($\Delta ldhA$, $\Delta pflB$, Δlpd), 5 additional independent mutations were also obtained. All 5 transformants carrying the altered *lpd* gene grew aerobically and anaerobically and produced ethanol as the main fermentation product. Sequencing the *lpd* gene in these 5 plasmids with the mutations showed that the amino acid change (E354K) is the same as that of the *lpd* gene in strain SE2378. Under similar conditions, error-prone PCR mutagenesis did not yield any mutation and was not pursued further. These results further confirm that a single mutation, such as the E353K, in the *lpd* gene is sufficient to support anaerobic growth of a *ldhA*, *pflB* mutant and the ethanologenic phenotype of *E. coli*.

Metabolic Routes of Pyruvate with the Mutated LPD in Various Backgrounds

In the presence of the *lpd* mutation (*lpd*^{*}), the PDH is active under anaerobic growth conditions. Transduction of this *lpd*^{*} mutation into wild type *E. coli* is expected to provide a third alternative route for pyruvate metabolism, in addition to lactate dehydrogenase and pyruvate formate-lyase (Figure 3-9). Of the three enzymes, PDH has the highest affinity for pyruvate (*K_m* of 0.4 mM). Based on its lower *K_m* for pyruvate, the PDH would be the expected primary enzyme metabolizing pyruvate rather than LDH or PFL. As seen with strain SE2378, metabolism of pyruvate through the PDH pathway leads to ethanol as the main fermentation

product to maintain redox balance. These observations suggest that the fermentation profile of strain W3110 with the *lpd** mutation will shift from mixed acid to mostly ethanol. Surprisingly, replacing the *lpd⁺* gene of wild type strain, W3110, with the *lpd** from strain SE2378 did not alter the fermentation profile and the primary product was lactic acid (Table 3-4).

Similar results were obtained with strain YK144 producing only LDH and PDH activities (Table 3-4). These results show that the PDH even with its 18-fold higher affinity for pyruvate failed to compete with LDH (127, 139). A distinguishing characteristic of anaerobic *E. coli* is the higher NADH/NAD⁺ ratio (31). This lower NAD⁺ concentration, the needed substrate of PDH, coupled with a higher NADH concentration, the substrate of LDH, is apparently the deciding factor in the flow of pyruvate in the anaerobic cell. Furthermore, LDH is activated by pyruvate and NADH (127).

In the presence of only PDH and PFL activities (*ldhA*) (strain YK146), the fermentation products were acetate, formate and ethanol during the initial growth phase. With a decline in the growth rate and at the stationary phase of growth, PDH became the main pyruvate-metabolizing enzyme as seen by an increase in ethanol during this phase. During the anaerobic growth phase, PFL pathway is favored because of the additional ATP per glucose produced at the acetate kinase step (Figure 1-1) to support a higher growth rate. As the culture reaches the stationary phase, PDH takes over pyruvate metabolism, because the additional ATP produced by ACK is apparently not needed to maintain the lower growth rate. These results indicate that lactate dehydrogenase pathway needs to be deleted in order for the mutated PDH to direct carbon flux from glucose to ethanol.

Aerobic and Anaerobic Expression Level of *pdh* Operon

In wild type *E. coli* cells, pyruvate dehydrogenase is responsible for oxidation of pyruvate only under aerobic conditions. Since the mapping of the mutation in the ethanologenic isolates

revealed that *pdh* is responsible for anaerobic growth, it was of interest to evaluate the expression level of *pdh* operon in the mutant during aerobic and anaerobic growth. The relative level of *aceE* gene mRNA of wild type strain W3110 was not significantly different under either aerobic or anaerobic growth conditions, indicating that the transcription of *pdh* operon is independent of the presence of O₂ (Table 3-5). Independence of *pdh* transcription to O₂ in the growth medium was also observed with the ethanologenic strain SE2378. These results were confirmed by the level of β-galactosidase activity (*Ppdh-lacZ*) produced by the cultures grown with or without O₂. Despite the same level of transcription of *pdh* operon in aerobic and anaerobic cultures of W3110, the activity of PDH measured as E1 component activity in the extracts of W3110 cells grown anaerobically was only about 50 % of that of aerobically grown cells. It is possible that the inactive PDH complex rapidly turned over in the anaerobic cell. In contrast to W3110, the mutant, strain SE2378, had similar levels of PDH enzyme activity regardless of the presence of O₂. The observed lower level of PDH activity in strain SE2378, compared to strain W3110, is in accordance with the lower mRNA levels in the mutant. These results show that the lack of PDH activity in the wild type *E. coli* (W3110) during anaerobic growth is attributable to lower protein level and inhibition of enzyme activity.

LPD Purification and Characterization

The dihydrolipoamide dehydrogenase (LPD), E3 component, in the pyruvate dehydrogenase (PDH) complex plays an important role not only in the catalytic activity of the complex but also in regulating PDH activity depending on the NADH/NAD⁺ ratio of the cell. It is known that the activity of E3 is inhibited by NADH (105, 111, 138). The mutation in the *lpd* gene in strain SE2378 and the other isolates apparently reversed the inhibitory effect of NADH on PDH activity. To evaluate this possibility both the LPD and PDH were purified and the

kinetic characteristics of these enzymes, especially the inhibition of activity by NADH, were determined.

NADH Sensitivity on Forward Reaction

The LPD from W3110 and SE2378 was purified to homogeneity for determination of enzyme activity (Figure 3-10). {Move this sentence to the Methods section. The LPD activity was linear up to 80 ng of the native protein and 200 ng of the mutated enzyme from strain SE2378 (Figure 3-11). For determination of the kinetic parameters of the enzyme, 53.8 ng of the native LPD and 200 ng of the mutated LPD were used per reaction. Both the native and the mutated LPD exhibited typical Michaelis-Menten type kinetics (Figure 3-12, 3-13). Kinetic constants for the native and the mutated LPD are presented in Table 3-6. The affinity of the two enzymes for NAD⁺ (0.4 mM) was the same. Turnover number for the mutated form of the enzyme was about 4-fold lower than the native enzyme and reduced the catalytic efficiency (K_{cat}/K_m) by about 4 fold, compared to that of the native LPD.

One of the distinctive characteristics of LPD is its high sensitivity to NADH/NAD⁺ (105, 111, 136, 138). In order to examine whether the mutation in *lpd* in strain SE2378 altered the sensitivity of the enzyme to NADH inhibition, LPD activity was determined in the presence of NADH. The activity of the native LPD was progressively inhibited by increasing NADH concentration (Figure 3-14; 3-15). The native LPD was completely inhibited at an NADH concentration of 0.16 mM. This concentration relates to an NADH/NAD⁺ ratio of 0.08. The mutated LPD (E354K) was significantly more sensitive to inhibition at a lower concentration of NADH (0.02 mM) than the native LPD (Figure 3-16). Increasing the NADH concentration reversed the inhibitory effect on the mutated LPD. Beyond an NADH concentration of 0.06 mM, increasing NADH concentration had minimal effect on the activity of the mutated enzyme. The physiological concentrations of NAD⁺ and NADH in *E. coli* growing under aerobic

conditions are 2.54 mM and 0.08 mM, respectively (NADH/NAD⁺ of 0.03) (31, 71). Both the native and the mutated LPD was inhibited equally at this ratio of NADH/NAD⁺ of 0.03 (Figure 3-15). The physiological significance of this in vitro observation with a PDH component to in vivo physiology is not clear. The NADH/NAD⁺ ratio of an anaerobic *E. coli* is about 0.7 (31). Since the native enzyme is inhibited by as low an NADH/NAD⁺ ratio as 0.08 (Figure 3-15), it is expected that the native LPD would have no activity under anaerobic growth conditions. In contrast, the mutated LPD still retained about 35% of the control activity at 0.16 mM NADH and the effect of NADH concentrations higher than this were not evaluated due to experimental difficulty. These results clearly show that the mutated LPD is less sensitive to NADH inhibition.

NADH Sensitivity of the Reverse Reaction of LPD

The reduced sensitivity of mutated LPD to NADH can be more readily seen by following the reverse reaction that transfers electrons from NADH to lipoamide producing dihydrolipoamide and NAD⁺. Although this is not the native reaction, this reaction is also inhibited by NADH although one of the substrates of the reaction is NADH. For this reaction to proceed, NAD⁺ is a required activator (105, 138). This requirement was also observed for the native LPD (Figure 3-17) and the reverse reaction of the enzyme was maximal only above an NAD⁺/NADH ratio of 1.5 or higher. Activation of the native LPD activity by NAD⁺ was biphasic. At a lower NAD⁺/NADH (up to 1.0), only about 35 % of the enzyme was activated and in a second higher phase, increasing the ratio from 1.0 to about 1.5 increased the activity to almost 100 %. This is in agreement with the previous report by Schmincke-Ott *et al.* (111), suggesting that LPD may have two NAD⁺ binding sites. In contrast, the mutated LPD retained about 80 % of its maximum specific activity even in the absence of NAD⁺. Maximal activity of the mutated enzyme was reached at an NAD⁺/NADH ratio of about 0.2. 0.2. (Figure 3-17). These results suggest that the E354K mutation overcame the need for binding of NAD⁺ to one of the

two sites for activation of the enzyme. In doing so, the mutated LPD apparently increased its catalytic capacity at higher NADH/NAD⁺ normally found in the cell under anaerobic conditions. An alternative possibility that the mutated form of the LPD has a tightly bound NAD⁺ in one of the activation sites can not be ruled out.

It is expected that this reduced sensitivity of LPD to NADH inhibition would be associated with reduced sensitivity of the pyruvate dehydrogenase complex of the mutant, strain SE2378, at supporting the activity of the enzyme at NADH/NAD⁺ ratios that is inhibitory to the native pyruvate dehydrogenase complex (136, 138).

PDH Purification and Characterization

The native PDH is composed of three enzymes including the LPD and has a molecular mass of about 4×10^6 Da. This complex was purified from strain YK175 (*ldhA*, *adhE*) and the mutated form of the enzyme was purified from strain YK176. Since neither strain grew anaerobically, cultures were grown aerobically for purification and kinetic characterization of the native and mutated PDH complex. Biochemical properties of purified enzyme are not expected to differ based on the growth conditions. Purification of the two forms of the complex is summarized in Table 3-7 (native PDH) and in Table 3-8 (mutated PDH). The ultracentrifugation step significantly removed most of the smaller proteins. While the recovery of mutated PDH was about 80 % after the ultracentrifugation step, only about 50 % of the native PDH was obtained after this step. Despite significant loss of activity in each of the steps, PDH was purified with only one contaminating protein (Figure 3-18). This contaminating protein (about 38,000 Da) co-purified with the PDH complex from both strains and had no detectable NADH oxidation activity including LDH, ADH, and NADH oxidase activity. The nature of the contaminating protein is not known.

Determination of Kinetic Constants of PDH Complex

Both forms of the enzyme fit the Michaelis-Menten kinetics (Figures 3-19, 20, 21, 22). Both forms of the PDH complex had similar affinity for the two substrates. Affinity for NAD^+ by the mutated form of PDH was similar to that of the native PDH (Table 3-9). This is in agreement with the observed similar affinity of the LPD component for NAD^+ (Table 3-6). However, the K_m for NAD^+ by the PDH complex was significantly lower than the isolated LPD component (0.1 mM vs. 0.4 mM for the LPD). These results indicate that the conformational changes associated with the formation of the complex form of PDH increased the affinity for NAD^+ in both cases. Turnover number and catalytic efficiency of the two enzymes were also comparable. These results indicate that the mutated form of PDH complex functions as efficiently as the native PDH complex converting pyruvate and NAD^+ to acetyl-CoA and NADH.

Inhibition of PDH activity by NADH

Under anaerobic conditions, the NADH/NAD^+ ratio of *E. coli* is significantly higher (about 0.70) than that of an aerobic cell (about 0.03) (31). Since the mutated form of LPD was found to be less sensitive to NADH, especially at the higher concentrations of NADH, it is possible that this effect is transferred to the PDH complex since the site of NADH inhibition is the LPD component. The native PDH was more severely inhibited by NADH than the mutated PDH and the progressive inhibition of the native PDH by NADH was observed as in the native LPD (Figures 3-14 and 3-23). Although the mutated PDH was also inhibited by NADH, its sensitivity to NADH inhibition was less than that of the native PDH (Figure 3-24). At a fixed NAD^+ concentration of 1.0 mM NAD^+ (10 times higher than K_m for NAD^+), while the native LPD was inhibited by about 60 % at an NADH/NAD^+ of about 0.03 (Figure 3-15), the PDH activity was reduced only by about 10 % at the same NADH/NAD^+ ratio (Figure 3-25). Inhibition of the native PDH activity by NADH was biphasic and about 80 % of its activity was inhibited at 0.1

mM NADH (NADH/NAD⁺ of 0.1) (Figure 3-25). In contrast, the mutated PDH still retained about 80 % of its activity at the same concentration of NADH (0.1 mM) (Figure 3-25). This difference in NADH sensitivity of the two enzymes is reflected in the K_i value for NADH of 1 μ M for native enzyme and 10 μ M for the mutated form (Table 3-9).

It is interesting to note that both the native PDH complex and purified LPD component were inhibited by about 70% in the presence of 0.1 mM NADH (Figures 3-15 and 3-25). However, the NADH inhibition characteristics of the PDH complex from the mutant, strain SE2378, differed from that of the LPD component from the same mutant. The observed sensitivity of the mutated LPD to low level of NADH was absent in the PDH complex indicating that the inhibition by 0.02 mM NADH was not physiological since the LPD only functions as part of the PDH complex in the cell. Discounting this part of the inhibition curve, the PDH complex and the LPD appear to be inhibited by about the same level by NADH. These results clearly demonstrate that the E354K mutation in *lpd* gene of strain SE2378 that reduced the severity of NADH inhibition of the LPD component is transferred to the PDH complex and is the main reason for the anaerobic growth phenotype of strain SE2378.

Fermentation of Sugars to Ethanol

Glucose Fermentation

The ability of strain SE2378 and similar isolates to produce ethanol as the main fermentation product provided an opportunity to evaluate these isolates as ethanologenic microbial biocatalysts that lack foreign genes for fermentation of sugars to ethanol. When wild type *E. coli* was cultured in a pH-controlled medium containing 50 g glucose L⁻¹, strain W3110 grew at a specific growth rate of 0.44 h⁻¹ (μ_{\max}), producing lactate, formate, acetate and ethanol as fermentation products (Figure 3-26; Table 3-10). Strain SE2378 grew after a lag of about 6 h

with a specific growth rate of 0.46 h^{-1} that is comparable to that of the wild type (Figure 3-27; Table 3-10). While wild type consumed almost all of the glucose in 24 h, strain SE2378 required about 72 h to consume the same amount of glucose. This difference can be attributed to the cell density of the culture at the end of the growth phase (2.4 mg ml^{-1} dry wt for the wild type vs. 1.7 mg ml^{-1} dry wt for the mutant) and also the highest rate of glucose consumption by wild type was slightly higher than that of strain SE2378 (4.1 to $3.26 \text{ g glucose h}^{-1} \text{ g cells}^{-1}$; Table 3-11). The highest concentration of ethanol produced by SE2378 with 5 % glucose was about 480 mM (22 g L^{-1}) and this accounted for 88 % of total fermentation products (Table 3-10). Considering the fermentation yield of ethanol from 1 mole of glucose is 2 moles of ethanol, ethanol yield of strain SE2378 with 50 g L^{-1} glucose was about 81 % (Table 3-10).

Xylose Fermentation

Since xylose is the major sugar present in hemicellulosic biomass, a microbial biocatalyst is required to ferment xylose efficiently. In a pH-controlled culture containing 50 g xylose /L , both the wild type and strain SE2378 grew at similar growth rate, although strain SE2378 exhibited a longer lag time (about 6 hours) before the beginning of growth (μ_{max} , 0.37 h^{-1} vs. 0.38 h^{-1} ; Figure 3-28, Figure 3-29; Table 3-12). This lower growth rate in xylose medium is in agreement with previous reports that anaerobic growth rate of *E. coli* on xylose is lower than that of *E. coli* on glucose (50). Also, wild type strain required more than 72 hours to ferment 50 g/L xylose while the same strain fermented the same amount of glucose within less than 36 hours. Since the cell mass of strain SE2378 at the end of the growth phase was the same as that of strain W3110, this difference in fermentation time is probably due to the higher rate of xylose consumption by strain SE2378. As expected, xylose fermentation led to an increase in acetate production by the wild type *E. coli* than in glucose fermentation, in agreement with the previous

report (50) that lower ATP generation on xylose directed more xylose to acetate production. While wild type produced about 190 mM ethanol in 72 hours, strain SE2378 produced approximately 440 mM ethanol within 48 hours. Ethanol yield by strain SE2378 was as 2.4fold higher than that of the wild type (0.82 vs. 0.34; Table 3-12).

It is interesting to note that the specific ethanol productivity of wild type and the *lpd* mutant was higher on xylose than on glucose (Table 3-11). This is probably a reflection of energy output of xylose fermentation. For wild type, the net ATP yield from xylose is only about 1.5 per xylose compared to 3.0 per glucose. This would require that the cells utilize more xylose to generate the same amount of energy. However, the specific rate of xylose consumption by the wild type was only slightly higher than that of glucose (4.93 vs. 4.10 g sugar h⁻¹ g cells⁻¹; Table 3-11) accounting for the lower cell yield and longer fermentation time compared to glucose fermentation (Figure 3-26, Figure 3-28). In contrast, strain SE2378 lacks pyruvate formate-lyase, an enzyme critical for xylose fermentation in minimal medium (50). Due to this mutation, the net calculated ATP yield from xylose fermentation in strain SE2378 is only 0.67 per xylose. It is apparent that this lower ATP yield is driving the high xylose flux in this ethanologen. These results suggest that the engineered ethanologenic *E. coli* without foreign genes has the potential to increase specific ethanol productivity in glucose fermentation by decreasing the net ATP yield from glucose.

Removal of Trace Amount of Lactic Acid

During glucose fermentation, small amounts of lactic acid were also produced by strain SE2378 (Table 3-10). Since the *ldhA* gene is deleted in this strain, it is unlikely that the LDH is responsible for this lactic acid. It is known that the metabolic pathways responsible for detoxification of methylglyoxal produced from dihydroxyacetone phosphate (DHAP) result in lactic acid formation (41, 43). By deleting the methylglyoxal synthase gene (*mgsA*), the first

enzyme in the methylglyoxal to lactic acid pathway, this trace amount of lactic acid could be eliminated, if this pathway is responsible for this lactic acid. Introducing a deletion into the *mgsA* in the chromosome of the ethanologenic strain SE2378, YK96, eliminated the lactic acid production during glucose fermentation (Figure 3-30; Table 3-13). In addition, the *mgsA* mutation also increased the ethanol yield to about 88 % of the glucose fermented without reduction in growth rate or cell yield (Table 3-13).

Proposed Ethanologenic Fermentation Pathway

In the ethanologenic mutant *E. coli* strain SE2378 isolated and described in this study, pyruvate dehydrogenase complex is active under fermentative conditions because a specific mutation in the LPD reduced the sensitivity of the enzyme to inhibition by high concentration of NADH associated with the anaerobic cell. This altered PDH complex supports anaerobic growth of *E. coli* without external electron acceptors even in the absence of LDH and PFL activity (Figure 3-31). The production of one acetyl-CoA per pyruvate yields an extra NADH, leading to a total of 4 NADHs per glucose. Since the glycolysis and PDH yields a total of 4 NADHs along with 2 acetyl-CoAs, the redox balance can be easily restored by the reduction of the 2 acetyl-CoAs with the 4 NADHs to 2 ethanols. For construction of an ethanologenic *E. coli* using the PDH system, the *ldhA* needs to be eliminated. Since the shift from PFL to PDH is accomplished by physiological means, a mutation in *pflB* is not required and indeed the presence of *pflB* may be beneficial to increasing the growth rate and higher cell yield especially with pentoses leading to a reduction in fermentation duration.

The PDH from almost all organisms is known to be inhibited by NADH to varying degrees and is probably a control mechanism that prevents excess production of NADH that cannot be oxidized under O₂ limitation conditions. Thus, an increase in NADH/NAD⁺ ratio is also a signal used by the cell to shift the metabolism from oxidative to fermentation. Introducing a mutation

similar to that of E352K in the LPD of other bacteria may exert a profound physiological change. Therefore, the development of biocatalyst, strain SE2378, provides a significant potential to avoid introduction of foreign genes for conversion of pentoses derived from cellulosic biomass to not only bioethanol but also other biobased products.

Table 3-1. Growth and fermentation profile of the anaerobic (+) derivatives of *E. coli* strain AH242 grown in LB+glucose (0.3 %, w/v) in a batch culture without pH control.

Isolate	O.D. (420 nm) at culture time (hrs)				Fermentation Products (mM)					
	24	48	72	91	Succinate	Lactate	Formate	Acetate	Ethanol	
1	-	0.0	0.7	0.9	2.8	-	-	3.1	31.1	
2	-	0.8			2.1	-	-	3.1	28.4	
3	-	0.0	0.4	0.8	2.7	-	-	3.6	30.6	
4	-	0.1	0.9		-	-	-	5.4	30.7	
5	-	0.5	0.9		3.3	-	-	3.9	29.4	(SE2382)
6	-	0.1	0.9		2.9	-	-	3.0	30.8	
7	-	0.9			1.7	-	-	4.8	30.3	
8	-	0.1	0.7		2.8	0.5	3.3	3.4	26.8	
9	-	0.9			2.4	-	-	3.1	30.4	
10	-	0.0	0.1	0.2	2.0	-	-	2.6	5.8	
11	-	0.6	0.9		2.8	-	-	3.2	32.0	
12	-	0.1	0.9		3.3	0.2	-	3.0	30.7	
13	-	0.1	0.9		2.5	0.2	-	2.4	32.4	
14	-	1.0			2.3	-	-	2.9	33.3	
15	-	0.2	0.9		2.6	-	-	3.1	32.7	(SE2383)
17	-	0.8			1.8	-	-	2.4	24.6	
18	+/-	0.9			2.3	-	2.7	4.0	31.2	(SE2377)
19	+/-	0.9			2.6	-	-	2.7	33.1	(SE2378)
20	-	0.8			0.9	7.6	-	2.2	11.4	
21	-	1.0			1.9	-	-	2.6	31.9	
22	-	0.2	0.5	0.8	2.5	4.9	-	2.9	28.2	
23	-	0.2	0.9		2.6	-	-	2.9	33.2	
24	-	0.3	0.9		2.5	3.8	-	3.0	29.2	
25	-	0.0	0.4	0.9	3.1	-	-	2.7	32.6	(SE2384)
26	-	0.5	0.9		2.4	4.5	-	2.7	27.4	
27	-	0.0	0.9		2.1	0.2	-	2.5	32.0	
28	-	0.5	0.5	0.6	3.3	0.6	3.5	4.9	26.3	

Table 3-1. Continued.

Isolate	O.D. (420 nm) at culture time (hrs)				Fermentation Products (mM)					Reference
	24	48	72	91	Succinate	Lactate	Formate	Acetate	Ethanol	
29	-	0.1	0.1	0.9	3.1	-	-	3.6	32.2	
30	-	0.0	0.0	0.7	2.1	-	-	2.8	23.5	
31	-	0.1	0.9		2.3	-	-	2.8	32.8	SE2385
32	-	0.4	0.9		2.9	-	-	3.0	32.0	
AH242	-	-	-	-	-	-	-	-	-	
W3110	0.6				4.2	18.5	2.6	9.3	7.3	wild type

-, No detectable growth

“-“ in fermentation products indicates undetectable level of the product.

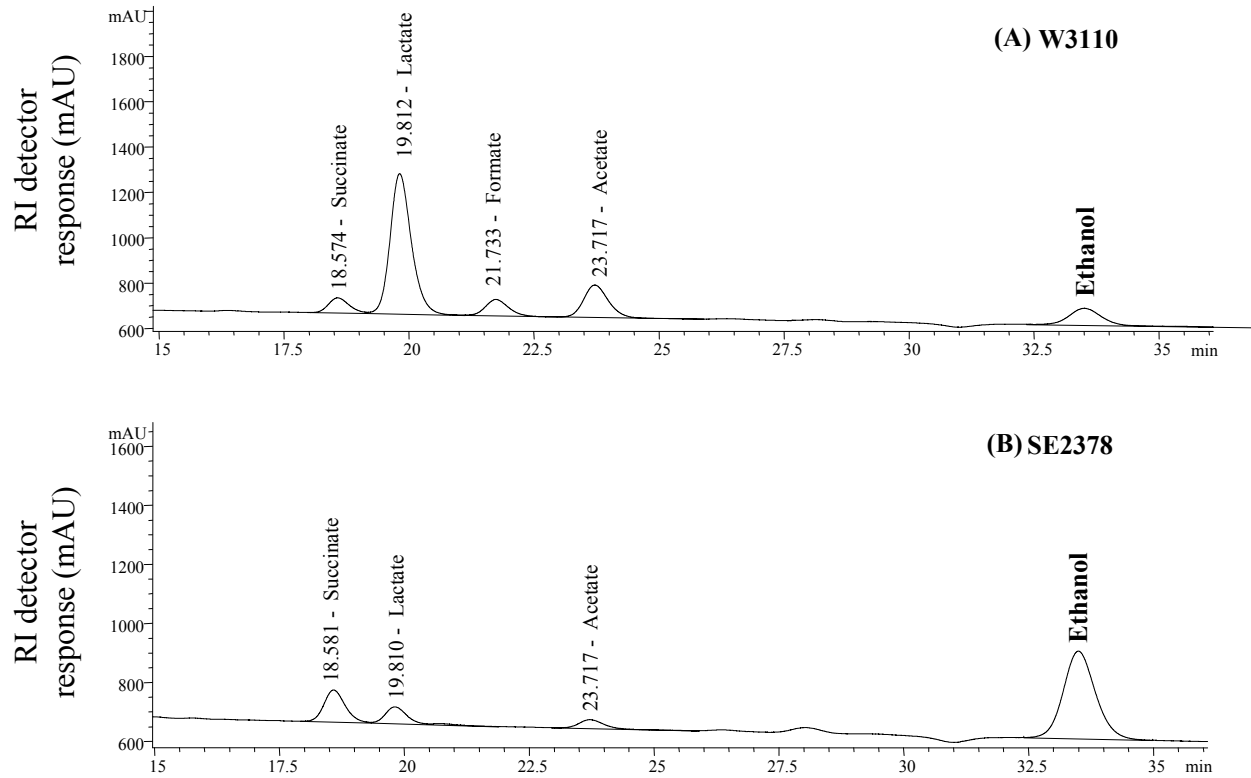


Figure 3-1. HPLC analysis of fermentation products. (A) strain W3110, (B) strain SE2378 in LB+glucose (1 %, w/v) in batch fermentations.

Cells were harvested after 36 hours.

See Methods for HPLC analysis.

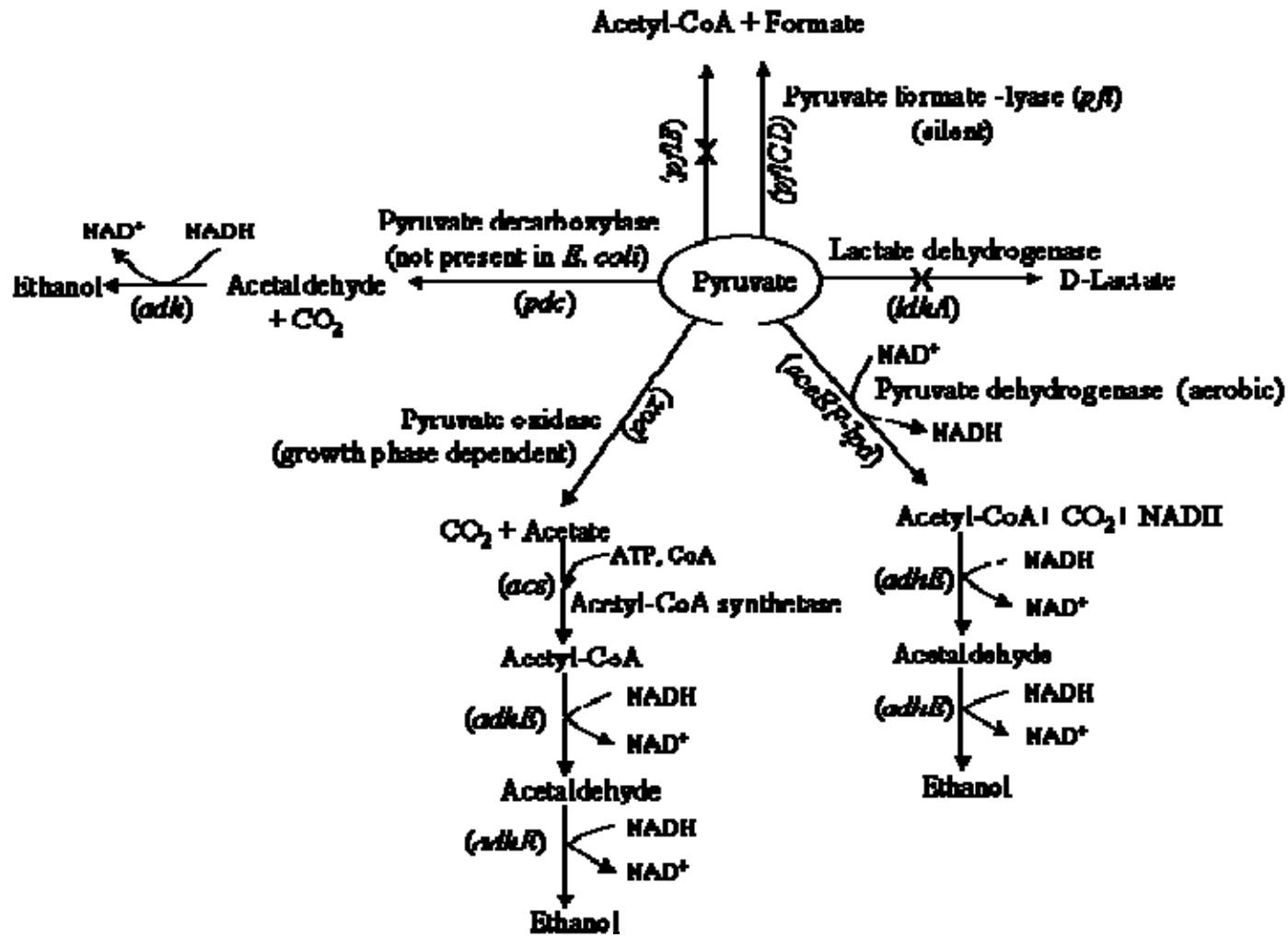


Figure 3-2. Metabolic fates of pyruvate in *E. coli*. X indicates deletion of the gene. *adhE*, alcohol dehydrogenase

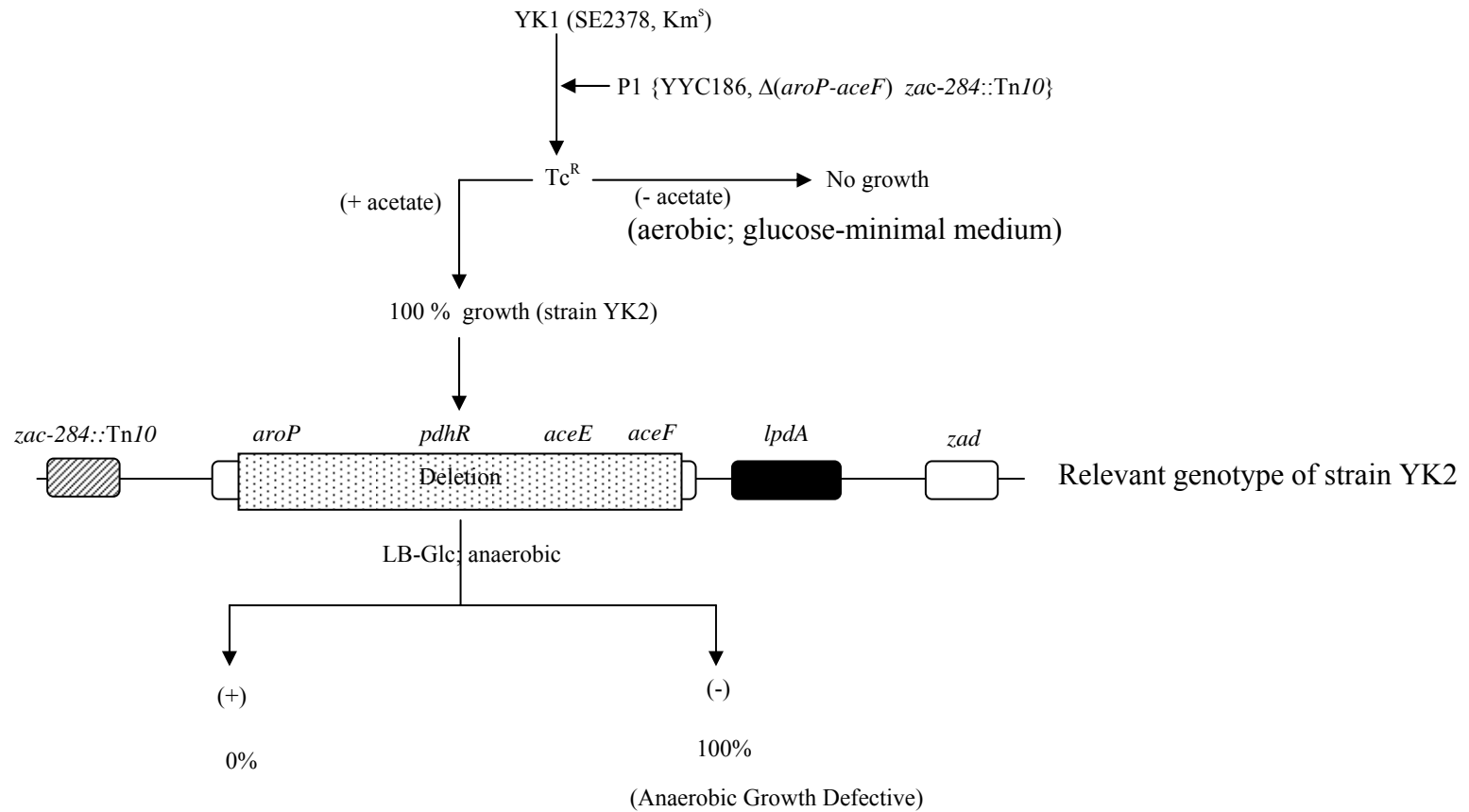


Figure 3-3. Effect of deleting *pdh* genes in strain SE2378 on anaerobic growth.

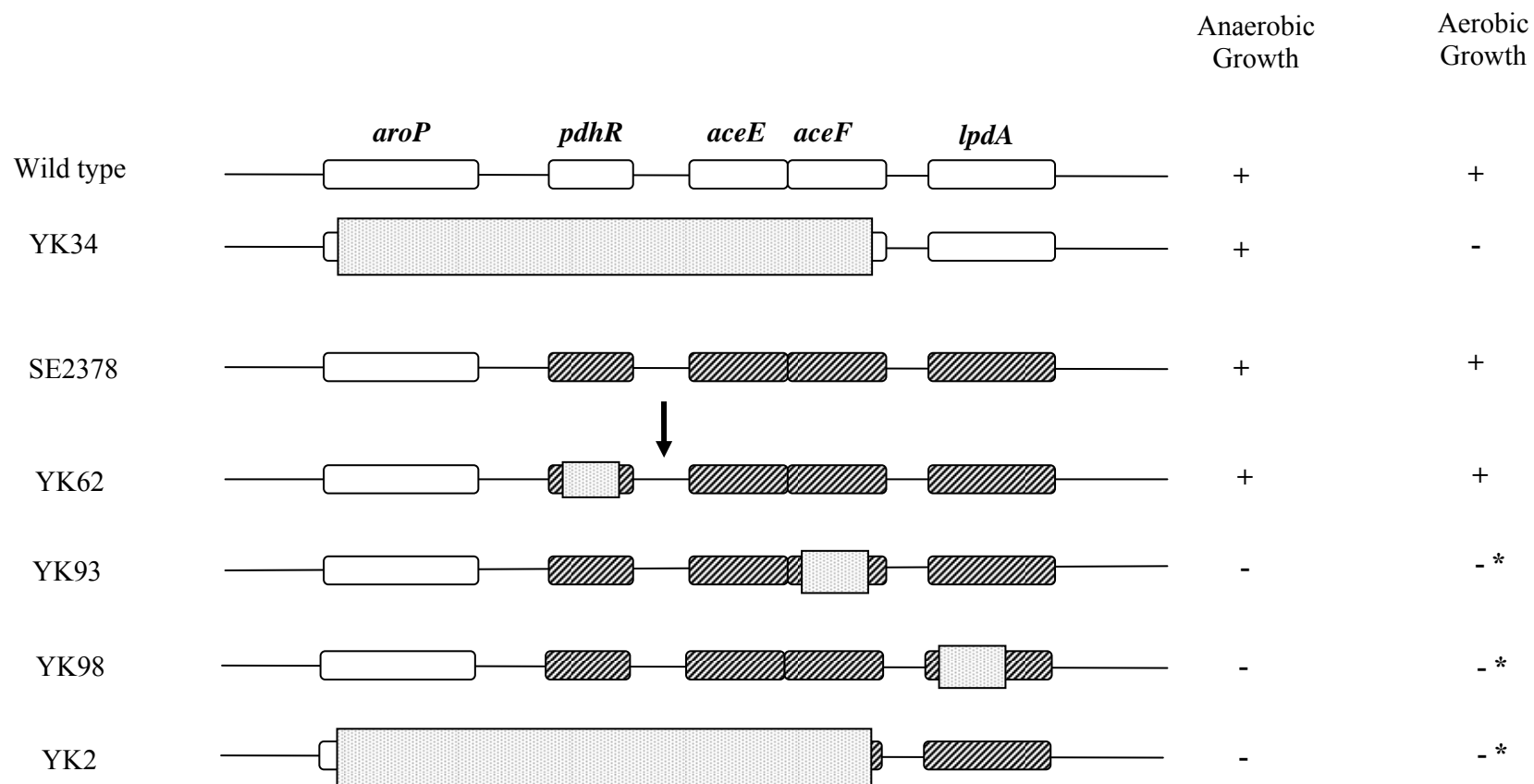


Figure 3-4. Growth characteristics of various deletion derivatives of wild type W3110 and strain SE2378.

Aerobic growth was tested in glucose-minimal medium.

* Growth (+) only with acetate supplementation ($1 \text{ mg} \cdot \text{ml}^{-1}$).

; wild type genes, ; mutant genes, ; deletion

Table 3-2. Growth characteristics of ethanologenic *E. coli* strain SE2378 with a mutation in *aceF* and its transductants.

Strain	Relevant genotype	Specific growth rate (h ⁻¹)			
		Aerobic		Anaerobic	
		LB	Minimal	LB	Minimal
W3110	wild type	1.31	1.05	0.98	0.51
AH242	$\Delta ldhA$, $\Delta(focA-pflB)$, Km ^R	1.21	0.97	-	-
SE2378	AH242, anaerobic+	1.18	0.51	0.46	NG*
YK153	W3110, <i>aceF</i>	0.46	NG (0.55)	1.07	0.44
YK152	AH242, <i>aceF</i>	0.83	NG (0.54)	NG	NG
YK157	YK152, <i>aceF</i> ⁺ (W3110)	1.32	0.96	NG	NG
YK158	YK152, <i>aceF</i> ⁺ (SE2378)	1.17	0.51	0.45	NG*

NG – no growth.

Values in parenthesis represent the specific growth rate in glucose minimal medium with acetate (1 mg ml⁻¹) under aerobic conditions.

* Growth in the presence of glutamate (100 µg/ml).

W3110	PdhR	1	MAYSKIRQPKL <u>S</u> DVIEQQLEFLILEGTLRPGEKLPPERELAKQFDVSRPS
SE2377	PdhR	1
SE2378	PdhR	1 <u>P</u>
SE2382	PdhR	1
W3110	PdhR	51	LREAIQRLEAKGLLLRRQGGGTFVQSSLWQSFSDPLVELLSDHPESQYDL
SE2377	PdhR	51
SE2378	PdhR	51
SE2382	PdhR	51
W3110	PdhR	101	LETRHALEGIAAYYAAL-RSTDEDKERIRELHHAIELAQQSGDLDAESNA
SE2377	PdhR	101-
SE2378	PdhR	101 <u>L</u>
SE2382	PdhR	101-
W3110	PdhR	150	VLQYQIAVTEAAHNVVLLHLLRCMEPMLAQNVRQNFELLYSRREMLPLVS
SE2377	PdhR	150
SE2378	PdhR	151
SE2382	PdhR	150
W3110	PdhR	200	SHRTRIFEAIMAGKPEEAREASHRHAFIEEILLDRSREESRRERSLRRLL
SE2377	PdhR	200
SE2378	PdhR	201
SE2382	PdhR	200
W3110	PdhR	250	EQRKN
SE2377	PdhR	250
SE2378	PdhR	251
SE2382	PdhR	250

Figure 3-6. Comparison of amino acid sequence of PdhR from wild-type (W3110), and three ethanogenic mutants (SE2378, SE2377 and SE2382).

```

W3110      1  CAACGAAAGAATTAGTGATTTTTCTGGTAAAAATTATCCAGAAGATGTTG
SE2377    1  .....
SE2378    1  .....
SE2385    1  .....

W3110     51  TAAATCAAGCGCATATAAAAGCGCGCAACTAAACGTAGAACCTGTCTTA
SE2377    51  .....
SE2378    51  .....
SE2385    51  .....

W3110     101 TTGAGCTTTCCGGCGAGGAGTTCAATGGGACAGGTTCCAGAAAACCTCAACG
SE2377    101 .....
SE2378    101 .....A.....
SE2385    101 .....

W3110     151 TTATTAGATAGATAAGGAATAACCCATGTCAGAACGTTTC
SE2377    151 .....
SE2378    151 .....
SE2385    151 .....

```

Figure 3-7. Nucleic acid sequence of intergenic region between *pdhR* and *aceE* genes of the ethanologenic mutants and the wild type. The mutated nucleotide is underlined and the translation start codon of *aceE* gene is in bold.

W3110	LPD	1	MSTEIKTQVVVLGAGPAGYSAAFRCADLGLETVIVERYNTLGGVCLNVGC
SE2377	LPD	1
SE2378	LPD	1
SE2382	LPD	1
SE2383	LPD	1
SE2384	LPD	1
SE2385	LPD	1
W3110	LPD	51	IPSKALLHVAKVIEEAKALAEHGIVFGEPKTDIDKIRTWKEKVINQLTGG
SE2377	LPD	51
SE2378	LPD	51
SE2382	LPD	51
SE2383	LPD	51
SE2384	LPD	51
SE2385	LPD	51
W3110	LPD	101	LAGMAKGRKVKVVNGLGKFTGANTLEVEGENGKTVINFDNAIIAAGSRPI
SE2377	LPD	101
SE2378	LPD	101
SE2382	LPD	101
SE2383	LPD	101
SE2384	LPD	101
SE2385	LPD	101
W3110	LPD	151	QLPFIPHEDPRIWDSTDALELKEVPERLLVMGGGIIGLEMGTVYHALGSQ
SE2377	LPD	151
SE2378	LPD	151
SE2382	LPD	151
SE2383	LPD	151
SE2384	LPD	151
SE2385	LPD	151
W3110	LPD	201	IDVVEVFDQVIPAADKDIVKVFTKRISKKNLMLLETKVTAVEAKEDGIYV
SE2377	LPD	201
SE2378	LPD	201
SE2382	LPD	201
SE2383	LPD	201
SE2384	LPD	201
SE2385	LPD	201
W3110	LPD	251	TMEGKKAPAEPQRYDAVLVAIGRVPNGKNLDAGKAGVEVDDRGFIRVVKQ
SE2377	LPD	251
SE2378	LPD	251
SE2382	LPD	251
SE2383	LPD	251
SE2384	LPD	251
SE2385	LPD	251

Figure 3-8. Comparison of the amino acid sequence of LPD among wild-type strain (W3110) and 6 isolates. The mutated nucleotides are in bold character and underlined.

W3110	LPD	301	LRTNVPHIFAIGDIVQPMLA <u>H</u> HKGVHEGHVAAEVIAGKKHYFDPKVIPSI
SE2377	LPD	301 <u>Y</u>
SE2378	LPD	301
SE2382	LPD	301
SE2383	LPD	301 <u>Y</u>
SE2384	LPD	301 <u>Y</u>
SE2385	LPD	301
W3110	LPD	351	AYT <u>E</u> PEVAWVGLTEKEAKEKGISYETATFPWAASGRAIASDCADGMTKLI
SE2377	LPD	351
SE2378	LPD	351	... <u>K</u>
SE2382	LPD	351	... <u>K</u>
SE2383	LPD	351
SE2384	LPD	351
SE2385	LPD	351	... <u>K</u>
W3110	LPD	401	FDKESHRVIGGAIVGTNGGELLGEIGLAIEMGCDAEDIALTIHAHPTLHE
SE2377	LPD	401
SE2378	LPD	401
SE2382	LPD	401
SE2383	LPD	401
SE2384	LPD	401
SE2385	LPD	401
W3110	LPD	451	SVGLAAEVFEFSITDLPNPKAKKK
SE2377	LPD	451
SE2378	LPD	451
SE2382	LPD	451
SE2383	LPD	451
SE2384	LPD	451
SE2385	LPD	451

Figure 3-8. Continued.

Table 3-3. Anaerobic growth and fermentation profile of *E. coli* with different *lpd* alleles.

Strain	Relevant Genotype	Anaerobic Growth	Fermentation products (mM)					
			Succinate	Lactate	Formate	Acetate	Ethanol	
AH242	$\Delta ldh, \Delta pfl, Km^R$	-						No growth
YK29	$\Delta ldh, \Delta pfl, Km^S$	-						No growth
YK100	YK29, $\Delta lpdA$	-						No growth
YK128	YK100 (+ <i>lpd</i> ⁺)	-						No growth
YK129	YK100 (+ <i>lpd</i> [*])	+	11.9	0.8	0.0	3.6	68.0	

Anaerobic growth and fermentation were in LB+glucose in batch fermentations without pH control. See text for other details.

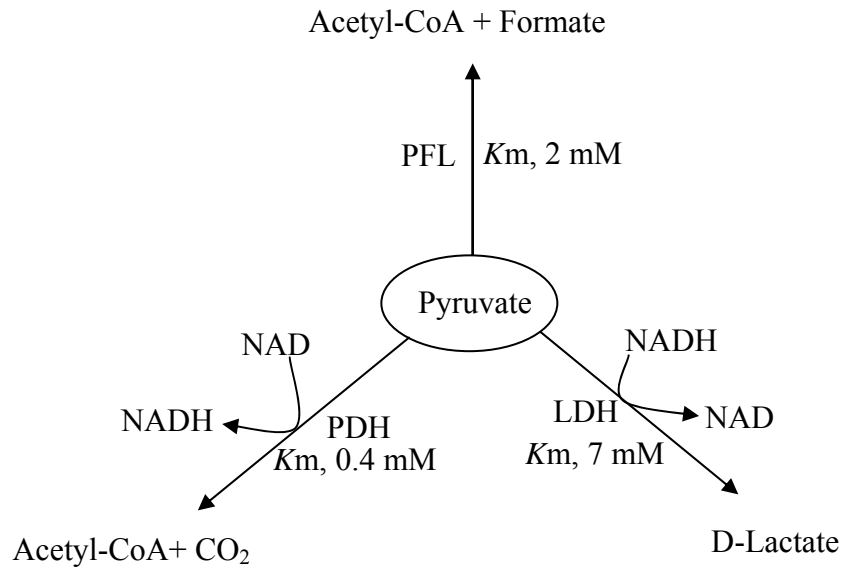


Figure 3-9. Pyruvate metabolic enzymes in strain SE2378 and their affinity for pyruvate.

Table 3-4. Fermentation profile of mutant strains with different pyruvate metabolic pathway composition^a.

Strain	Relevant Genotype	Enzyme(s) present	Growth	Fermentation Products (mM)					% of ethanol in products
				Succinate	Lactate	Formate	Acetate	Ethanol	
W3110	wild type	PFL, LDH	+	4.2	18.5	2.6	9.3	7.3	22.8
YK142	Δlpd , lpd^*	PFL, LDH, PDH*	+	3.6	15.8	3.7	8.8	8.7	23.6
AH240	$\Delta(focA-pflB)$	LDH	+	3.9	24.9	-	5.1	-	0
YK144	$\Delta(focA-pflB)$, lpd^*	LDH, PDH*	+	3.8	24.4	-	4.5	-	0
AH241	$\Delta ldhA$	PFL	+	2.2	0.6	4.7	5.5	10.8	56.5
YK146	$\Delta ldhA$, lpd^*	PFL, PDH*	+	2.3	1.2	7.2	6.9	49.1	82.5
AH242	$\Delta ldhA$, $\Delta(focA-pflB)$		No Growth						
SE2378	$\Delta ldhA$, $\Delta(focA-pflB)$, lpd^*	PDH*	+	4.1	0.8	0	4.7	107.3	91.5

^a Fermentation was conducted in LB+glucose in batch fermentations.

* Pyruvate dehydrogenase with the mutated LPD (lpd^*).

Table 3-5. Pyruvate dehydrogenase mRNA, transcription and protein levels in aerobic and anaerobic *E. coli* wild type, strain W3110 and ethanologenic mutant, strain SE2378.

Strain	Relative mRNA level ^a		β -galactosidase Activity ^b		PDH Activity ^c	
	+ O ₂	- O ₂	+ O ₂	- O ₂	+ O ₂	- O ₂
W3110	1.00	0.98	600	630	370	185
SE2378	0.71	0.77	570	680	240	200

^a Relative mRNA levels were determined by quantitative RT-PCR and the level of *aceE* mRNA in cells grown under aerobic conditions was taken as 1.0 and the relative level of *aceE* mRNA for the other growth conditions and strain SE2378 was determined.

^b β -galactosidase activity of *pdhR-lacZ* fusion is presented as nmoles min⁻¹ (mg protein)⁻¹.

^c PDH activity represents the pyruvate decarboxylase (E1) activity of the PDH complex - nmoles ferricyanide reduced min⁻¹ (mg protein)⁻¹.

See Methods section for details.

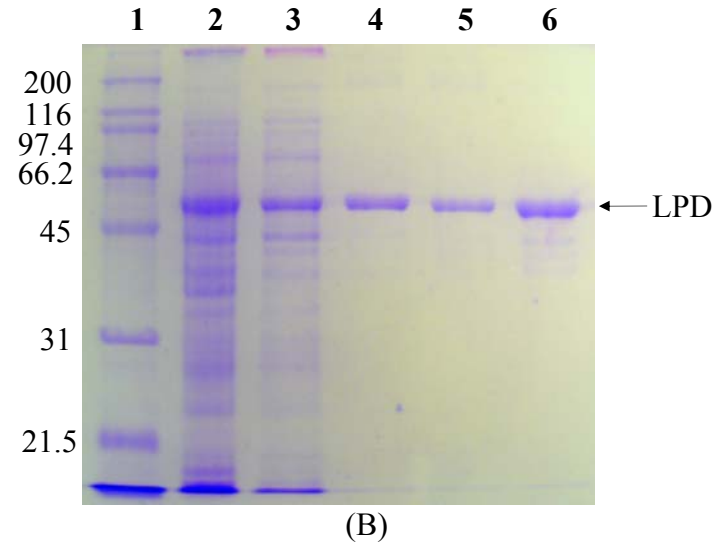
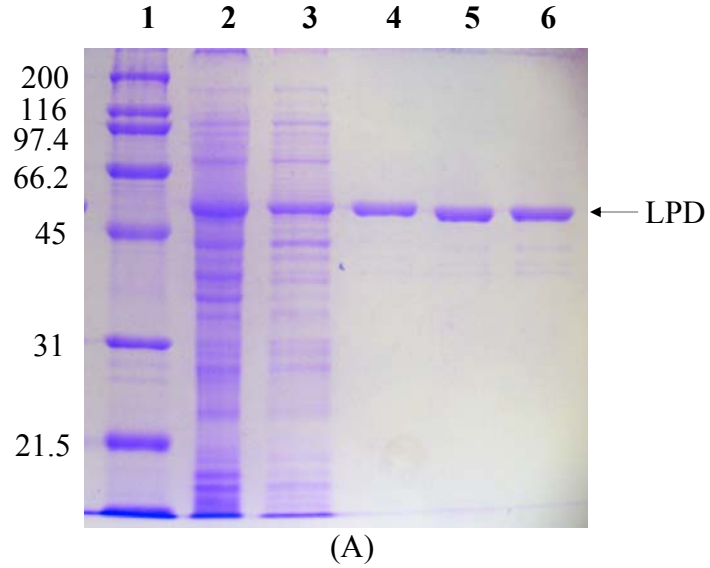


Figure 3-10. SDS-Polyacrylamide gel electrophoresis of purified dihydrolipoamide dehydrogenase (LPD) from wild-type, A) W3110 and B) the ethanologenic strain SE2378. Lane 1, Molecular weight markers in KDa, lane 2, cells; lane 3, crude extract; lane 4, after affinity chromatography (Ni^{2+} column); lane 5, after Thrombin treatment; lane 6, after gel filtration.

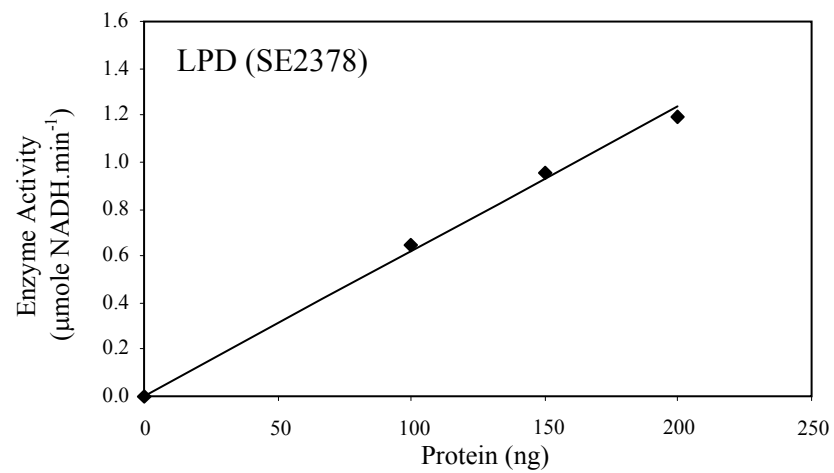
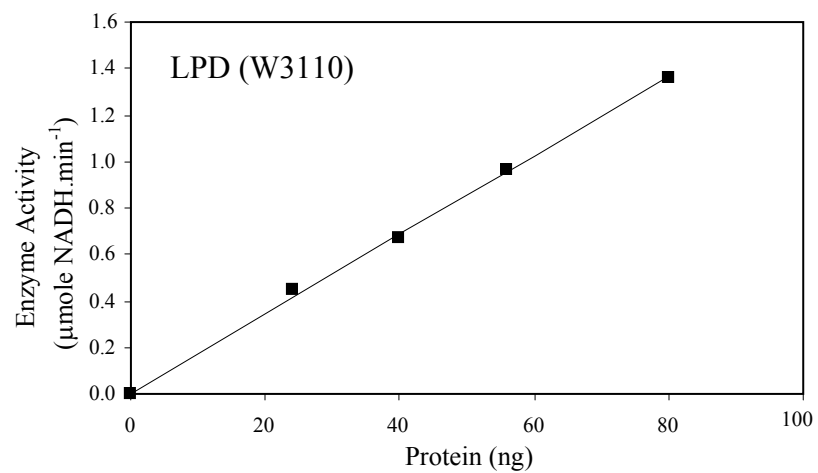


Figure 3-11. Linearity of LPD protein concentration vs. activity of the enzyme in the forward reaction.

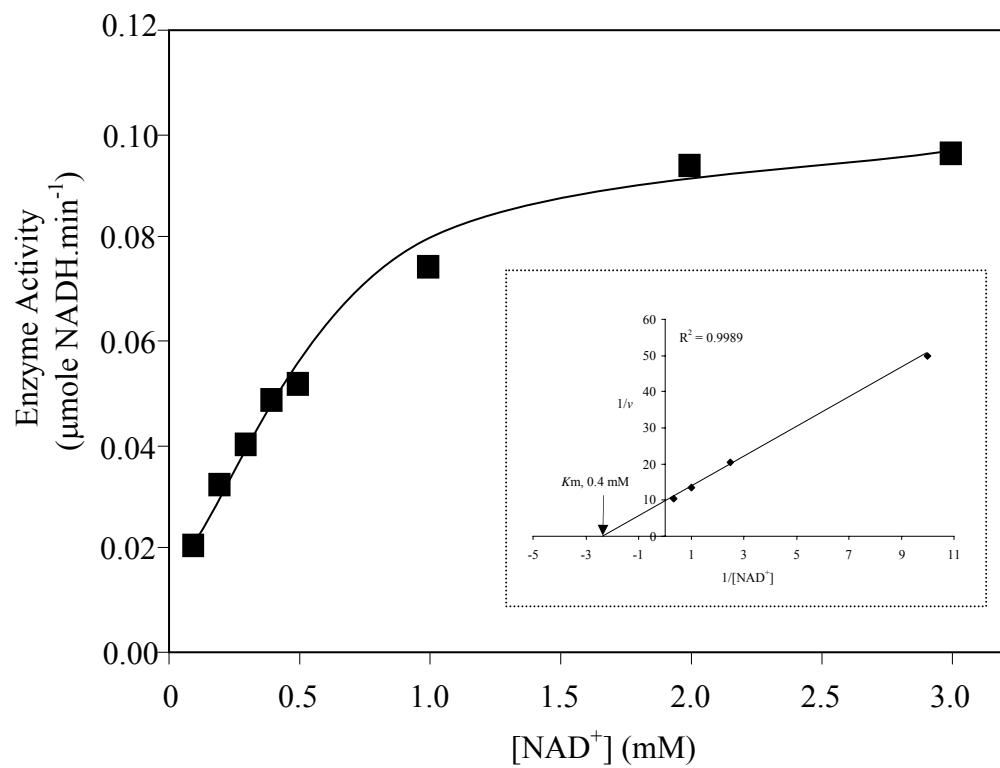


Figure 3-12. Native LPD (W3110) activity with various NAD⁺ concentrations.

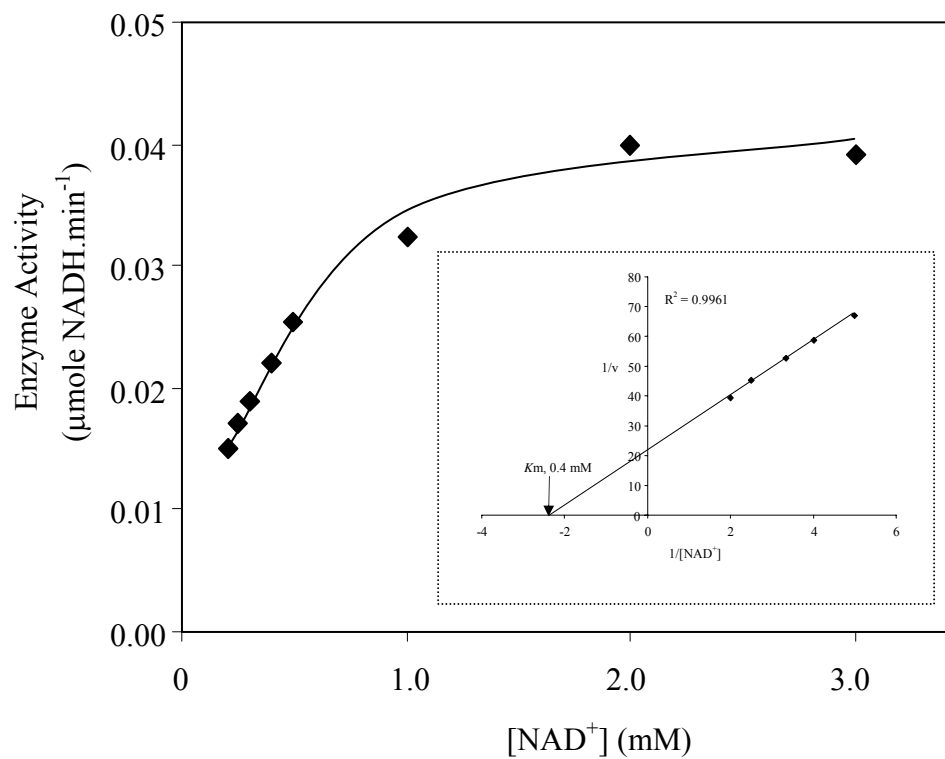


Figure 3-13. Mutated LPD (SE2378) activity with various NAD⁺ concentrations.

Table 3-6. Kinetic constants of the native (W3110) and the mutated (SE2378) LPD .

	<i>K_m</i>	<i>K_i</i>	<i>K_{cat}</i>	<i>K_{cat}/K_m</i>
	NAD ⁺ (mM)	NADH (mM)	S ⁻¹	M ⁻¹ S ⁻¹
Native LPD	0.4	5.2	1.7 x 10 ³	4.2 x 10 ⁶
Mutated LPD	0.4	not determined	4.3 x 10 ²	1.1 x 10 ⁶

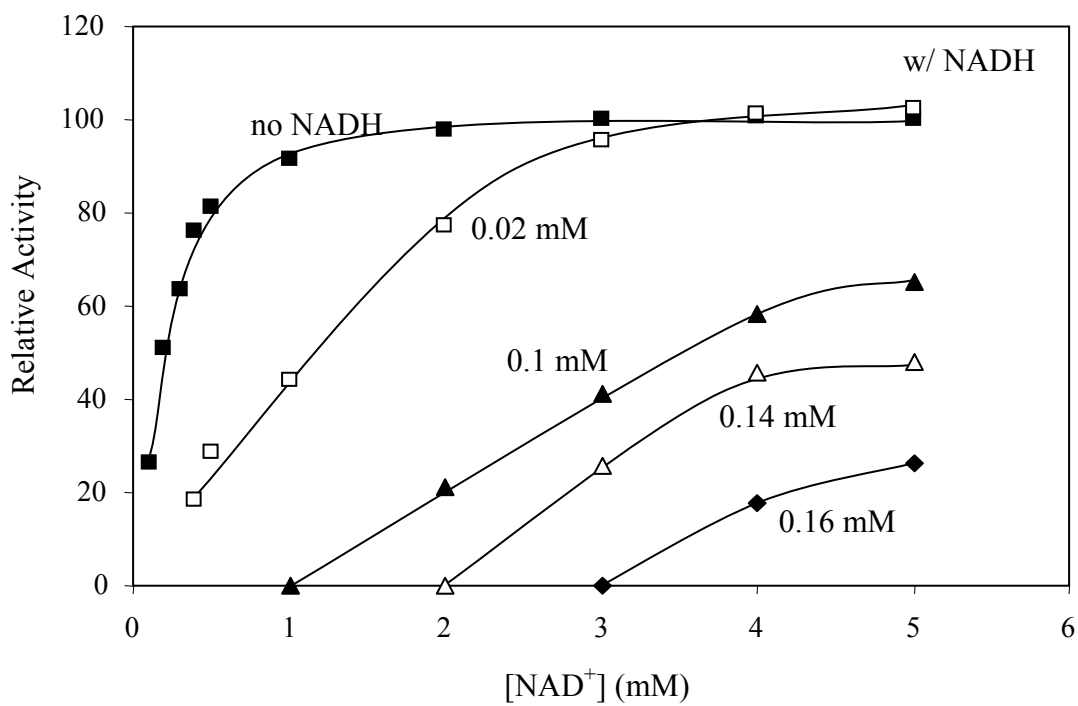


Figure 3-14. Inhibition of native LPD (W3110) forward activity by NADH. Relative activity was calculated from specific activity, $\mu\text{moles NADH min}^{-1} (\text{mg protein})^{-1}$.

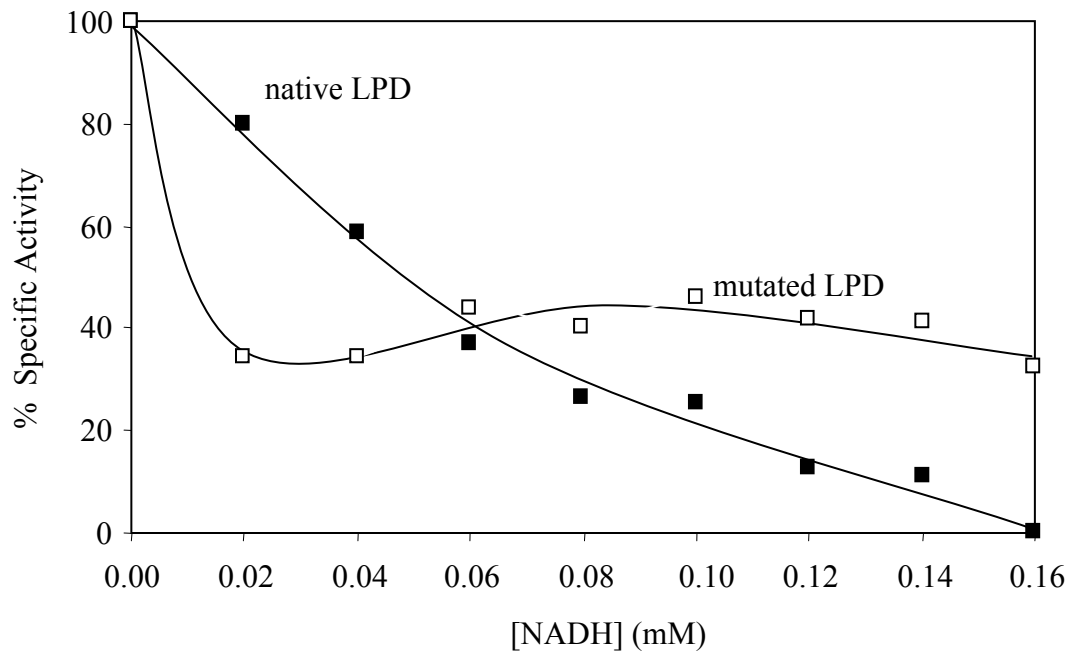


Figure 3-15. Inhibition of LPD activity by NADH (2.0 mM NAD⁺) on forward reaction.

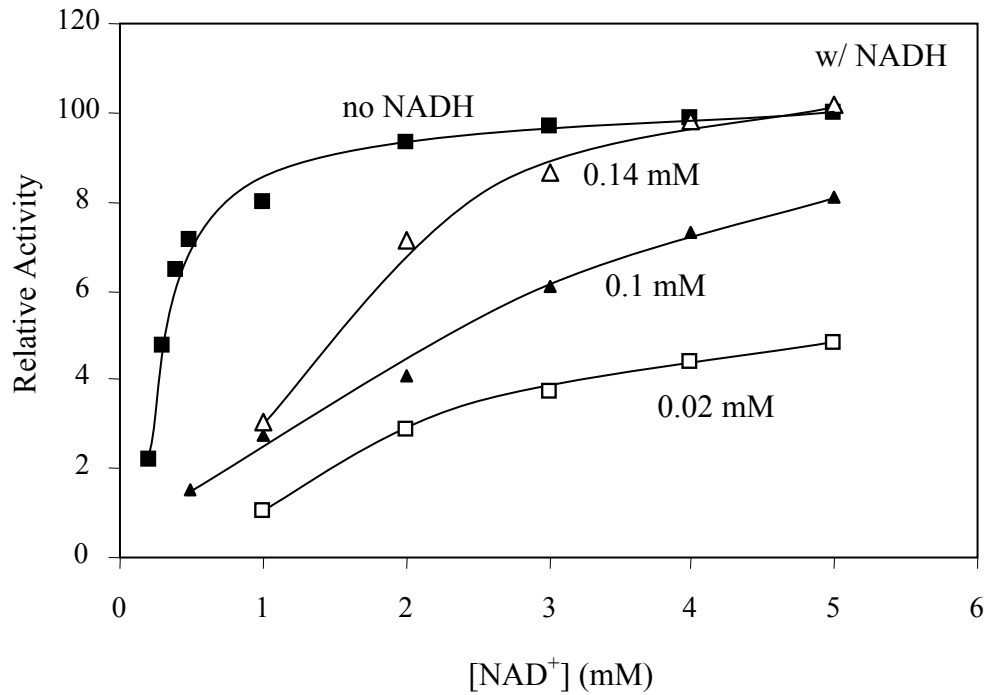


Figure 3-16. Inhibition of mutated LPD (SE2378) by NADH.
 Relative activity was calculated from specific activity, $\mu\text{moles NADH min}^{-1} (\text{mg protein})^{-1}$.

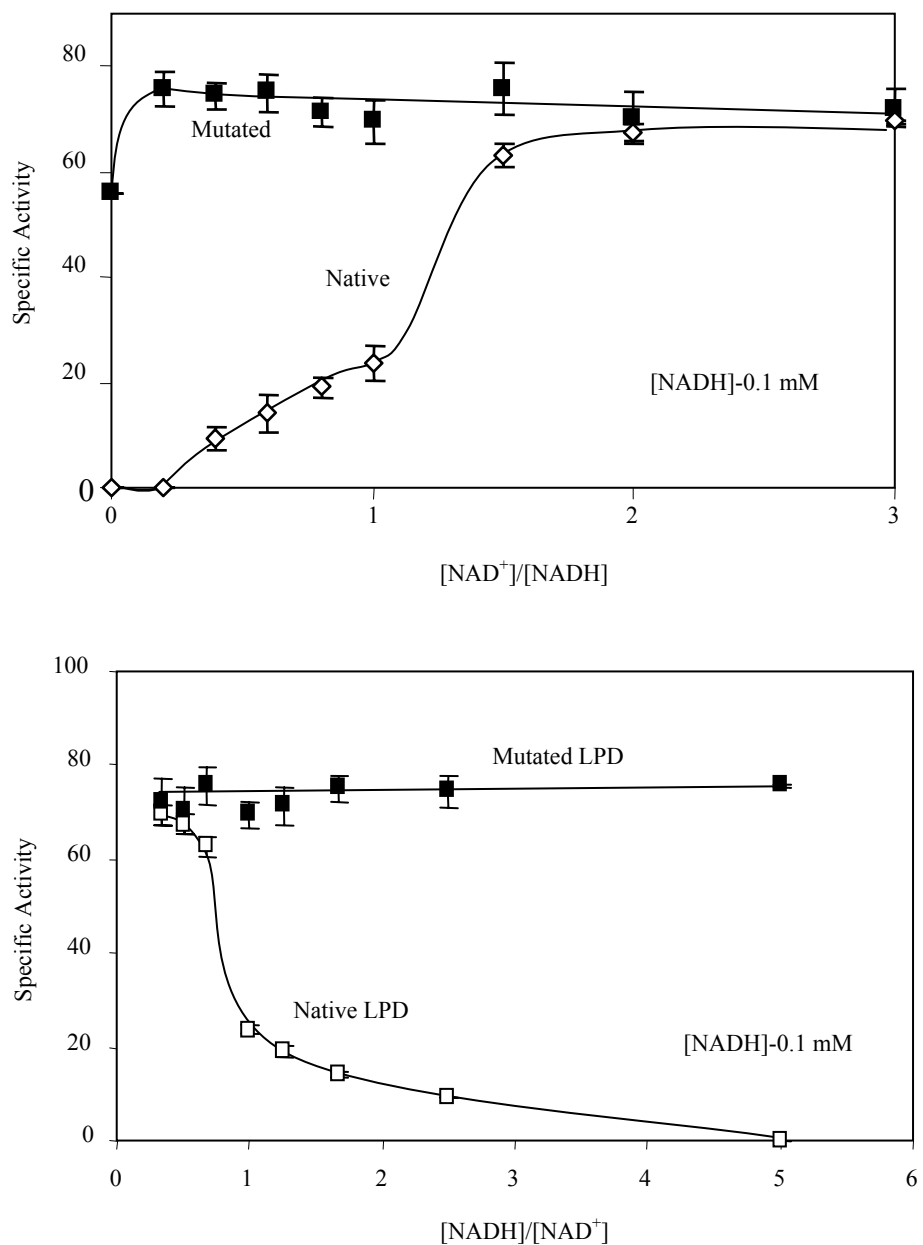


Figure 3-17. Activation of LPD reverse reaction by increasing $NAD^+/NADH$ ratio. Top panel, $NAD^+/NADH$; Bottom panel, $NADH/NAD^+$. $NADH$ (0.1 mM) and various concentrations of NAD^+ were used in the determination of LPD activity by the reverse reaction. Specific activity, $\mu\text{moles } NADH \text{ min}^{-1} (\text{mg protein})^{-1}$.

Table 3-7. Purification of native PDH complex from *E. coli* strain W3110.

Purification step	Volume (ml)	Protein Conc. (mg/ml)	Total protein (mg)	Specific activity ^a	Total activity ^b	yield (%)	purification fold
Crude extract	25	15.41	385.3	1.6	628.0	100	1
Ultra centrifugation	6	13.68	82.1	3.8	309.4	49	2.3
Hydroxyapatite	15	0.91	13.7	6.0	81.2	13	3.7
Gel filtration	20	0.14	2.8	8.9	24.8	4	5.4

^a $\mu\text{mole NADH min}^{-1}\text{mg protein}^{-1}$

^b $\mu\text{mole NADH min}^{-1}$

Table 3-8. Purification of the mutated PDH complex from strain YK176.

Purification step	Volume (ml)	Protein Conc. (mg/ml)	Total Protein (mg)	Specific Activity ^a	Total Activity ^b	yield (%)	Purification fold
Crude extract	20	27.4	548.0	1.2	657.6	100	1
Ultra centrifugation	5	22.6	112.9	4.6	523.9	80	3.9
Hydroxyapatite	10	1.45	14.5	7.6	109.5	17	6.3
Gel filtration	25	0.29	7.3	9.4	68.2	10	7.8

^a $\mu\text{mole NADH min}^{-1}\text{mg protein}^{-1}$

^b $\mu\text{mole NADH min}^{-1}$

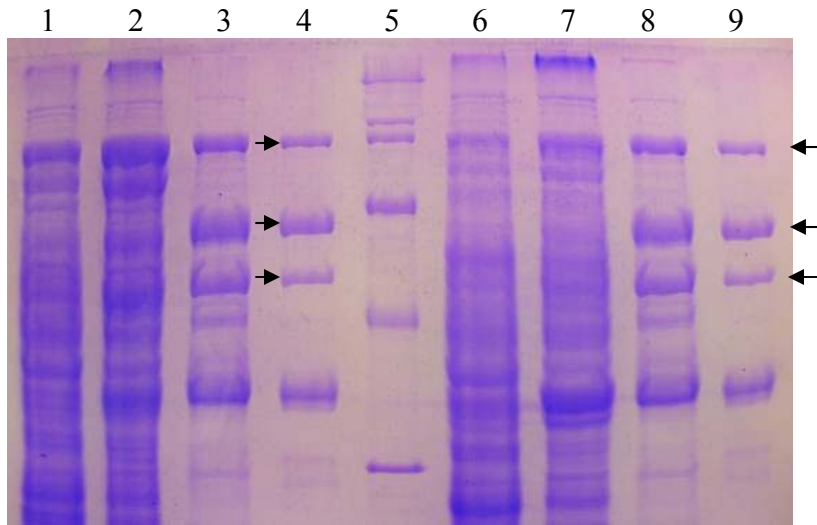


Figure 3-18. SDS-PAGE of partially purified PDH complex. 1,6-crude extract; 2,7-after ultracentrifugation; 3, 8-after hydroxyapatite chromatography; 4, 9-after gel-filtration; 5-molecular weight marker. sizes, top to bottom: 200, 116, 97.4, 66.2, 45, 31, 21.5 (KDa). Lane 1-4, Native enzyme, Lane 6-9, Mutated form of the enzyme. Arrows indicate the components of the PDH complex from top to bottom, E1 (AceE), E2 (AceF), and E3 (LPD).

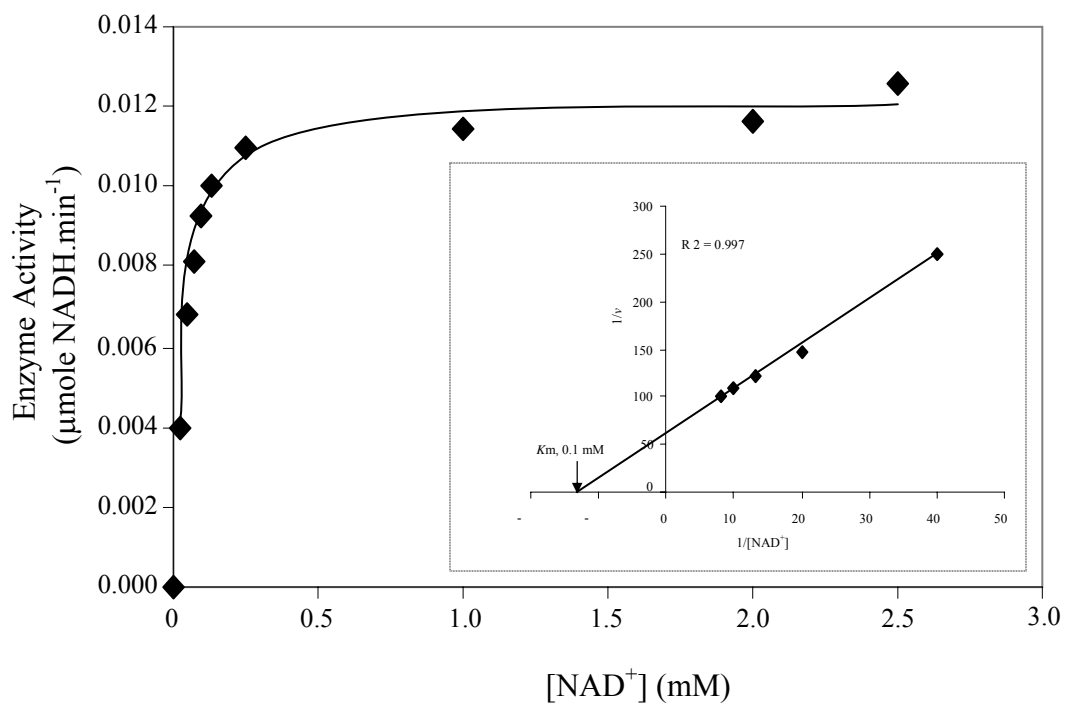


Figure 3-19. Native PDH (W3110) activity with various NAD⁺ concentrations. Enzyme activity is measured with 1.4 µg protein.ml⁻¹.

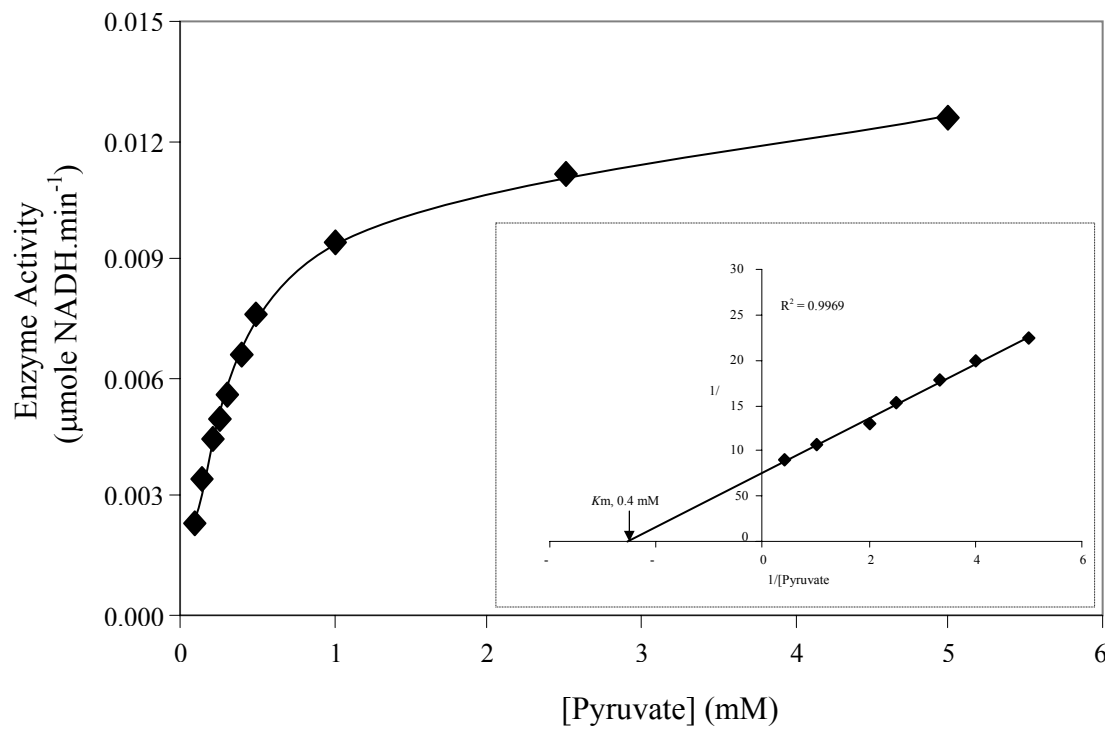


Figure 3-20. Native PDH (W3110) activity with various pyruvate concentrations. Enzyme activity is measured with 1.4 µg protein.ml⁻¹.

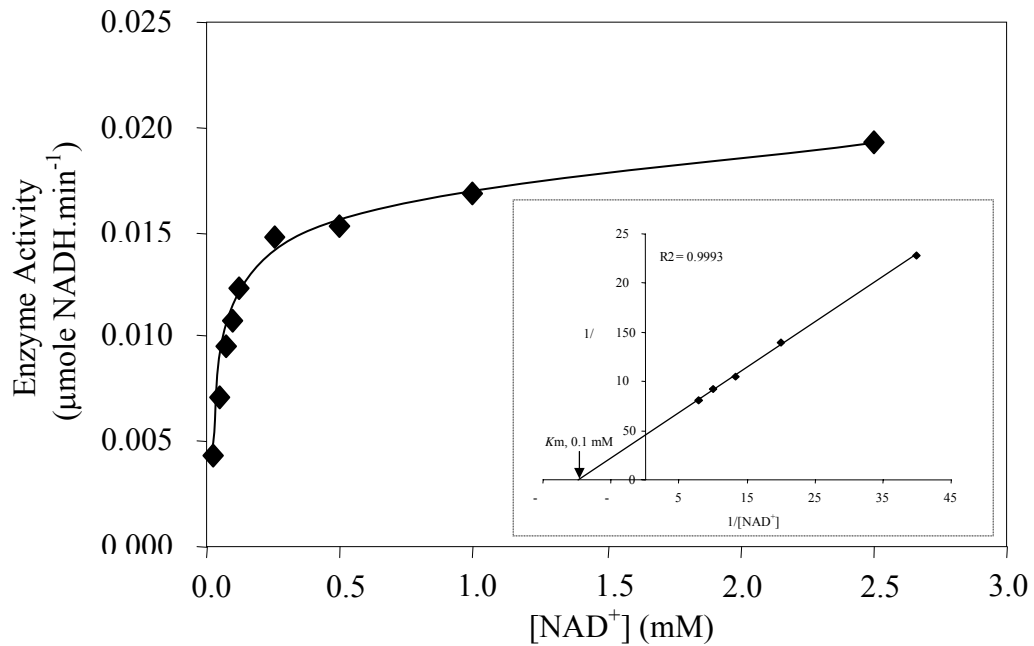


Figure 3-21. Mutated PDH (SE2378) activity with various NAD^+ concentrations. Enzyme activity is measured with $2.9 \mu\text{g protein}\cdot\text{ml}^{-1}$.

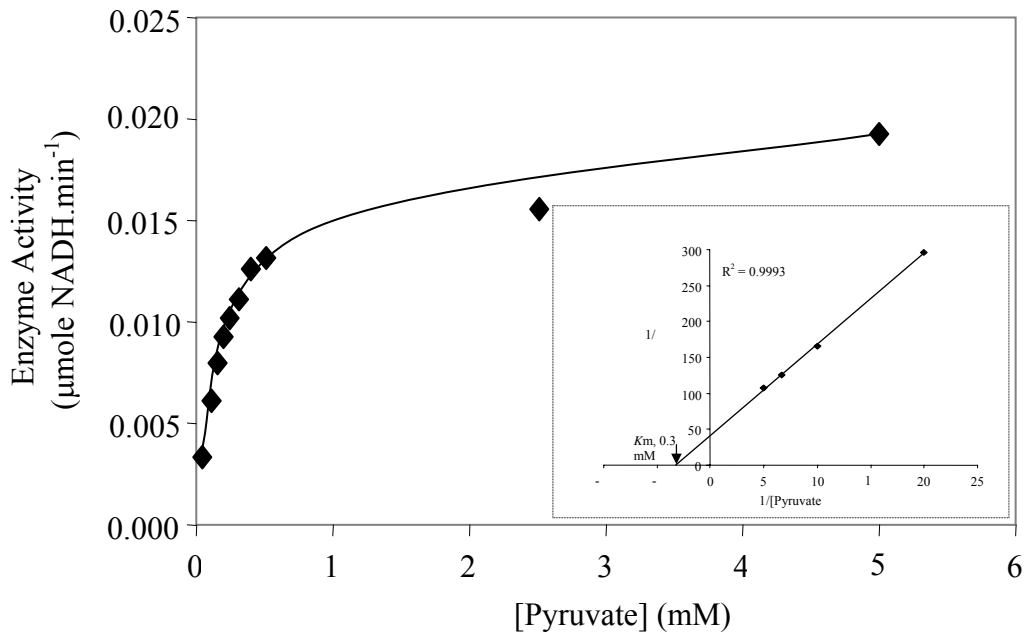


Figure 3-22. Mutated PDH (SE2378) activity with various pyruvate concentrations. Enzyme activity is measured with 2.9 µg protein.ml⁻¹.

Table 3-9. Kinetics constants of the native (W3110) and the mutated (SE2378) PDH.

	<i>K_m</i>		<i>K_{cat}</i>	<i>K_{cat}/K_m</i>	<i>K_i</i>
	NAD ⁺ (mM)	Pyruvate (mM)	S ⁻¹	M ⁻¹ S ⁻¹	NADH (μM)
Native PDH	0.1	0.4	4.5 x 10 ²	4.6 x 10 ⁶	1.0
Mutated PDH	0.1	0.3	3.0 x 10 ²	3.1 x 10 ⁶	10.0

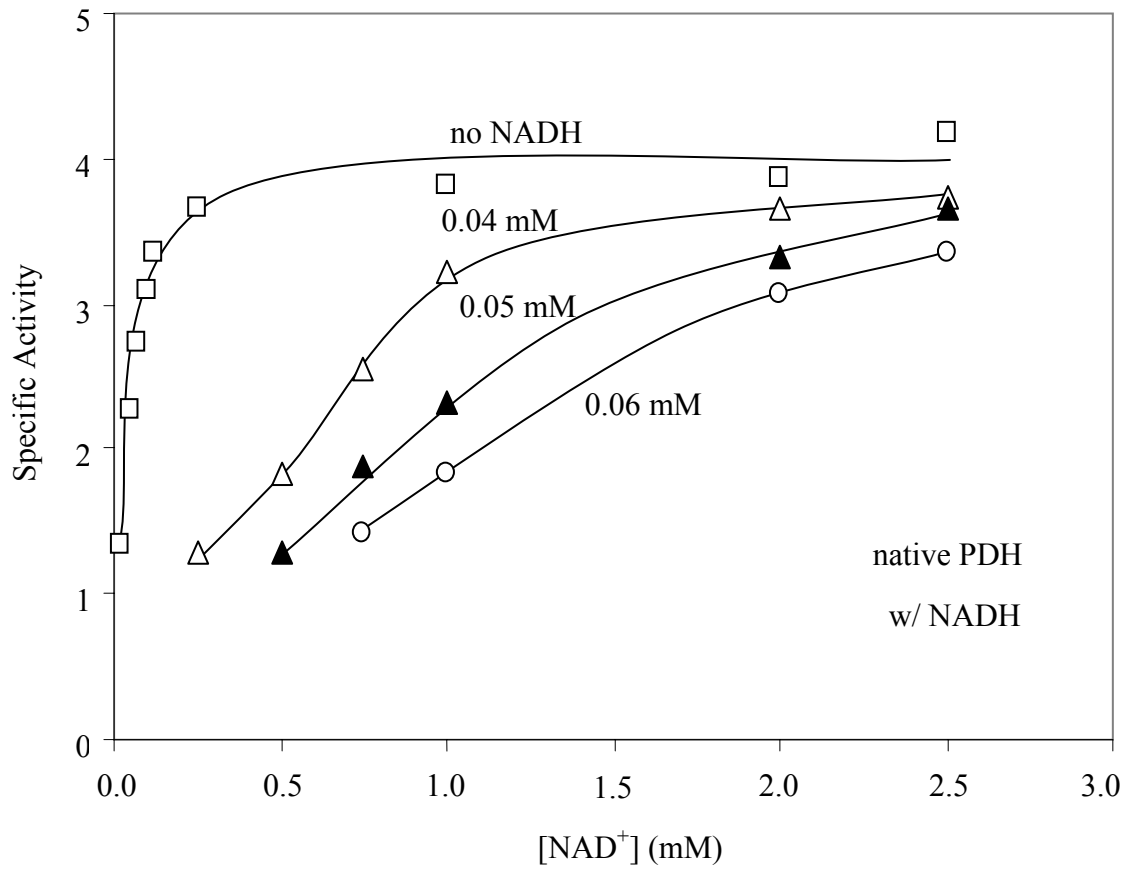


Figure 3-23. Inhibition of native PDH (W310) activity by NADH.
 Specific activity, $\mu\text{mole NADH min}^{-1} \text{mg Protein}^{-1}$.

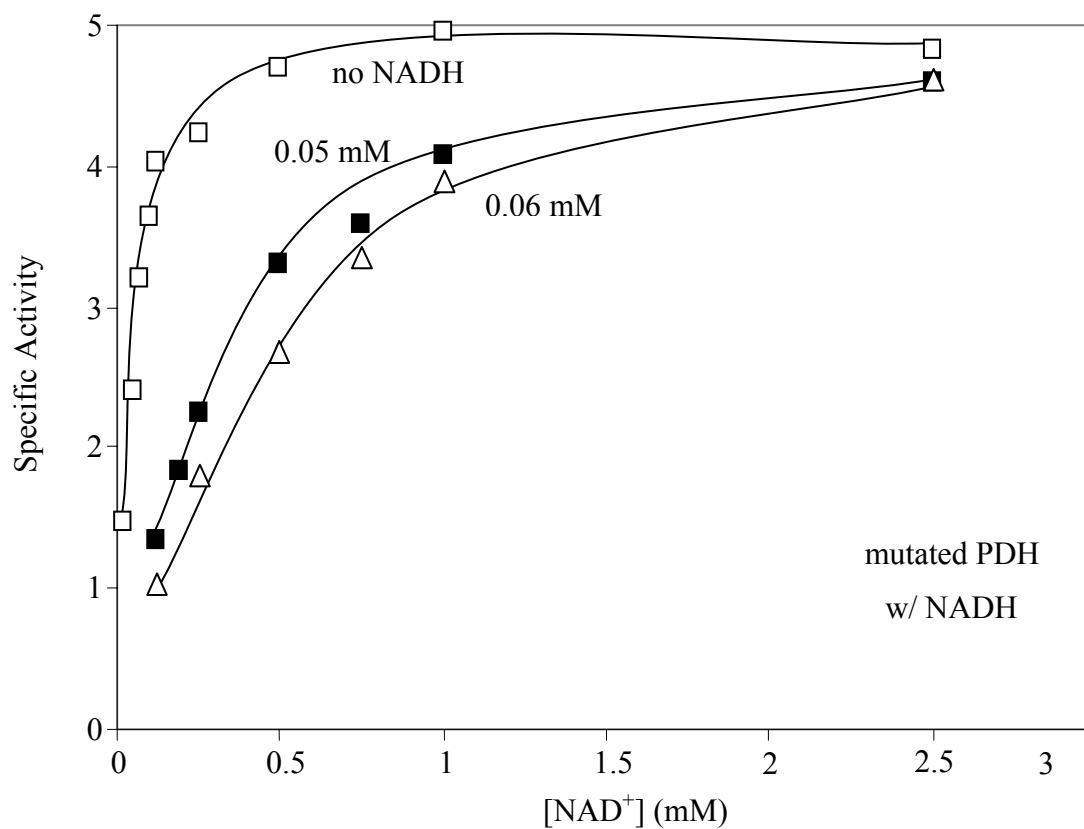


Figure 3-24. Inhibition of mutated PDH (SE2378) by NADH.
 Specific activity, $\mu\text{mole NADH min}^{-1} \text{mg Protein}^{-1}$

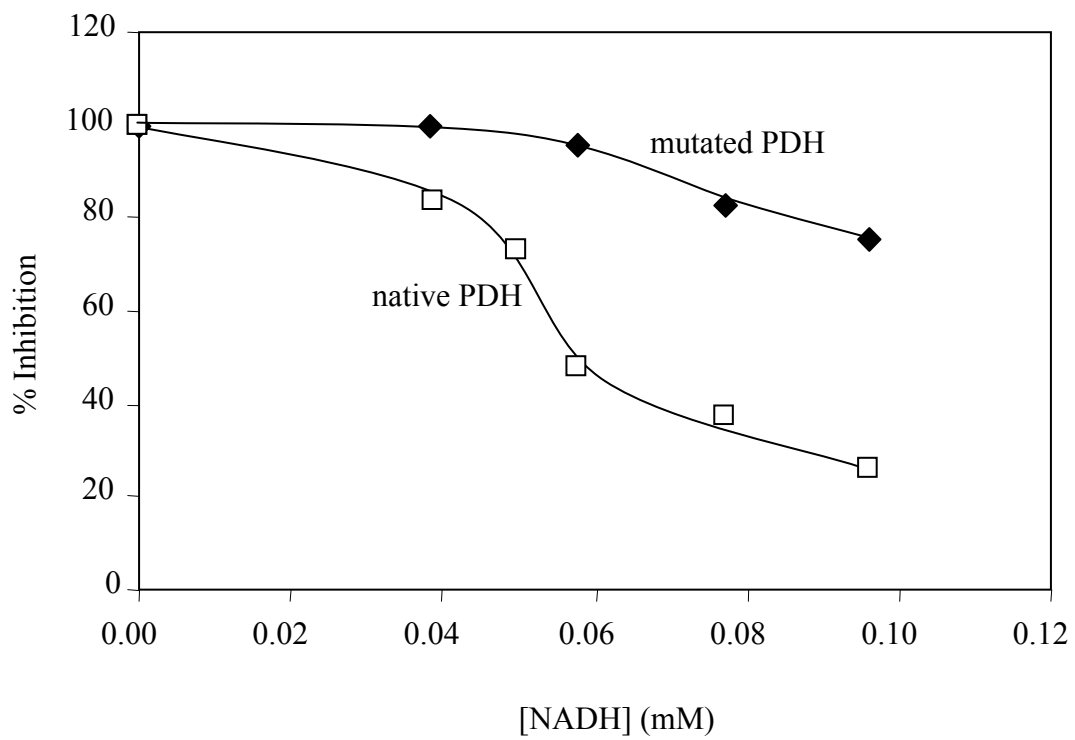


Figure 3-25. Inhibition of PDH complex by NADH at a fixed NAD^+ concentration of 1.0 mM.

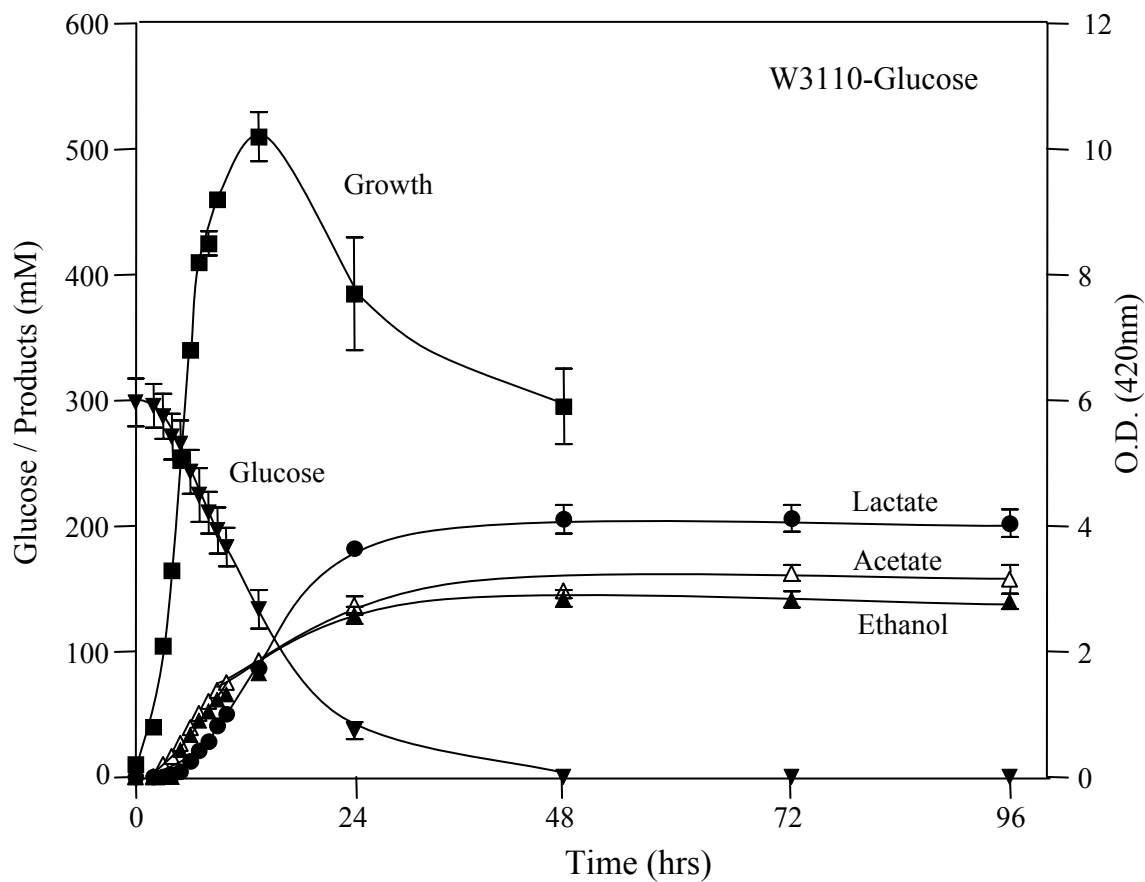


Figure 3-26. Growth and fermentation characteristics of wild type strain W3110 in LB + glucose (50 g L^{-1}) at pH 7.0 and $37 \text{ }^\circ\text{C}$.

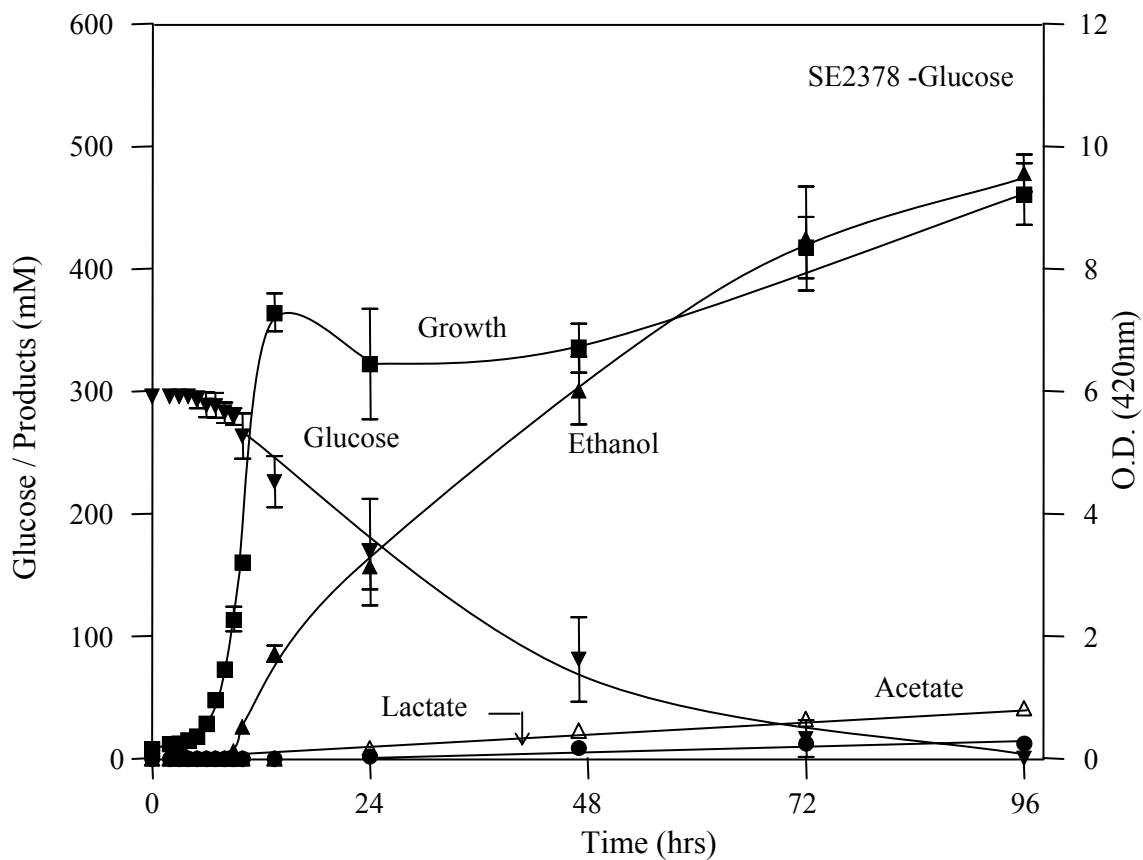


Figure 3-27. Growth and fermentation characteristics of ethanologenic strain SE2378 in LB+ glucose (50 g L^{-1}) at pH 7.0 and 37°C .

Table 3-10. Glucose fermentation characteristics of *E. coli* strain SE2378 and wild type strain W3110.

Strain	Glucose consumed (mM)	μ (h^{-1})	Product Concentration (mM)				Ethanol	
			Succinate	Lactate	Formate	Acetate	Yield	
W3110	298.4 \pm 19.0	0.44	18.4 \pm 0.7	206.1 \pm 10.5	205.6 \pm 11.4	162.4 \pm 6.4	142.4 \pm 6.6	0.24 \pm 0.01
SE2378	295.7 \pm 4.0	0.46	26.6 \pm 2.3	12.7 \pm 2.1	0.0	27.4 \pm 2.3	478.4 \pm 15.4	0.81 \pm 0.02

Table 3-11. Growth and ethanol production by *E. coli* strain SE2378 grown on glucose or xylose^a.

	W3110		SE2378	
	Glucose	Xylose	Glucose	Xylose
μ_{Max}	0.44	0.37	0.46	0.38
$Y_{\text{X/S}}$	0.04	0.04	0.04	0.04
Q_{S}	2.94	1.58	1.29	1.65
Q_{P}	0.50	0.36	0.61	0.53
$Y_{\text{P/S}}$	0.12	0.18	0.41	0.42
q_{S}	4.10	4.93	3.26	5.33
q_{P}	0.49	0.89	1.34	2.24

μ_{Max} - specific growth rate, h^{-1}

$Y_{\text{X/S}}$ - $\text{g cells (g substrate)}^{-1}$

Q_{S} - $\text{g sugar consumed L}^{-1} \text{h}^{-1}$

Q_{P} - $\text{g ethanol L}^{-1} \text{h}^{-1}$

$Y_{\text{P/S}}$ - $\text{g ethanol (g substrate)}^{-1}$

q_{S} - $\text{g sugar consumed (g cells-dry weight)}^{-1} \text{h}^{-1}$

q_{P} - $\text{g ethanol (g cells-dry weight)}^{-1} \text{h}^{-1}$

^aGlucose and xylose fermentations by strains W3110 and SE2378 in LB broth are presented in Tables 3-10 and 11 and Figures 3-26, 27, 28 and 29. The reported values are calculated maximum values.

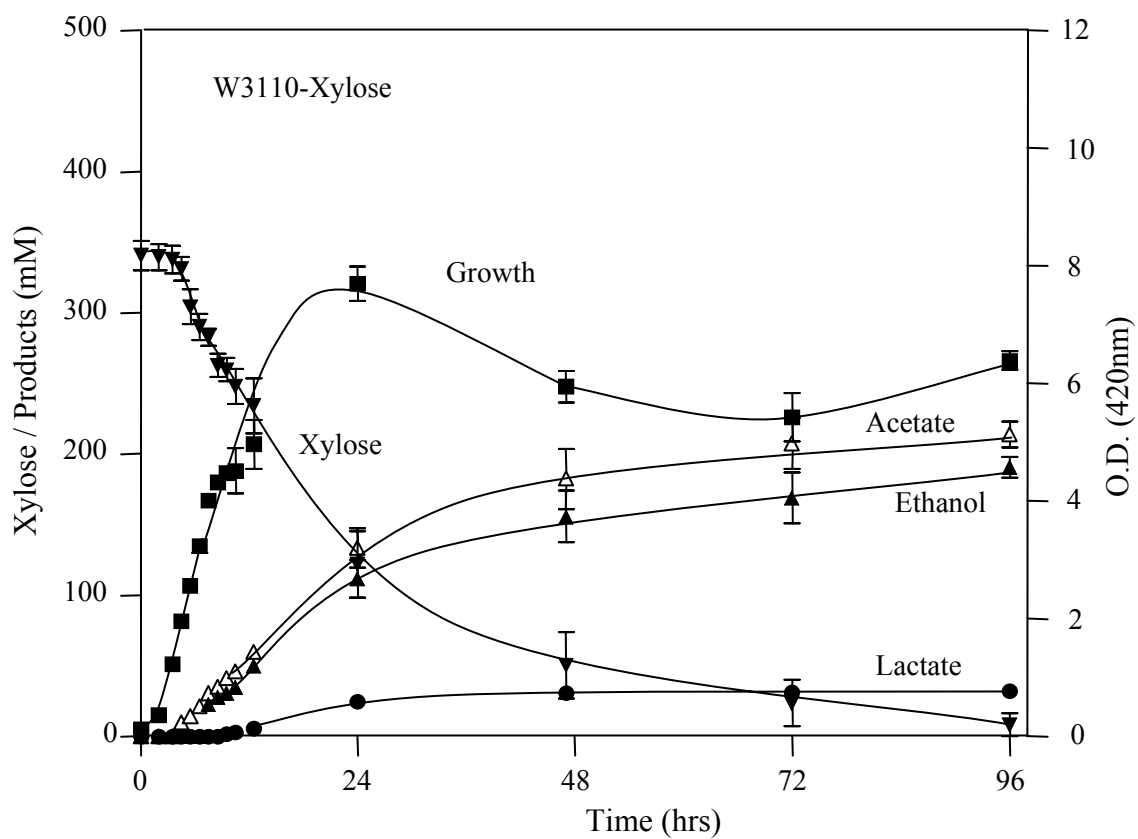


Figure 3-28. Growth and fermentation characteristics of wild type strain W3110 in LB+xylose (50 g L^{-1}) at pH 7.0 and 37°C .

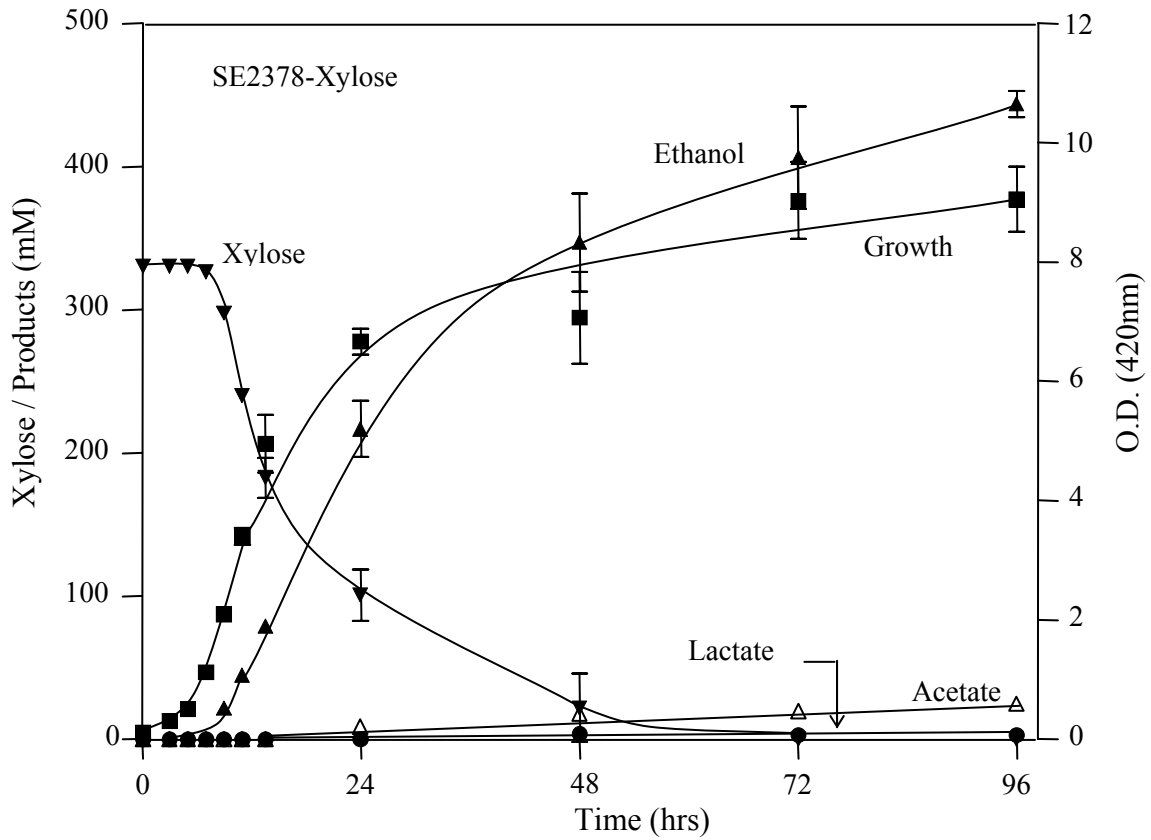


Figure 3-29. Growth and fermentation characteristics of ethanologenic strain SE2378 in LB+xylose (50 g L^{-1}) at pH 7.0 and 37°C .

Table 3-12. Xylose fermentation characteristics of *E. coli* strain SE2378 and wild type strain W3110.

Strain	Xylose consumed (mM)	μ (h ⁻¹)	Product Concentration (mM)					Ethanol
			Succinate	Lactate	Formate	Acetate	Ethanol	Yield
W3110	332.5 ± 8.3	0.37	57.2 ± 1.0	32.4 ± 2.5	248.3 ± 52.5	214.7 ± 10.0	190.8 ± 7.4	0.34 ± 0.00
SE2378	324.7 ± 1.5	0.38	32.9 ± 5.4	0.0	0.0	24.9 ± 2.3	444.0 ± 9.17	0.82 ± 0.01

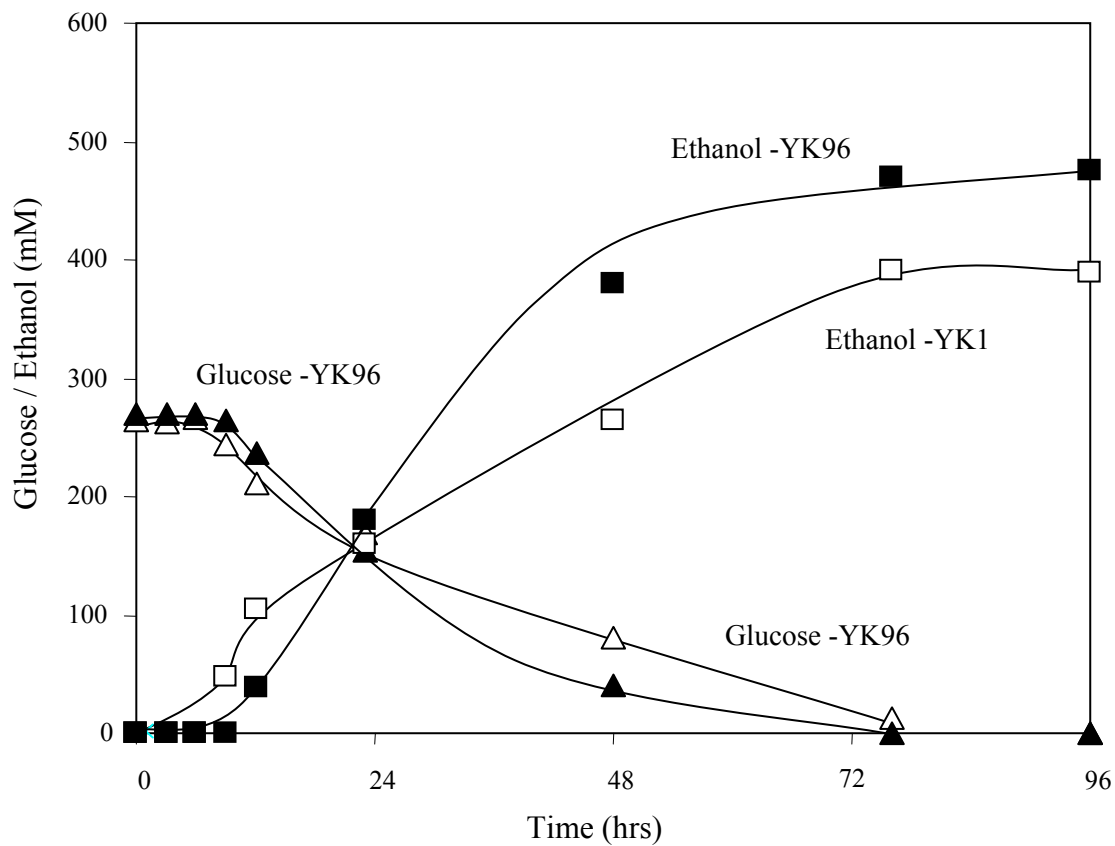


Figure 3-30. Fermentation characteristics of kanamycin-sensitive derivative of ethanologenic strain SE2378, YK1, and its $\Delta mgsA$ derivative strain YK96 in LB+glucose (50 g L^{-1}) at pH 7.0, 37°C .

Table 3-13. Fermentation characteristics of kanamycin-sensitive derivative of ethanologenic strain SE2378, YK1, and its $\Delta mgsA$ derivative strain YK96 in LB+glucose (50 g L⁻¹) at pH 7.0 and 37 °C.

Strain	Glucose consumed (mM)	μ (h ⁻¹)	Product Concentration (mM)					Ethanol	Carbon
			Succinate	Lactate	Formate	Acetate	Ethanol	Yield	Recovery
YK1	263.8	0.45	35.2	12.7	0	42.4	390.2	0.79	0.91
YK96	270.3	0.46	12.5	0	0	10.5	476.1	0.88	0.92

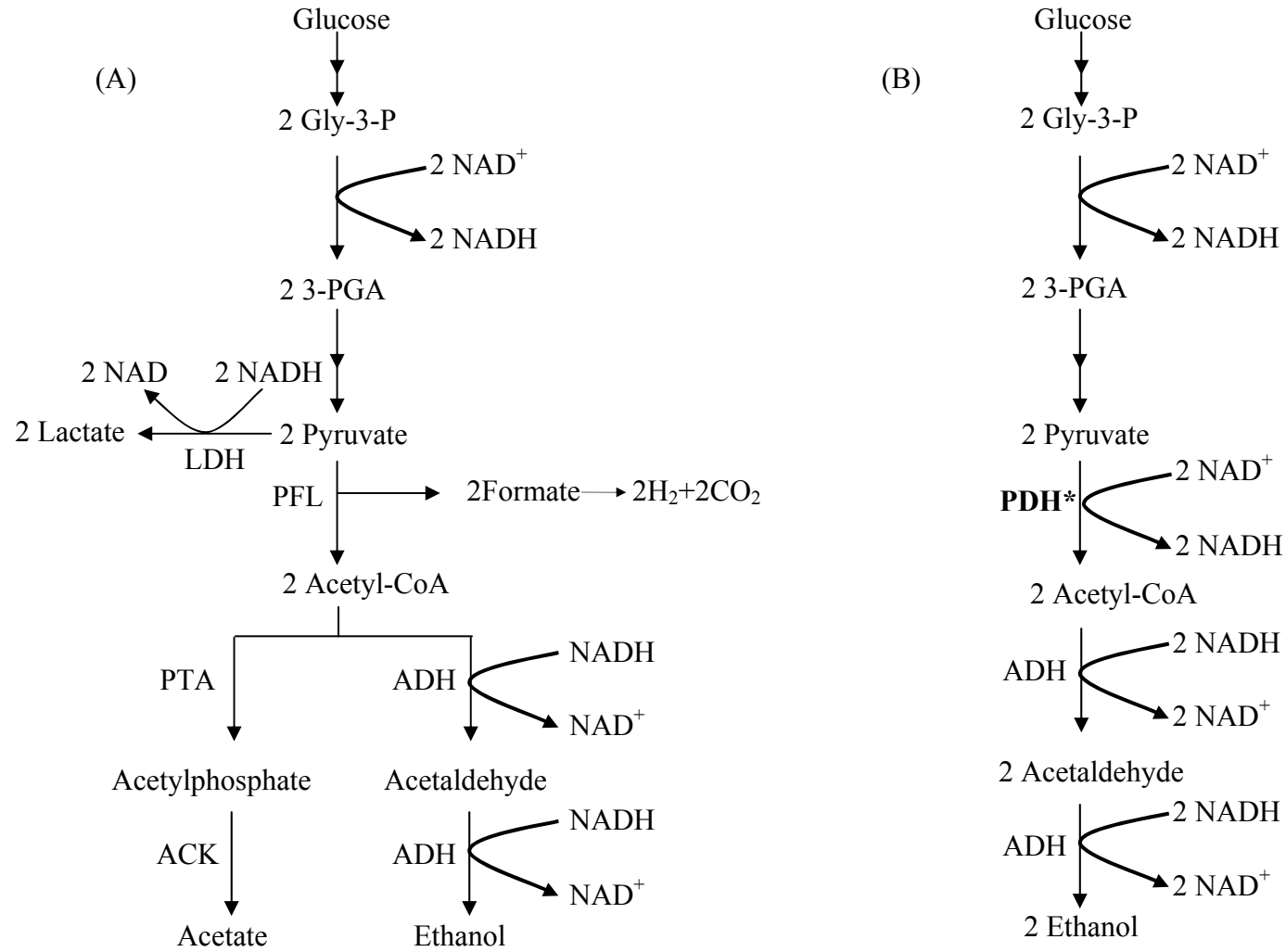


Figure 3-31. Ethanologenic fermentation pathway. (A) Mixed acid fermentation and (B) ethanologenic fermentation pathway of strain SE2378.

LIST OF REFERENCES

1. **Abdel-Hamid, A. M., M. M. Attwood, and J. R. Guest.** 2001. Pyruvate oxidase contributes to the aerobic growth efficiency of *Escherichia coli*. *Microbiology* **147**:1483-1498.
2. **Alam, K. Y., and D. P. Clark.** 1989. Anaerobic fermentation balance of *Escherichia coli* as observed by in vivo nuclear magnetic resonance spectroscopy. *J Bacteriol* **171**:6213-6217.
3. **Amore, R., P. Kotter, C. Kuster, M. Ciriacy, and C. P. Hollenberg.** 1991. Cloning and expression in *Saccharomyces cerevisiae* of the NAD(P)H-dependent xylose reductase-encoding gene (XYL1) from the xylose-assimilating yeast *Pichia stipitis*. *Gene* **109**:89-97.
4. **Ausubel, F. M., R. Brent, R. E. Kingston, D. D. Moore, J. A. Smith, J. G. Seidman, and K. Struhl.** 1987. *Current Protocols in Molecular Biology*. Greene Publishing Associates and Wiley-Interscience, Brooklyn, NY.
5. **Badger, P. C.** 2002. Ethanol from cellulose: A General Review. Trends in new crops and new uses., J. Janick and A. Whipkey ed. ASHA Press, Alexandria, VA.
6. **Bagramyan, K., N. Mnatsakanyan, A. Poladian, A. Vassilian, and A. Trchounian.** 2002. The roles of hydrogenases 3 and 4, and the F₀F₁-ATPase, in H₂ production by *Escherichia coli* at alkaline and acidic pH. *FEBS Lett* **516**:172-178.
7. **Bagramyan, K., and A. Trchounian.** 2003. Structural and functional features of formate hydrogen lyase, an enzyme of mixed-acid fermentation from *Escherichia coli*. *Biochemistry (Mosc)* **68**:1159-1170.
8. **Baltz, R. H.** 2006. Molecular engineering approaches to peptide, polyketide and other antibiotics. *Nat Biotechnol* **24**:1533-1540.
9. **Bennett, R., D. R. Taylor, and A. Hurst.** 1966. D- and L-lactate dehydrogenases in *Escherichia coli*. *Biochim Biophys Acta* **118**:512-521.
10. **Berger, E. A.** 1973. Different mechanisms of energy coupling for the active transport of proline and glutamine in *Escherichia coli*. *Proc Natl Acad Sci U S A* **70**:1514-1518.
11. **Bisswanger, H.** 1981. Substrate specificity of the pyruvate dehydrogenase complex from *Escherichia coli*. *J Biol Chem* **256**:815-822.
12. **Bothast, R. J., N. N. Nichols, and B. S. Dien.** 1999. Fermentations with new recombinant organisms. *Biotechnol Prog* **15**:867-875.
13. **Bothast, R. J., and M. A. Schlicher.** 2005. Biotechnological processes for conversion of corn into ethanol. *Appl Microbiol Biotechnol* **67**:19-25.

14. **Bradford, M. M.** 1976. A rapid and sensitive method for the quantitation of microgram quantities of protein utilizing the principle of protein-dye binding. *Anal Biochem* **72**:248-254.
15. **Bunch, P. K., F. Mat-Jan, N. Lee, and D. P. Clark.** 1997. The *ldhA* gene encoding the fermentative lactate dehydrogenase of *Escherichia coli*. *Microbiology* **143 (Pt 1)**:187-195.
16. **CaJacob, C. A., G. R. Gavino, and P. A. Frey.** 1985. Pyruvate dehydrogenase complex of *Escherichia coli*. Thiamin pyrophosphate and NADH-dependent hydrolysis of acetyl-CoA. *J Biol Chem* **260**:14610-14615.
17. **Cassey, B., J. R. Guest, and M. M. Attwood.** 1998. Environmental control of pyruvate dehydrogenase complex expression in *Escherichia coli*. *FEMS Microbiol Lett* **159**:325-329.
18. **Causey, T. B., S. Zhou, K. T. Shanmugam, and L. O. Ingram.** 2003. Engineering the metabolism of *Escherichia coli* W3110 for the conversion of sugar to redox-neutral and oxidized products: homoacetate production. *Proc Natl Acad Sci U S A* **100**:825-832.
19. **Chang, Y. Y., and J. E. Cronan, Jr.** 1983. Genetic and biochemical analyses of *Escherichia coli* strains having a mutation in the structural gene (*poxB*) for pyruvate oxidase. *J Bacteriol* **154**:756-762.
20. **Chang, Y. Y., A. Y. Wang, and J. E. Cronan, Jr.** 1994. Expression of *Escherichia coli* pyruvate oxidase (PoxB) depends on the sigma factor encoded by the *rpoS(katF)* gene. *Mol Microbiol* **11**:1019-1028.
21. **Chen, Y. M., and E. C. Lin.** 1991. Regulation of the *adhE* gene, which encodes ethanol dehydrogenase in *Escherichia coli*. *J Bacteriol* **173**:8009-8013.
22. **Clark, D. P.** 1989. The fermentation pathways of *Escherichia coli*. *FEMS Microbiol Rev* **5**:223-234.
23. **Clark, D. P., P. R. Cunningham, S. G. Reams, F. Mat-Jan, R. Mohammedkhani, and C. R. Williams.** 1988. Mutants of *Escherichia coli* defective in acid fermentation. *Appl Biochem Biotechnol* **17**:163-173.
24. **Conway, A., and D. E. Koshland, Jr.** 1968. Negative cooperativity in enzyme action. The binding of diphosphopyridine nucleotide to glyceraldehyde 3-phosphate dehydrogenase. *Biochemistry* **7**:4011-4023.
25. **Creaghan, I. T., and J. R. Guest.** 1978. Succinate dehydrogenase-dependent nutritional requirement for succinate in mutants of *Escherichia coli* K12. *J Gen Microbiol* **107**:1-13.

26. **Cunningham, L., D. Georgellis, J. Green, and J. R. Guest.** 1998. Co-regulation of lipoamide dehydrogenase and 2-oxoglutarate dehydrogenase synthesis in *Escherichia coli*: characterisation of an ArcA binding site in the *lpd* promoter. *FEMS Microbiol Lett* **169**:403-408.
27. **Dalgaard, T., U. Jorgensen, J. E. Olesen, E. S. Jensen, and E. S. Kristensen.** 2006. Looking at biofuels and bioenergy. *Science* **312**:1743-1744.
28. **Danson, M. J., and R. N. Perham.** 1976. Evidence for two lipoic acid residues per lipoate acetyltransferase chain in the pyruvate dehydrogenase multienzyme complex of *Escherichia coli*. *Biochem J* **159**:677-682.
29. **Datsenko, K. A., and B. L. Wanner.** 2000. One-step inactivation of chromosomal genes in *Escherichia coli* K-12 using PCR products. *Proc Natl Acad Sci U S A* **97**:6640-5.
30. **Davis, R. W., D. Botstein, and J. R. Roth.** 1980. *A Manual for Genetic Engineering: Advanced Bacterial Genetics*. Cold Spring Harbor Laboratory, Cold Spring Harbor, NY
31. **de Graef, M. R., S. Alexeeva, J. L. Snoep, and M. J. Teixeira de Mattos.** 1999. The steady-state internal redox state (NADH/NAD) reflects the external redox state and is correlated with catabolic adaptation in *Escherichia coli*. *J Bacteriol* **181**:2351-2357.
32. **Deanda, K., M. Zhang, C. Eddy, and S. Picataggio.** 1996. Development of an arabinose-fermenting *Zymomonas mobilis* strain by metabolic pathway engineering. *Appl Environ Microbiol* **62**:4465-4470.
33. **Deckers-Hebestreit, G., J. Greie, W. Stalz, and K. Altendorf.** 2000. The ATP synthase of *Escherichia coli*: structure and function of F(0) subunits. *Biochim Biophys Acta* **1458**:364-373.
34. **Derosier, D. J., R. M. Oliver, and L. J. Reed.** 1971. Crystallization and preliminary structural analysis of dihydrolipoyl transsuccinylase, the core of the 2-oxoglutarate dehydrogenase complex. *Proc Natl Acad Sci U S A* **68**:1135-1137.
35. **Dien, B. S., M. A. Cotta, and T. W. Jeffries.** 2003. Bacteria engineered for fuel ethanol production: current status. *Appl Microbiol Biotechnol* **63**:258-266.
36. **Dien, B. S., C. P. Kurtzman, B. C. Saha, and R. J. Bothast.** 1996. Screening for L-arabinose fermenting yeasts. *Appl Biochem Biotechnol* **57-58**:233-242.
37. **Dietrich, J., and U. Henning.** 1970. Regulation of pyruvate dehydrogenase complex synthesis in *Escherichia coli* K 12. Identification of the inducing metabolite. *Eur J Biochem* **14**:258-269.

38. **Dombek, K. M., and L. O. Ingram.** 1987. Ethanol production during batch fermentation with *Saccharomyces cerevisiae*: changes in glycolytic enzymes and internal pH. *Appl Environ Microbiol* **53**:1286-1291.
39. **Eliasson, A., C. Christensson, C. F. Wahlbom, and B. Hahn-Hagerdal.** 2000. Anaerobic xylose fermentation by recombinant *Saccharomyces cerevisiae* carrying XYL1, XYL2, and XKS1 in mineral medium chemostat cultures. *Appl Environ Microbiol* **66**:3381-3386.
40. **Farrell, A. E., R. J. Plevin, B. T. Turner, A. D. Jones, M. O'Hare, and D. M. Kammen.** 2006. Ethanol can contribute to energy and environmental goals. *Science* **311**:506-508.
41. **Ferguson, G. P., S. Totemeyer, M. J. MacLean, and I. R. Booth.** 1998. Methylglyoxal production in bacteria: suicide or survival? *Arch Microbiol* **170**:209-218.
42. **Goodlove, P. E., P. R. Cunningham, J. Parker, and D. P. Clark.** 1989. Cloning and sequence analysis of the fermentative alcohol-dehydrogenase-encoding gene of *Escherichia coli*. *Gene* **85**:209-14.
43. **Grabar, T. B., S. Zhou, K. T. Shanmugam, L. P. Yomano, and L. O. Ingram.** 2006. Methylglyoxal bypass identified as source of chiral contamination in l(+) and d(-)-lactate fermentations by recombinant *Escherichia coli*. *Biotechnol Lett* **28**:1527-1535.
44. **Graumann, K., and A. Premstaller.** 2006. Manufacturing of recombinant therapeutic proteins in microbial systems. *Biotechnol J* **1**:164-186.
45. **Gray, K. A., L. Zhao, and M. Emptage.** 2006. Bioethanol. *Curr Opin Chem Biol* **10**:141-146.
46. **Guest, J. R., S. J. Angier, and G. C. Russell.** 1989. Structure, expression, and protein engineering of the pyruvate dehydrogenase complex of *Escherichia coli*. *Ann N Y Acad Sci* **573**:76-99.
47. **Hakes, J.** 2000. Presented at the American Association of Petroleum Geologists, New Orleans, LA.
48. **Hallborn, J., M. F. Gorwa, N. Meinander, M. Penttila, S. Keranen, and B. Hahn-Hagerdal.** 1994. The influence of cosubstrate and aeration on xylitol formation by recombinant *Saccharomyces cerevisiae* expressing the XYL1 gene. *Appl Microbiol Biotechnol* **42**:326-333.
49. **Hansen, H. G., and U. Henning.** 1966. Regulation of pyruvate dehydrogenase activity in *Escherichia coli* K12. *Biochim Biophys Acta* **122**:355-358.

50. **Hasona, A., Y. Kim, F. G. Healy, L. O. Ingram, and K. T. Shanmugam.** 2004. Pyruvate formate lyase and acetate kinase are essential for anaerobic growth of *Escherichia coli* on xylose. *J Bacteriol* **186**:7593-7600.
51. **Haydon, D. J., M. A. Quail, and J. R. Guest.** 1993. A mutation causing constitutive synthesis of the pyruvate dehydrogenase complex in *Escherichia coli* is located within the *pdhR* gene. *FEBS Lett* **336**:43-47.
52. **Hernandez-Montalvo, V., A. Martinez, G. Hernandez-Chavez, F. Bolivar, F. Valle, and G. Gosset.** 2003. Expression of *galP* and *glk* in a *Escherichia coli* PTS mutant restores glucose transport and increases glycolytic flux to fermentation products. *Biotechnol Bioeng* **83**:687-694.
53. **Hernandez-Montalvo, V., F. Valle, F. Bolivar, and G. Gosset.** 2001. Characterization of sugar mixtures utilization by an *Escherichia coli* mutant devoid of the phosphotransferase system. *Appl Microbiol Biotechnol* **57**:186-191.
54. **Hill, J., E. Nelson, D. Tilman, S. Polasky, and D. Tiffany.** 2006. Environmental, economic, and energetic costs and benefits of biodiesel and ethanol biofuels. *Proc Natl Acad Sci U S A* **103**:11206-11210.
55. **Hillman, J. D., and D. G. Fraenkel.** 1975. Glyceraldehyde 3-phosphate dehydrogenase mutants of *Escherichia coli*. *J Bacteriol* **122**:1175-1179.
56. **Hinman, L. M., and J. P. Blass.** 1981. An NADH-linked spectrophotometric assay for pyruvate dehydrogenase complex in crude tissue homogenates. *J Biol Chem* **256**:6583-6586.
57. **Ho, N. W., Z. Chen, A. P. Brainard, and M. Sedlak.** 1999. Successful design and development of genetically engineered *Saccharomyces* yeasts for effective cofermentation of glucose and xylose from cellulosic biomass to fuel ethanol. *Adv Biochem Eng Biotechnol* **65**:163-192.
58. **Holms, H.** 2001. Flux analysis: a basic tool of microbial physiology. *Adv Microb Physiol* **45**:271-340.
59. **Ingledeew, W. J., and R. K. Poole.** 1984. The respiratory chains of *Escherichia coli*. *Microbiol Rev* **48**:222-271.
60. **Ingram, L. O., H. C. Aldrich, A. C. Borges, T. B. Causey, A. Martinez, F. Morales, A. Saleh, S. A. Underwood, L. P. Yomano, S. W. York, J. Zaldivar, and S. Zhou.** 1999. Enteric bacterial catalysts for fuel ethanol production. *Biotechnol Prog* **15**:855-866.
61. **Ingram, L. O., T. Conway, D. P. Clark, G. W. Sewell, and J. F. Preston.** 1987. Genetic engineering of ethanol production in *Escherichia coli*. *Appl Environ Microbiol* **53**:2420-2425.

62. **Ingram, L. O., P. F. Gomez, X. Lai, M. Moniruzzaman, B. E. Wood, L. P. Yomano, and S. W. York.** 1998. Metabolic engineering of bacteria for ethanol production. *Biotechnol Bioeng* **58**:204-214.
63. **Jeffries, T. W.** 2006. Engineering yeasts for xylose metabolism. *Curr Opin Biotechnol* **17**:320-6.
64. **Jeffries, T. W.** 2005. Ethanol fermentation on the move. *Nat Biotechnol* **23**:40-41.
65. **Jeffries, T. W., and Y. S. Jin.** 2004. Metabolic engineering for improved fermentation of pentoses by yeasts. *Appl Microbiol Biotechnol* **63**:495-509.
66. **Jones, H. M., and R. P. Gunsalus.** 1987. Regulation of *Escherichia coli* fumarate reductase (*frdABCD*) operon expression by respiratory electron acceptors and the *fnr* gene product. *J Bacteriol* **169**:3340-3349.
67. **Kern, A., E. Tilley, I. S. Hunter, M. Legisa, and A. Glieder.** 2007. Engineering primary metabolic pathways of industrial micro-organisms. *J Biotechnol* **129**:6-29.
68. **Kline, E. S., and H. R. Mahler.** 1965. The lactic dehydrogenases of *E. coli*. *Ann N Y Acad Sci* **119**:905-919.
69. **Knappe, J., and G. Sawers.** 1990. A radical-chemical route to acetyl-CoA: the anaerobically induced pyruvate formate-lyase system of *Escherichia coli*. *FEMS Microbiol Rev* **6**:383-398.
70. **Kotter, P., R. Amore, C. P. Hollenberg, and M. Ciriacy.** 1990. Isolation and characterization of the *Pichia stipitis* xylitol dehydrogenase gene, *XYL2*, and construction of a xylose-utilizing *Saccharomyces cerevisiae* transformant. *Curr Genet* **18**:493-500.
71. **Kroll, R. G., and I. R. Booth.** 1981. The role of potassium transport in the generation of a pH gradient in *Escherichia coli*. *Biochem J* **198**:691-698.
72. **Laemmli, U. K.** 1970. Cleavage of structural proteins during the assembly of the head of bacteriophage T4. *Nature* **227**:680-685.
73. **Lin, E. C., and S. Iuchi.** 1991. Regulation of gene expression in fermentative and respiratory systems in *Escherichia coli* and related bacteria. *Annu Rev Genet* **25**:361-387.
74. **Lin, Y., and S. Tanaka.** 2006. Ethanol fermentation from biomass resources: current state and prospects. *Appl Microbiol Biotechnol* **69**:627-42.
75. **Lindsay, H., E. Beaumont, S. D. Richards, S. M. Kelly, S. J. Sanderson, N. C. Price, and J. G. Lindsay.** 2000. FAD insertion is essential for attaining the assembly

- competence of the dihydrolipoamide dehydrogenase (E3) monomer from *Escherichia coli*. *J Biol Chem* **275**:36665-36670.
76. **Lineweaver, H., and D. Burk.** 1934. The Determination of Enzyme Dissociation Constants. *J. Am. Chem. Soc.* **56**:658—666.
 77. **Linn, T., and R. St Pierre.** 1990. Improved vector system for constructing transcriptional fusions that ensures independent translation of *lacZ*. *J Bacteriol* **172**:1077-1084.
 78. **Lynd, L. R., C. E. Wyman, and T. U. Gerngross.** 1999. Biocommodity Engineering. *Biotechnol Prog* **15**:777-793.
 79. **Maniatis, T., E. F. Fritsch, and J. Sambrook.** 1982. *Molecular Cloning*. Cold Spring Harbor Laboratory, New York.
 80. **Martinez, A., S. W. York, L. P. Yomano, V. L. Pineda, F. C. Davis, J. C. Shelton, and L. O. Ingram.** 1999. Biosynthetic burden and plasmid burden limit expression of chromosomally integrated heterologous genes (*pdc*, *adhB*) in *Escherichia coli*. *Biotechnol Prog* **15**:891-897.
 81. **Mat-Jan, F., C. R. Williams, and D. P. Clark.** 1989. Anaerobic growth defects resulting from gene fusions affecting succinyl-CoA synthetase in *Escherichia coli* K12. *Mol Gen Genet* **215**:276-280.
 82. **Matsumura, I., and A. D. Ellington.** 2001. *Methods in Molecular Biology*, 2nd ed. Humana Press Inc., Totowa, NJ.
 83. **Miles, J. S., and J. R. Guest.** 1987. Molecular genetic aspects of the citric acid cycle of *Escherichia coli*. *Biochem Soc Symp* **54**:45-65.
 84. **Miller, J. H.** 1992. *A Short Course in Bacterial Genetics-A Laboratory Manual and Handbook for Escherichia coli and Related Bacteria*. Cold Spring Harbor Laboratory Press, New York, NY.
 85. **Millichip, R. J., and Doelle, H. W.** 1989. Large-scale ethanol production from Mil (Sorghum) using *Zymomonas mobilis*. *Process Biochem* **24**:141-145.
 86. **Mitchell, W. J.** 1985. The phosphoenolpyruvate-dependent phosphotransferase system: a central feature of carbohydrate accumulation by enteric bacteria. *Microbiol Sci* **2**:330-4, 339.
 87. **Mnatsakanyan, N., A. Vassilian, L. Navasardyan, K. Bagramyan, and A. Trchounian.** 2002. Regulation of *Escherichia coli* formate hydrogenlyase activity by formate at alkaline pH. *Curr Microbiol* **45**:281-286.

88. **Moniruzzaman, M., Dien, B. S., Skory, C. D., Chen, Z. D., Hespell, R. B., Ho, N. W. Y., Dale, B. E. and Bothast, R. J.** 1997. Fermentation of corn fibre sugars by an engineered xylose utilizing *Saccharomyces* yeast strain. *World J. Microbiol. Biotechnol* **13**:341-346.
89. **Moniruzzaman, M., X. Lai, S. W. York, and L. O. Ingram.** 1997. Isolation and molecular characterization of high-performance cellobiose-fermenting spontaneous mutants of ethanologenic *Escherichia coli* KO11 containing the *Klebsiella oxytoca* *casAB* operon. *Appl Environ Microbiol* **63**:4633-4637.
90. **Nagradova, N. K.** 2001. Study of the properties of phosphorylating D-glyceraldehyde-3-phosphate dehydrogenase. *Biochemistry (Mosc)* **66**:1067-1076.
91. **Narayanan, N., M. Y. Hsieh, Y. Xu, and C. P. Chou.** 2006. Arabinose-induction of lac-derived promoter systems for penicillin acylase production in *Escherichia coli*. *Biotechnol Prog* **22**:617-625.
92. **Ogino, T., Y. Arata, S. Fujiwara, H. Shoun, and T. Beppu.** 1978. Proton correlation nuclear magnetic resonance study of anaerobic metabolism of *Escherichia coli*. *Biochemistry* **17**:4742-4745.
93. **Ohta, K., D. S. Beall, J. P. Mejia, K. T. Shanmugam, and L. O. Ingram.** 1991. Genetic improvement of *Escherichia coli* for ethanol production: chromosomal integration of *Zymomonas mobilis* genes encoding pyruvate decarboxylase and alcohol dehydrogenase II. *Appl Environ Microbiol* **57**:893-900.
94. **Ostergaard, S., L. Olsson, and J. Nielsen.** 2000. Metabolic engineering of *Saccharomyces cerevisiae*. *Microbiol Mol Biol Rev* **64**:34-50.
95. **Park, S. J., G. Chao, and R. P. Gunsalus.** 1997. Aerobic regulation of the *sucABCD* genes of *Escherichia coli*, which encode alpha-ketoglutarate dehydrogenase and succinyl coenzyme A synthetase: roles of ArcA, Fnr, and the upstream *sdhCDAB* promoter. *J Bacteriol* **179**:4138-4142.
96. **Patel, M. A., M. S. Ou, R. Harbrucker, H. C. Aldrich, M. L. Buszko, L. O. Ingram, and K. T. Shanmugam.** 2006. Isolation and characterization of acid-tolerant, thermophilic bacteria for effective fermentation of biomass-derived sugars to lactic acid. *Appl Environ Microbiol* **72**:3228-3235.
97. **Ponce, E.** 1999. Effect of growth rate reduction and genetic modifications on acetate accumulation and biomass yields in *Escherichia coli*. *J Biosci Bioeng* **87**:775-780.
98. **Quail, M. A., and J. R. Guest.** 1995. Purification, characterization and mode of action of PdhR, the transcriptional repressor of the *pdhR-aceEF-lpd* operon of *Escherichia coli*. *Mol Microbiol* **15**:519-529.

99. **Quail, M. A., D. J. Haydon, and J. R. Guest.** 1994. The *pdhR-aceEF-lpd* operon of *Escherichia coli* expresses the pyruvate dehydrogenase complex. *Mol Microbiol* **12**:95-104.
100. **Ragauskas, A. J., C. K. Williams, B. H. Davison, G. Britovsek, J. Cairney, C. A. Eckert, W. J. Frederick, Jr., J. P. Hallett, D. J. Leak, C. L. Liotta, J. R. Mielenz, R. Murphy, R. Templer, and T. Tschaplinski.** 2006. The path forward for biofuels and biomaterials. *Science* **311**:484-489.
101. **RD, P., W. LL, T. AF, G. RL, S. BJ, and E. DC** 2005, posting date. Biomass as feedstock for a bioenergy and bioproducts industry: the technical feasibility of a billion-ton annual supply. <http://www.osti.gov/bridge>. [Online.]
102. **Reed, L. J.** 2001. A trail of research from lipoic acid to alpha-keto acid dehydrogenase complexes. *J Biol Chem* **276**:38329-38336.
103. **Reed, L. J., F. H. Pettit, M. H. Eley, L. Hamilton, J. H. Collins, and R. M. Oliver.** 1975. Reconstitution of the *Escherichia coli* pyruvate dehydrogenase complex. *Proc Natl Acad Sci U S A* **72**:3068-3072.
104. **Rogers P. L. K, L. J., Skotnicki M. L. and Tribe D. E.** 1982. Ethanol production by *Zymomonas mobilis*. *Advances Biochem. Eng* **23**:37-84.
105. **Sahlman, L., and C. H. Williams, Jr.** 1989. Lipoamide dehydrogenase from *Escherichia coli*. Steady-state kinetics of the physiological reaction. *J Biol Chem* **264**:8039-8045.
106. **Sanderson, K. E., and J. R. Roth.** 1988. Linkage map of *Salmonella typhimurium*, edition VII. *Microbiol Rev* **52**:485-532.
107. **Sauer, U., and B. J. Eikmanns.** 2005. The PEP-pyruvate-oxaloacetate node as the switch point for carbon flux distribution in bacteria. *FEMS Microbiol Rev* **29**:765-794.
108. **Saumweber, H., R. Binder, and H. Bisswanger.** 1981. Pyruvate dehydrogenase component of the pyruvate dehydrogenase complex from *Escherichia coli* K12. Purification and characterization. *Eur J Biochem* **114**:407-411.
109. **Sauter, M., and R. G. Sawers.** 1990. Transcriptional analysis of the gene encoding pyruvate formate-lyase-activating enzyme of *Escherichia coli*. *Mol Microbiol* **4**:355-363.
110. **Sawers, G., and B. Suppmann.** 1992. Anaerobic induction of pyruvate formate-lyase gene expression is mediated by the ArcA and FNR proteins. *J Bacteriol* **174**:3474-3478.
111. **Schmincke-Ott, E., and H. Bisswanger.** 1981. Dihydrolipoamide dehydrogenase component of the pyruvate dehydrogenase complex from *Escherichia coli* K12.

- Comparative characterization of the free and the complex-bound component. Eur J Biochem **114**:413-420.
112. **Schwartz, E. R., and L. J. Reed.** 1970. Regulation of the activity of the pyruvate dehydrogenase complex of *Escherichia coli*. Biochemistry **9**:1434-1439.
 113. **Shalel-Levanon, S., K. Y. San, and G. N. Bennett.** 2005. Effect of oxygen, and ArcA and FNR regulators on the expression of genes related to the electron transfer chain and the TCA cycle in *Escherichia coli*. Metab Eng **7**:364-374.
 114. **Shen, L. C., and D. E. Atkinson.** 1970. Regulation of pyruvate dehydrogenase from *Escherichia coli*. Interactions of adenylate energy charge and other regulatory parameters. J Biol Chem **245**:5974-5978.
 115. **Slininger, P. J., Bothast, R. J. Okos, M. R. and Ladisch, M. R.** 1985. Comparative evaluation of ethanol production by xylose-fermenting yeasts presented high xylose concentrations. Biotechnol. Lett **7**:431-436.
 116. **Smith, M. W., and F. C. Neidhardt.** 1983. 2-Oxoacid dehydrogenase complexes of *Escherichia coli*: cellular amounts and patterns of synthesis. J Bacteriol **156**:81-88.
 117. **Snoep, J. L., M. R. de Graef, A. H. Westphal, A. de Kok, M. J. Teixeira de Mattos, and O. M. Neijssel.** 1993. Differences in sensitivity to NADH of purified pyruvate dehydrogenase complexes of *Enterococcus faecalis*, *Lactococcus lactis*, *Azotobacter vinelandii* and *Escherichia coli*: implications for their activity in vivo. FEMS Microbiol Lett **114**:279-283.
 118. **Soberon, X., and M. H. Saier, Jr.** 2006. Engineering transport protein function: theoretical and technical considerations using the sugar-transporting phosphotransferase system of *Escherichia coli* as a model system. J Mol Microbiol Biotechnol **11**:302-307.
 119. **Spencer, M. E., and J. R. Guest.** 1973. Isolation and properties of fumarate reductase mutants of *Escherichia coli*. J Bacteriol **114**:563-570.
 120. **Spencer, M. E., and J. R. Guest.** 1985. Transcription analysis of the *sucAB*, *aceEF* and *lpd* genes of *Escherichia coli*. Mol Gen Genet **200**:145-154.
 121. **Sprenger, G. A.** 1996. Carbohydrate metabolism in *Zymomonas mobilis*: a catabolic highway with some scenic routes. FEMS. Microbiol Lett **145**:301-307.
 122. **Stephens, P. E., M. G. Darlison, H. M. Lewis, and J. R. Guest.** 1983. The pyruvate dehydrogenase complex of *Escherichia coli* K12. Nucleotide sequence encoding the dihydrolipoamide acetyltransferase component. Eur J Biochem **133**:481-489.

123. **Stephens, P. E., M. G. Darlison, H. M. Lewis, and J. R. Guest.** 1983. The pyruvate dehydrogenase complex of *Escherichia coli* K12. Nucleotide sequence encoding the pyruvate dehydrogenase component. *Eur J Biochem* **133**:155-162.
124. **Stephens, P. E., H. M. Lewis, M. G. Darlison, and J. R. Guest.** 1983. Nucleotide sequence of the lipoamide dehydrogenase gene of *Escherichia coli* K12. *Eur J Biochem* **135**:519-527.
125. **Sticklen, M.** 2006. Plant genetic engineering to improve biomass characteristics for biofuels. *Curr Opin Biotechnol* **17**:315-319.
126. **Tantirungkij, M., T. Seki, and T. Yoshida.** 1994. Genetic improvement of *Saccharomyces cerevisiae* for ethanol production from xylose. *Ann N Y Acad Sci* **721**:138-147.
127. **Tarmy, E. M., and N. O. Kaplan.** 1968. Kinetics of *Escherichia coli* B D-lactate dehydrogenase and evidence for pyruvate-controlled change in conformation. *J Biol Chem* **243**:2587-2596.
128. **Toivari, M. H., A. Aristidou, L. Ruohonen, and M. Penttila.** 2001. Conversion of xylose to ethanol by recombinant *Saccharomyces cerevisiae*: importance of xylulokinase (XKS1) and oxygen availability. *Metab Eng* **3**:236-49.
129. **Underwood, S. A., S. Zhou, T. B. Causey, L. P. Yomano, K. T. Shanmugam, and L. O. Ingram.** 2002. Genetic changes to optimize carbon partitioning between ethanol and biosynthesis in ethanologenic *Escherichia coli*. *Appl Environ Microbiol* **68**:6263-6272.
130. **Van Dyk, T. K., D. R. Smulski, and Y. Y. Chang.** 1987. Pleiotropic effects of *poxA* regulatory mutations of *Escherichia coli* and *Salmonella typhimurium*, mutations conferring sulfometuron methyl and alpha-ketobutyrate hypersensitivity. *J Bacteriol* **169**:4540-4546.
131. **van Maris, A. J., D. A. Abbott, E. Bellissimi, J. van den Brink, M. Kuyper, M. A. Luttik, H. W. Wisselink, W. A. Scheffers, J. P. van Dijken, and J. T. Pronk.** 2006. Alcoholic fermentation of carbon sources in biomass hydrolysates by *Saccharomyces cerevisiae*: current status. *Antonie Van Leeuwenhoek* **90**:391-418.
132. **Vertes, A. A., M. Inui, and H. Yukawa.** 2006. Implementing biofuels on a global scale. *Nat Biotechnol* **24**:761-764.
133. **Vik, S. B., and R. R. Ishmukhametov.** 2005. Structure and function of subunit a of the ATP synthase of *Escherichia coli*. *J Bioenerg Biomembr* **37**:445-449.
134. **Vik, S. B., J. C. Long, T. Wada, and D. Zhang.** 2000. A model for the structure of subunit a of the *Escherichia coli* ATP synthase and its role in proton translocation. *Biochim Biophys Acta* **1458**:457-466.

135. **Walfridsson, M., J. Hallborn, M. Penttila, S. Keranen, and B. Hahn-Hagerdal.** 1995. Xylose-metabolizing *Saccharomyces cerevisiae* strains overexpressing the TKL1 and TAL1 genes encoding the pentose phosphate pathway enzymes transketolase and transaldolase. *Appl Environ Microbiol* **61**:4184-4190.
136. **Wei, W., H. Li, N. Nemeria, and F. Jordan.** 2003. Expression and purification of the dihydrolipoamide acetyltransferase and dihydrolipoamide dehydrogenase subunits of the *Escherichia coli* pyruvate dehydrogenase multienzyme complex: a mass spectrometric assay for reductive acetylation of dihydrolipoamide acetyltransferase. *Protein Expr Purif* **28**:140-150.
137. **Wendisch, V. F., M. Bott, and B. J. Eikmanns.** 2006. Metabolic engineering of *Escherichia coli* and *Corynebacterium glutamicum* for biotechnological production of organic acids and amino acids. *Curr Opin Microbiol* **9**:268-274.
138. **Wilkinson, K. D., and C. H. Williams, Jr.** 1981. NADH inhibition and NAD activation of *Escherichia coli* lipoamide dehydrogenase catalyzing the NADH-lipoamide reaction. *J Biol Chem* **256**:2307-2314.
139. **Wittenberger, C. L., and J. G. Fulco.** 1967. Purification and allosteric properties of a nicotinamide adenine dinucleotide-linked D(-)-specific lactate dehydrogenase from *Butyribacterium rettgeri*. *J Biol Chem* **242**:2917-2924.
140. **Wood, B. E., and Ingram, L. O.** 1992. Ethanol-production from cellobiose, amorphous cellulose, and crystalline cellulose by recombinant *Klebsiella oxytoca* containing chromosomally integrated *Zymomonas mobilis* genes for ethanol-production and plasmids expressing thermostable cellulase genes from *Clostridium thermocellum*. *Appl. Environ. Microbiol* **58**:2103-2110.
141. **Wood, J., G. Long, and D. Morehouse.** 2000. Presented at the meeting of the American Association of Petroleum Geologists, New Orleans, Louisiana.
142. **Wyman, C. E.** 1994. Alternative fuels from biomass and their impact on carbon dioxide accumulation. *Appl. Biochem. Biotechnol* **45/46**:897-915.
143. **Zhang, M., Eddy, C., Deanda, K., Finkestein, M., and Picataggio, S.** 1995. Metabolic engineering of a pentose metabolism pathway in ethanologenic *Zymomonas mobilis*. *Science* **267**:240-243.
144. **Zhou, S., F. C. Davis, and L. O. Ingram.** 2001. Gene integration and expression and extracellular secretion of *Erwinia chrysanthemi* endoglucanase CelY (*celY*) and CelZ (*celZ*) in ethanologenic *Klebsiella oxytoca* P2. *Appl Environ Microbiol* **67**:6-14.
145. **Zhou, S., and L. Ingram.** 1999. Engineering endoglucanase-secreting strains of ethanologenic *Klebsiella oxytoca* P2. *J Ind Microbiol Biotechnol* **22**:600-607.

146. **Zhu, J., and K. Shimizu.** 2004. The effect of *pfl* gene knockout on the metabolism for optically pure D-lactate production by *Escherichia coli*. *Appl Microbiol Biotechnol* **64**:367-375.

BIOGRAPHICAL SKETCH

Youngnyun Kim was born in Seoul, Korea, in 1971. He attended Shin-sa Middle school and Kujung High School. He received his bachelor's degree and master's degree in biotechnology from Ajou University. He worked in Dr. Ryu's laboratory for his master's degree. After he received his master's degree, he worked in the environmental engineering field in Hyosung Co. before he came to the USA.

He was accepted to the Ph.D program in the in the Department of Biological Engineering at Utah State University. He transferred to the Department of Microbiology and Cell Science at the University of Florida in 2002, to work in Dr. Shanmugam's laboratory. He was employed by Amyris Biotechnology before his graduation.